NASA CR-72841

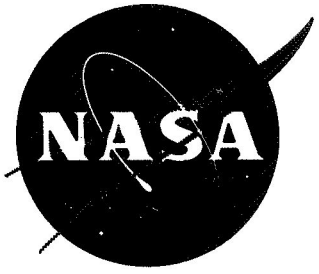

MECHANICAL PROPERTIES AND LOX COMPATIBILITY OF STAINLESS STEEL-CLAD TITANIUM PREPARED BY EXPLOSIVE WELDING AND VACUUM DEPOSITION

by

K. E. Meiners, Program Director

BATTELLE MEMORIAL INSTITUTE

prepared for

NATIONAL AERONAUTICS AND SPACE ADMINISTRATION

NASA Lewis Research Center
Cleveland, Ohio
Contract NAS 3-12007
Thomas W. Godwin, Project Manager

Requests for copies of this report should be referred to

National Aeronautics and Space Administration
Scientific and Technical Information Facility
P.O. Box 33
College Park, Md. 20740

NASA CR-72841

FINAL REPORT

MECHANICAL PROPERTIES AND LOX COMPATIBILITY OF STAINLESS STEEL-CLAD TITANIUM PREPARED BY EXPLOSIVE WELDING AND VACUUM DEPOSITION

by

K. E. Meiners, Program Director

BATTELLE MEMORIAL INSTITUTE
505 King Avenue
Columbus, Ohio 43201

prepared for

NATIONAL AERONAUTICS AND SPACE ADMINISTRATION

December 31, 1969

CONTRACT NAS 3-12007

NASA Lewis Research Center
Cleveland, Ohio
Thomas W. Godwin, Project Manager

TABLE OF CONTENTS

LIST OF TABLES

LIST OF TABLES
(Continued)

LIST OF FIGURES

LIST OF FIGURES
(Continued)

LIST OF FIGURES
(Continued)

LIST OF FIGURES
(Continued)

FINAL REPORT

on

MECHANICAL PROPERTIES AND LOX COMPATIBILITY OF STAINLESS STEEL-CLAD TITANIUM PREPARED BY EXPLOSIVE WELDING AND VACUUM DEPOSITION

(Contract NAS 3-12007)

to

NATIONAL AERONAUTICS AND SPACE ADMINISTRATION
Lewis Research Center
Cleveland, Ohio

Submitted by

K. E. Meiners, Program Director

BATTELLE MEMORIAL INSTITUTE
Columbus Laboratories

ABSTRACT

Explosive welding and physical vapor deposition were investigated as candidate techniques for production of the bilaminate composite, Type 304 L stainless steel/Ti-5Al-2.5Sn (ELI grade). Clad 0.5-inch plate and 0.050-inch sheet were prepared by explosive welding. Physical vapor deposition was employed to prepare sheet clad with 0.0001 to 0.010 inch of stainless steel. Drop-weight impact in the presence of liquid oxygen (LOX) was used to demonstrate the protection offered by a thin stainless cladding against titanium-LOX reaction under a variety of impact situations, cladding thicknesses, and intentional defect sizes. Fatigue, tensile, and fracture-toughness properties of the products of both fabrication methods were determined at ambient and cryogenic temperature.

SUMMARY

To decrease overall weight of current launch vehicles, it is desirable to employ materials with high strength-to-weight ratios, such as titanium alloys, in such components as fuel and oxidizer tanks, pump impellers and cases, and the interconnecting plumbing. Although such alloys as Ti-5Al-2.5Sn (ELI) are commonly used in cryogenic applications, they cannot be used in launch vehicles because of potential reactivity with the propellants, especially oxygen. However, titanium alloys could be employed if they were physically separated from the propellants by a layer of nonreactive material such as Type 304L stainless steel which is also an accepted construction material for cryogenic-temperature applications. The objective of this program was to show how this composite could be manufactured and to determine several of its properties.

Two candidate methods were selected for the preparation of Ti-5Al-2.5Sn (ELI) sheet and plate clad with Type 304L stainless steel. Explosive-welding parameters were studied in a limited development effort aimed at producing 0.050-inch titanium-alloy sheet clad with 0.008-inch stainless steel and 0.5-inch titanium-alloy plate clad with 0.020 inch stainless. Similarly, a limited development effort was conducted to establish electron-beam-evaporation parameters to produce stainless steel coatings of various thicknesses up to 0.010 inch on Ti-5Al-2.5Sn sheet. The parameter-development efforts of both processes employed a guided bend-ductility test with subsequent metallographic examination to evaluate coating adherence of the stainless steel and overall room-temperature ductility of the composite. Process parameters that could yield a satisfactory product were identified for both techniques. The composite produced could be bent through 105 degrees about a radius equivalent to 2.5 times the Ti-5Al-2.5Sn substrate thickness without separation of the cladding from the substrate.

A detailed study was conducted to determine the response of the composite to drop-weight impact in the presence of liquid oxygen (LOX). In this study, cladding thicknesses ranging from less than 0.0001 inch to 0.008 inch were evaluated. No reaction between the composite and LOX could be initiated as long as the stainless steel cladding remained physically intact. A limited investigation into the effect of cladding-defect size was performed. The results indicated that flaw sizes of 0.004 inch and below would not permit reaction between LOX and titanium. The probability of reaction during complete puncture of the composite was found to be very high.

Fatigue life, tensile properties, and fracture-toughness properties of various thicknesses of the composite were evaluated at room temperature and -320 F. The fatigue evaluation revealed that a thin film of intermetallic compound had formed at the junction of the cladding and Ti-5Al-2.5Sn substrate

during both fabrication techniques. The presence of the brittle intermetallics which form in this metallurgical system was judged to be responsible for the severely decreased fatigue life exhibited by the composite. Tensile properties of the composite were, for the most part, unchanged from that of unclad Ti-5Al-2.5Sn (ELI). For the fracture-toughness evaluation, both a compact tension specimen to determine plain-strain fracture toughness (K_{Ic}) and three types of flawed sheet tensile specimens were employed. The latter were used, where applicable, to estimate plain-stress fracture toughness (K_c) of the clad sheet. Fracture toughness (K_{Ic}) of the bilaminate was found to be essentially the same as that of the unclad titanium alloy. The K_c values from flawed-tensile-specimen tests indicated a degradation of sheet fracture toughness in the case of the explosive-welding fabrication procedure.

The principal objective of this program was fully realized. A thin film of stainless steel was shown conclusively to be a fully protective barrier to Ti-5Al-2.5Sn reaction with LOX. Owing to the complications of intermetallic-compound formation between the constituents of the composite, the fabrication-process-demonstration and mechanical-property-determination phases of the effort could not be so conclusively completed. Satisfactory composites were produced by both explosive welding and physical vapor deposition. However, the product that was achieved did not represent in either case the optimized bilaminate that could have been produced with a ductilizing intermediate material to prevent intermetallic-compound formation. The bilaminate containing intermetallic exhibits a degraded fatigue life and other mechanical properties that indicate neither a particular improvement nor degradation as a result of cladding. Hence, from a mechanical-properties standpoint, hopes for improvement by cladding did not materialize. Further work will be necessary to determine the mechanical properties of a stainless steel/Ti-5Al-2.5Sn (ELI) composite not complicated by brittle compounds.

INTRODUCTION

It is the goal of all designers of aerospace systems to develop structures with adequate strength for the intended mission, but with minimum weight and maximum payload. This goal has led to intense interest in composite structures of various types which could yield the desirable properties of two or more engineering materials with the diminution of the undesirable features of one or more of the component materials. Such is the broad objective behind the present study. Currently, the bulk of the structural support of large space booster systems consists of high-strength aluminum alloys. The weight of the overall structure could be reduced if the major components were constructed with titanium alloys which have yet higher strength-to-weight ratios. However, prior studies indicate negating disadvantages to the use of titanium in this application. Most seriously, titanium and its alloys can react violently with liquid oxygen (LOX) under certain circumstances which could feasibly occur during booster operation. To render titanium stable in the system, it must be physically isolated from the LOX by a reliable barrier. The barrier must not degrade the structural efficiency of the titanium alloy to any appreciable extent.

The NASA Marshall Space Flight Center conducted a rather broad study on protective coatings for titanium. The coatings ranged from organics to metals. In addition, the mechanism of the LOX-titanium reaction was studied in some detail by Boyd, Berry, and Miller of Battelle Memorial Institute. The combined results of these and other studies in the field pointed toward the need for a metallurgical composite which would retain the strength-to-density ratio, in essence, of the high-strength titanium alloys and add compatibility with LOX.

Controlled-carbon-content stainless steel is very stable in the presence of liquid oxygen and possesses favorable mechanical properties at cryogenic temperatures. Of the titanium alloys, the alpha alloy, Ti-5Al-2.5Sn with controlled interstitial impurity content, is one of the more commonly used at liquid oxygen and hydrogen temperatures. It was of interest, therefore, to prepare and evaluate experimental quantities of material consisting of a Ti-5Al-2.5Sn (ELI grade) substrate clad with a thin (less than 15 percent of the composite thickness) layer of Type 304L stainless steel.

The alloy ingredients of stainless steel are metallurgically incompatible with the constituents of Ti-5Al-2.5Sn. At moderate temperatures, intermetallic aluminides, titanides, etc., are formed. These behave in a fashion expected of most intermetallic compounds which as a class are, in general, prone to brittle failure at room temperature. The scope of the present investigation was limited to those preparation techniques that held promise of producing a metallurgical composite at temperatures below which the intermetallics are generally known to form. Explosive welding and electron-beam

evaporation, a form of physical vapor deposition, were explored. Work on the vapor-deposition technique was directed toward the thinner coatings utilizing sheet substrate which would be applied to tank and plumbing components of the system. The explosive-welding work concentrated on thicker stainless steel layers and on plate substrate which would be applied to pump components. Material prepared by these methods were to be evaluated with respect to the protection afforded against LOX-titanium contact and reaction that can occur during impact and with respect to the following mechanical properties:

Tensile strength at room temperature and -320 F

Fatigue life at room temperature and -320 F

Fracture toughness at -320 F.

The overall objective of the program was to explore selected methods of preparing a titanium alloy/stainless steel composite for use as a potential basic construction material for deep cryogenic fueled booster tankage, plumbing, and pump components. The scope of the program did not allow an evaluation of all conceivable preparation methods nor was it possible to generate statistically complete design data within the limits of the study. Thus, the results which follow should be regarded as indicative rather than fully conclusive. It is believed that the composite approach to space booster construction is a workable one. Further research, however, is required to complete judgment on the composite explored during the course of this program.

CLADDING-METHOD INVESTIGATION

Procurement and Characterization of Materials

Ti-5Al-2.5Sn (ELI Grade) Substrate

Two gages, 0.050-inch sheet and 0.05-inch plate, of Ti-5Al-2.5Sn substrate stock were procured. Both gages were from the same master heat. The vendor certification and subsequent evaluations performed at Battelle were compared against Specification MIL-T-9046-F for this alloy, and the material received was found to meet this specification. The data obtained during this characterization are summarized in Table 1. Metallographic examination of samples taken from the plate and sheet revealed little, if any, visible anisotropy in either gage. Photomicrographs of the sheet material are shown in Figure 1. The as-received microstructure of the plate material is illustrated in Figure 2.

Type 304L Stainless Steel Cladding

A quantity of 0.060-inch-gage stainless steel was procured and characterized in the manner of the substrate alloy. Similarly, the material received was found to meet Specification AMS 5647A for this alloy. The results of that characterization are summarized in Table 2. The 0.060-inch-gage sheet was employed to produce quantities of 0.020- and 0.008-inch-gage stock by room-temperature rolling. Samples of the 0.060-, 0.020-, and 0.008-inch material were examined metallographically. The microstructures of these starting materials are presented for reference in Figure 3.

Explosive Welding

(E. G. Smith, Jr., and V. D. Linse)

Explosive welding offers the capability of joining thin and thick gages of stainless steel sheet to titanium-alloy sheet or plate substrate. This process appeared most applicable to hardware articles such as pump components where a relatively thick stainless steel layer may be desired. There are several potential technical and economic advantages to be realized from fabricating the composite stock by this technique. First, the explosive-welding process produces very little alloying (melting or diffusion) when proper welding parameters are employed. This is particularly important for the stainless steel – titanium alloy system. The components of this system form brittle

TABLE 1. TITANIUM-ALLOY CHARACTERIZATION SUMMARY

Composition, weight percent	Heat G-7622	MIL-T-9046-F Specification
Al	5.0	4.5-5.75
Sn	2.6	2.0-3.0
C	0.022	0.05 max
N	0.008	0.035 max
H	0.004	0.0125 max
O	0.08	0.12 max
Fe	0.15	0.25 max
Mn	0.003	---
Ti	Balance	Balance

Mechanical Properties (Annealed Condition)	Battelle-Columbus Tests[a]	Vendor Tests[a]	Specification
Ultimate Tensile Strength, psi	116,000 114,000 119,000	115,300 115,000 140,200	100,000 (min)
Yield Strength at 0.2 Percent Offset, psi	105,000 103,000 114,000	106,900 106,700 134,300	95,000 (min)
Elongation in 2 Inches, percent	16.5 16.0 17.0	18.5 20.0 20.0	10 (min)
Hardness, R_C	31 31 29		36 (typical value)

(a) Initial two values are for 0.050-inch sheet; the third value is for 0.5-inch plate.

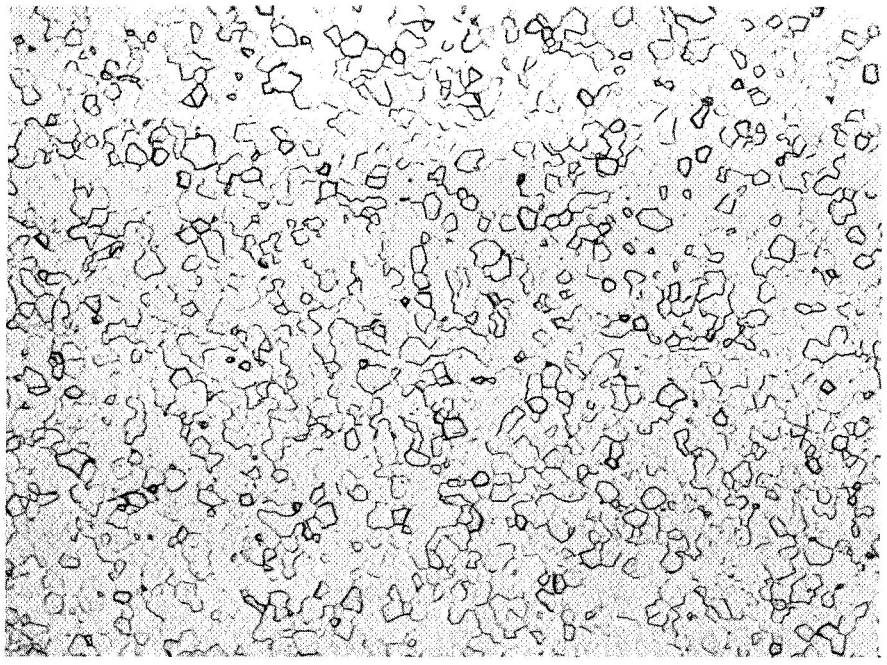

100X 95 H_2O-3 HNO_3-1 HF 5D024

a. Longitudinal Section

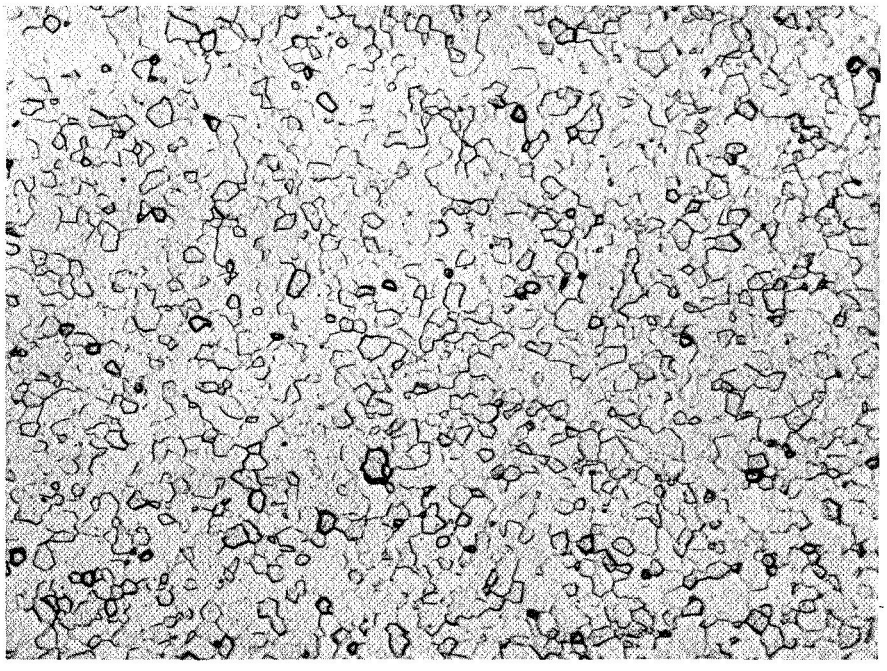

100X 95 H_2O-3 HNO_3-1 HF 5D023

b. Transverse Section

FIGURE 1. TYPICAL MICROSTRUCTURE OF AS-RECEIVED Ti-5Al-2.5Sn SHEET

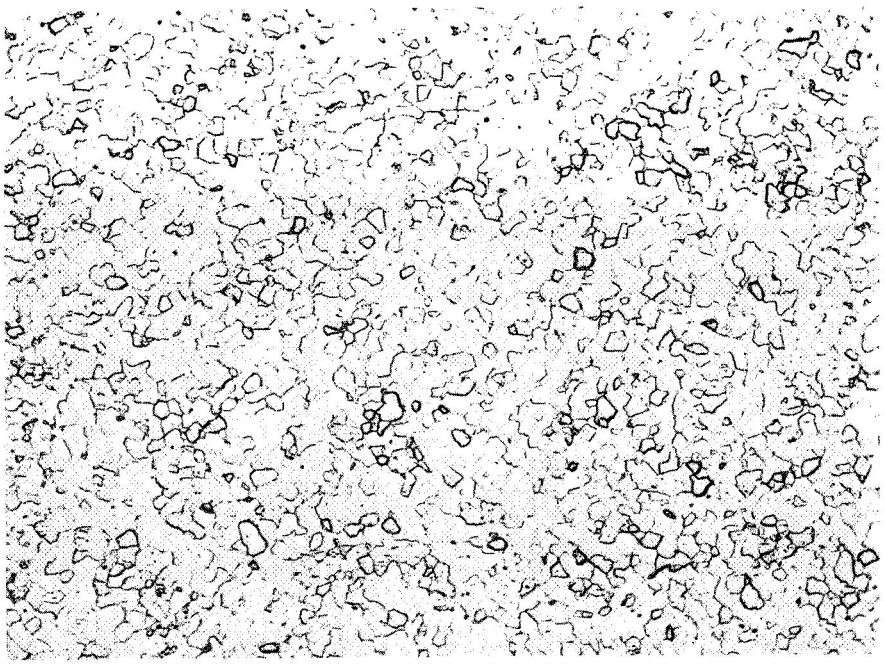

100X 95 H_2O-3 HNO_3-1 HF 5D028

a. Longitudinal Section

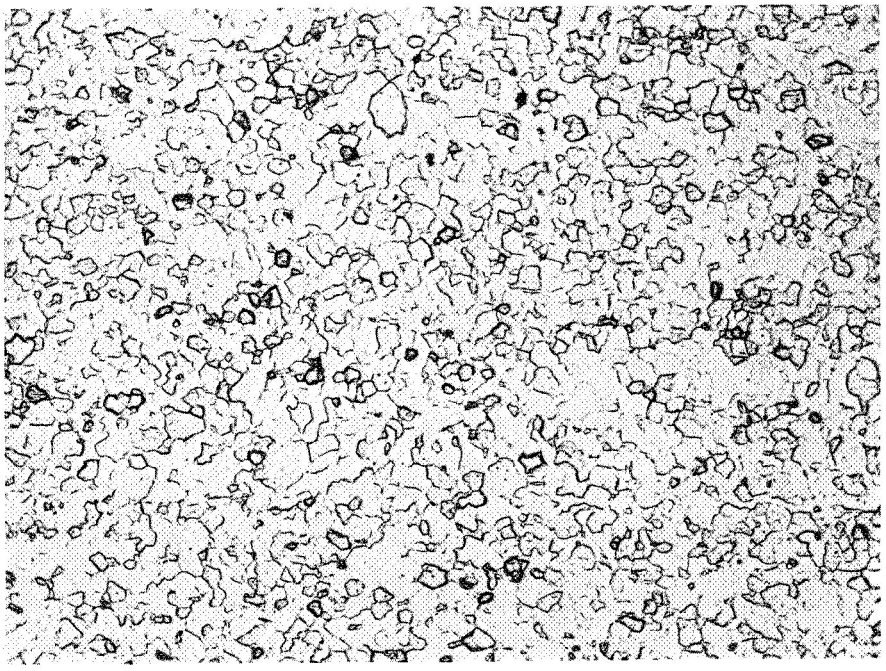

100X 95 H_2O-3 HNO_3-1 HF 5D027

b. Transverse Section

FIGURE 2. TYPICAL MICROSTRUCTURE OF AS-RECEIVED Ti-5Al-2.5Sn PLATE

TABLE 2. TYPE 304L STAINLESS STEEL CHARACTERIZATION SUMMARY

Composition, weight percent	Heat 334292H	AMS 5647A Specification
C	0.026	0.03 max
Mn	1.83	2.00 max
P	0.013	0.040 max
S	0.008	0.030 max
Si	0.44	1.00 max
Cr	18.20	18.00 - 20.00
Ni	9.92	8.00 - 11.00
Cu	0.19	0.5
Mo	0.10	0.5
Co	0.09	---
Fe	Balance	Balance

Mechanical Properties (Annealed Condition)	Battelle-Columbus Tests	Vendor Tests	Typical Values
Ultimate Tensile Strength, psi	83,000 84,000	79,360	80,000
Yield Strength at 0.2 Percent Offset, psi	34,150 34,900	34,880	30,000
Elongation in 2 Inches, Percent	64 69	60	55
Hardness, R_B	73 74	71	76

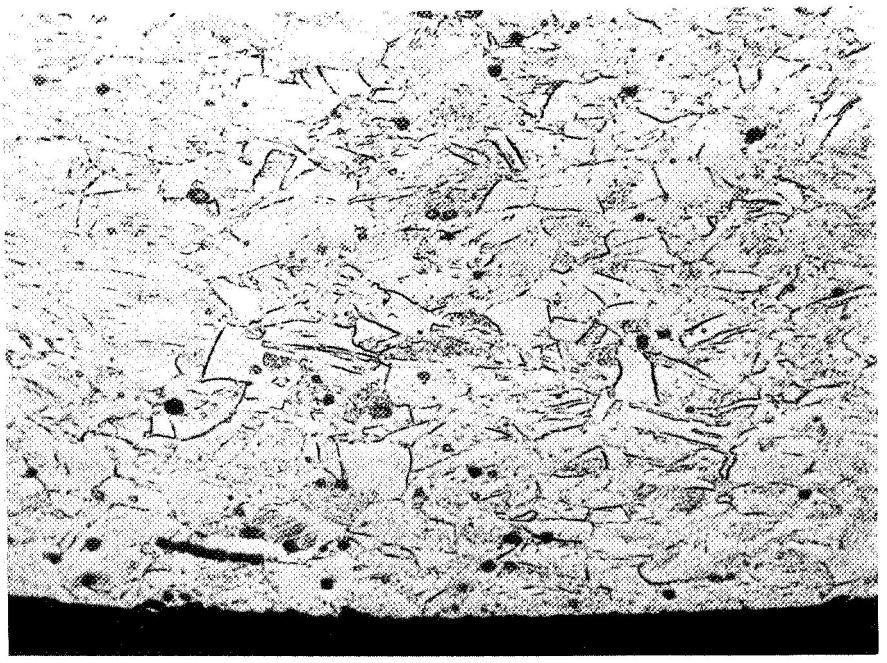

500X 0.5 G $CuCl_3$-98 HCl-2 HNO_3 5D114

a. As Rolled 0.008-Inch Foil

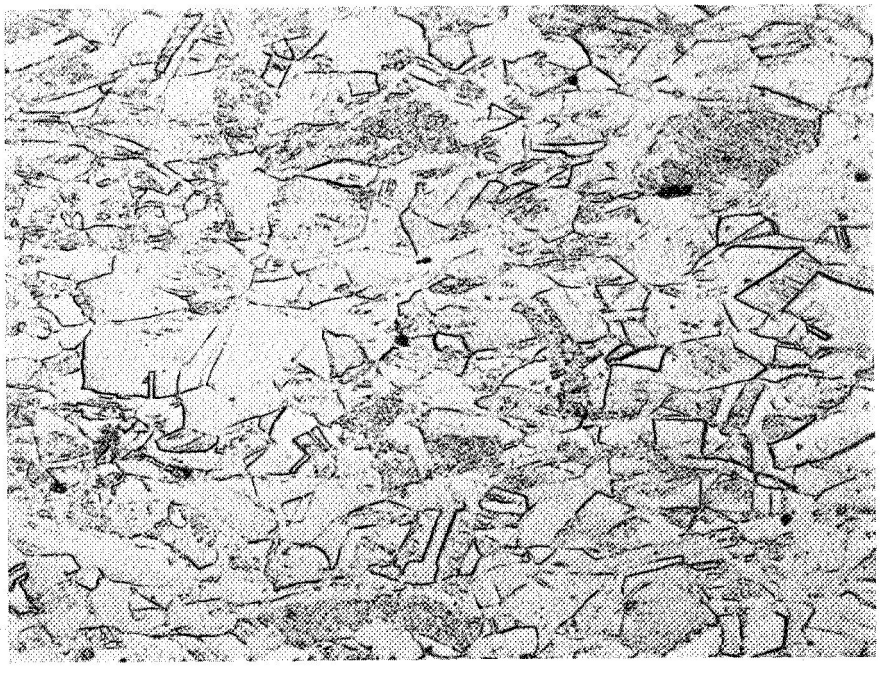

500X 0.5 G $CuCl_3$-98 HCl-2 HNO_3 5D115

b. As Rolled 0.020-Inch Foil

FIGURE 3. TYPICAL MICROSTRUCTURES OF TYPE 304L STAINLESS STEEL EMPLOYED IN CLADDING STUDIES

compounds when alloyed. The presence of these compounds at the interface of the composite can severely reduce the formability of the composite. Second, explosive welds typically exhibit 100 percent joint efficiency. The nature of the explosive-welding process makes it particularly well suited for joining large surface areas. Considering the usefulness of sheet or plate (thick section) stock for the intended application and the modest tooling requirements for these flat forms, this inherent convenience can offer a significant economic advantage relative to other fabrication processes.

Parametric Studies

Preliminary experiments were conducted primarily to determine the parameters for achieving sound explosive welds between 304L stainless steel and Ti-5Al-2.5Sn (ELI) in two thickness combinations. These combinations were (1) 0.008-inch stainless steel on 0.050-inch titanium alloy (thin composite) and (2) 0.020-inch stainless steel on 0.5-inch titanium alloy (thick composite). In addition, available 0.002-inch Type 302 stainless steel and 0.004-inch Type 301 stainless steel were used with 0.050-inch titanium alloy sheet to demonstrate a capability for welding thinner claddings. In these welding experiments, the parameters of explosive type, amount of explosive, and standoff distance were systematically varied from specimen to specimen. The weld integrity of the resulting composites was then correlated with these variables to establish suitable welding parameters.

A second purpose of these preliminary studies was to evaluate the ductility of explosively welded composite, since this stock, once made, would generally be used in a forming operation to prepare the desired finished component. Ductility was measured by bend tests and hardness tests. Samples from both as-welded and welded and heat-treated composites were evaluated. These results were compared with results of similar tests on as-received titanium-alloy control samples.

Materials. Commercial Type 304L stainless steel sheet 0.060-inch thick was reduced by rolling to produce quantities of 0.008 and 0.020-inch-thick sheet. These were employed in both the as-rolled (cold worked) and annealed condition in subsequent experiments. Other, 0.002-inch Type 302 and 0.004-inch Type 301, stainless steel foils were purchased from a commercial vendor and used only in the as-rolled condition. The Ti-5Al-2.5Sn (ELI) sheet (0.050 inch) and plate (0.5 inch) employed in this program were described previously. The titanium alloy was used in the as-received (stress relieved) condition.

Assembly and Welding of Parametric Specimens. All parametric specimens were welded using essentially the procedure which follows. The lay-up of a typical specimen ready for welding is illustrated in Figure 4. The base component, a 5 by 8-inch sheet of Ti-5Al-2.5Sn, was attached to a somewhat larger 0.5-inch-thick steel anvil plate with double-coated tape. The cladding, a 5 by 8-inch piece of stainless steel, was next similarly taped to a sheet of mild steel, 0.062 by 6 by 12 inches. The purpose of this shield is to provide a means for keeping the cladding flat and to protect it from the erosive effects of the detonating explosive. The cladding-shield laminate was then positioned as shown in Figure 4 with the cladding facing towards the base. Spacer shims placed between the anvil and cladding maintained the laminate parallel with and at a constant standoff distance from the titanium-alloy base.

Assembly of the specimen was completed by positioning first a 0.125-inch rubber buffer and then the explosive charge on the protection shield. The purpose of the buffer is to reduce the opportunity for spalling of the cladding or separating of the cladding and shield assembly as they are accelerated. The explosive charge consisted of a rectangular container uniformly loaded with explosive powder to a density of 16 g/in.^{3}. The charge was detonated at one end of the specimen and the detonation front was allowed to travel some distance to stabilize itself before reaching the cladding and base components being welded.

Eleven welding experiments were conducted using the combinations of parameters shown in Table 3. Two essentially identical types of explosive, Trojan 70C* and SWP-1*, were used for all except one experiment (Specimen SS/Ti-11) for which Pentolite* was used. The amount of explosive was controlled by the charge thickness, which, for a given packing density, is equivalent to a specific mass of explosive for a unit area of charge. A more meaningful parameter for explosive amount as applied to welding is the ratio of the explosive mass to the total mass of the cladding assembly for a unit area of specimen. The cladding assembly in these experiments consisted of the cladding, shield, and buffer which are accelerated by the explosive as a unit. Standoff distance for each experiment was controlled by the height of spacer shims which separated the cladding-shield laminate from the base. The explosive-cladding assembly mass ratio along with the cladding-base standoff distance and the explosive detonation velocity determines the collision conditions for welding.

Evaluation of Parametric Specimens. The parametric specimens were evaluated in terms of weld integrity and ductility. Weld integrity was assessed by metallography. Metallographic samples were taken from the center of the

*Product of the Trojan Powder Company.

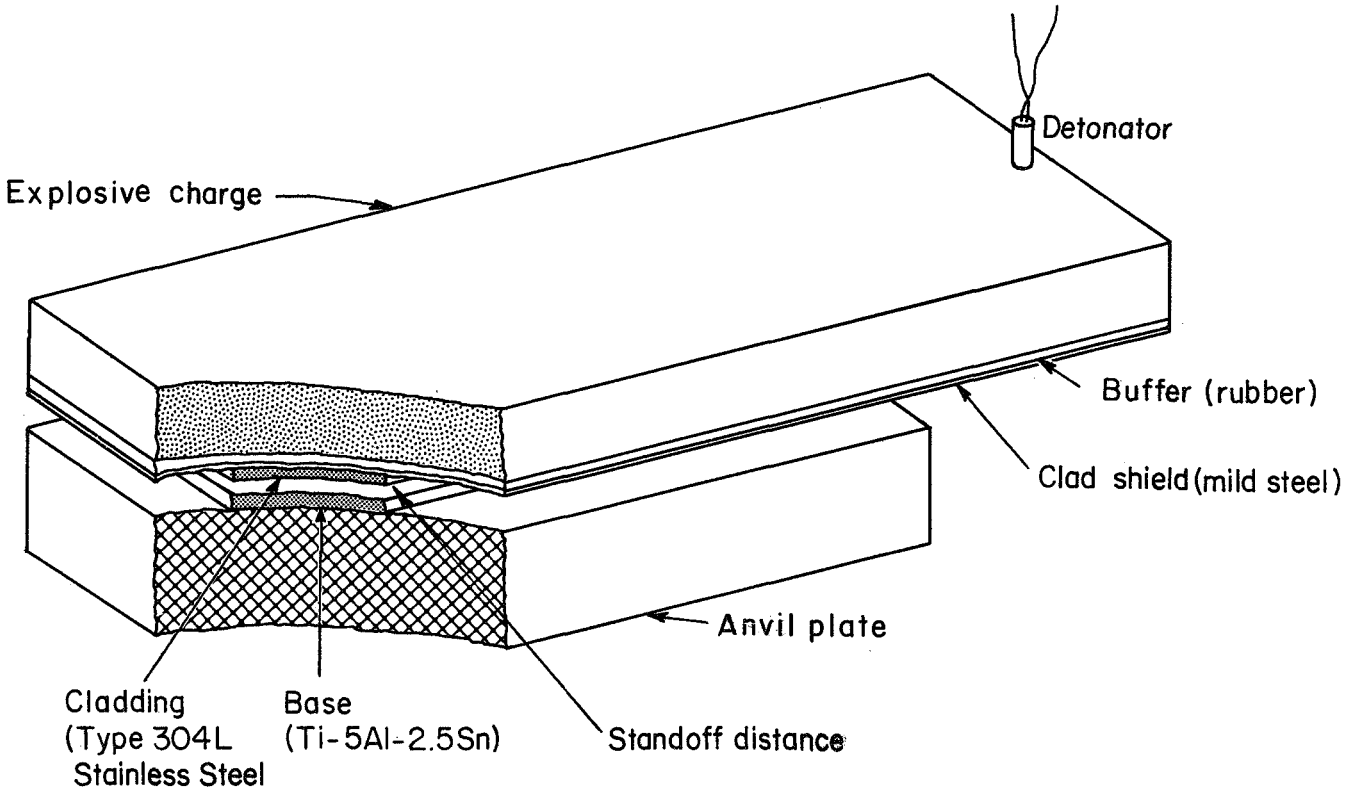

FIGURE 4. COMPONENT ARRANGEMENT FOR PARAMETRIC WELDING SPECIMEN

TABLE 3. EXPLOSIVE-WELDING DATA FOR STAINLESS STEEL/ TITANIUM-ALLOY PARAMETRIC SPECIMENS

Specimen	Specimen Component Thickness, in.		Explosive-Welding Parameters			Remarks
	304L SS Cladding	Ti-5Al-2.5Sn Base	Standoff Distance, in.	Charge Loading[a], g/in.^{2}	Mass Ratio[b]	
			Thin Composites			
SS/Ti-1	0.008	0.050	0.050	7	0.59	Cold-rolled cladding
-3	0.008	0.050	0.100	7	0.59	Annealed cladding
-5	0.002[c]	0.050	0.050	7	0.63	Cold-rolled cladding
-6	0.004[d]	0.050	0.050	7	0.62	Cold-rolled cladding
			Thick Composites			
SS/Ti-2	0.020	0.500	0.050	7	0.52	Cold-rolled cladding
-4	0.020	0.500	0.100	7	0.52	Cold-rolled cladding
-7	0.020	0.500	0.125	9	0.67	Cold-rolled cladding
-8	0.020	0.500	0.125	10	0.75	Annealed cladding
-9	0.020	0.500	0.125	7	0.52	Annealed cladding
-10	0.020	0.500	0.125	9	0.67	Annealed cladding
-11	0.020	0.500	0.125	5[e]	0.37	Annealed cladding

(a) Either Trojan 70C or SWP-1 explosive was used except where noted.
(b) The ratio of explosive mass to that of the cladding, shield, and buffer per unit area of specimen.
(c) 302 stainless steel cladding used.
(d) 301 stainless steel cladding used.
(e) Pentolite explosive used.

composite specimens and viewed parallel to the welding direction. In addition, the thick-section specimens — 0.020-inch cladding on 0.5-inch substrate — were amenable to evaluation by a qualitative "peel" test. This test gages the relative difficulty encountered in mechanically removing the cladding from the substrate; subsequent observations indicate whether the separation occurs in the weld or base metals.

Composite formability was determined primarily from bend tests. Duplicate samples from as-welded, welded and heat-treated, and as-received titanium-alloy material were tested. Each set of two samples was bent through a 105-degree angle around anvils of increasingly smaller radius until failure occurred. Anvils having radii of from 0.5 to 0.031 inch were used for the thin composites, while anvils for the thicker composites had radii of from 2 to 0.5 inch. One sample was bent with the stainless steel and weld interface stressed in tension, while a second sample was bent with the titanium alloy stressed in tension (cladding and interface in compression). Metallography was used in some instances to determine the mode of failure.

Microhardness measurements (Knoop indentor with 500-gram load) were made on samples from a few composite specimens to determine changes resulting from the welding environment and subsequent heat treatments. These measurements were made at specific locations relative to the weld interface. The resulting data were correlated with the bend-test results in evaluating composite ductility.

Thin Composites. Explosive welds were readily achieved between each of the 0.002-, 0.004-, and 0.008-inch stainless steel claddings and 0.050-inch titanium-alloy substrate (Specimens SS/Ti-1 through -4 in Table 3). These welds exhibited well-defined ripple patterns as shown in Figure 5. When viewed at high magnifications, typical pockets of solidified melt were found periodically distributed along the interfaces. The welds produced using annealed stainless steel were not visibly different from those made using cold-rolled foils. Both conditions are shown in Figure 5.

Bend-test results for selected samples from thin composite specimens are summarized in Table 4. Data for unclad 0.050-inch titanium-alloy samples have been included for comparison purposes. Relative ductility is indicated by comparing the minimum bend radius to sample-thickness ratios (R/t) in the last column. Lower values of this ratio indicate greater ductility. The ductility of as-welded samples from Specimen SS/Ti-1 was less than that of the control samples from the as-received sheet material. This difference was particularly large for samples tested with the stainless steel cladding stressed in tension. Samples from this specimen are shown after bending to the R/t values indicated with the titanium alloy stressed in tension (Figure 6a), and with the cladding stressed in tension (Figure 6b).

TABLE 4. SUMMARY OF BEND-TEST RESULTS FOR EXPLOSIVELY WELDED STAINLESS STEEL-CLAD TITANIUM-ALLOY SPECIMENS

Specimen	Condition of Test Sample	Bend Test Data: Tensile Member	Nominal Sample Thickness, in.	Minimum Anvil Radius Prior to Failure[a], in.	Minimum Bend Ratio of Radius to Sample Thickness[a], R/t
		Thin Composite Specimens			
Ti-Control	As-received titanium-alloy sheet	Titanium alloy	0.050	0.125	2.50
SS/Ti-1	As welded	Ditto	0.058	0.250	4.32
Ditto	Ditto	Stainless steel	Ditto	1.00	17.2
SS/Ti-3	As welded and heat treated at 1200 F	Titanium alloy	"	0.156	2.69
Ditto	Ditto	Stainless steel	"	0.188	3.24
"	As welded and heat treated at 1400 F	Titanium alloy	"	0.094[b]	1.62[b]
"	Ditto	Stainless steel	"	Ditto	Ditto
		Thick Composite Specimens			
Ti-Control	As-received titanium-alloy plate	Titanium alloy	0.500	1.00	2.00
SS/Ti-10	As welded	Stainless steel	Ditto	>2.00[c]	>3.73[c]
Ditto	Ditto	Titanium alloy	"	0.50	1.44
"	As welded and heat treated at 1200 F	Stainless steel	"	>2.00[c]	>3.73[c]
"	Ditto	Titanium alloy	"	<0.5[d]	<0.96[d]

(a) The minimum value for which no external damage was observed.
(b) This sample was found to be internally damaged.
(c) This sample failed in bending with the largest available anvil radius of 2.0 inch.
(d) This sample did not fail in bending the smallest available anvil radius of 0.5 inch.

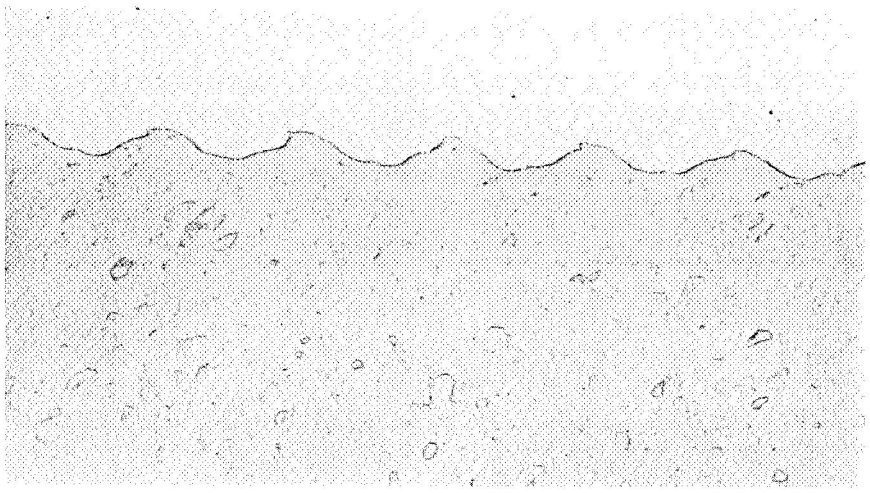

Annealed 0.008-inch
Type 304L stainless steel

Annealed 0.060-inch
Ti-5Al-2.5Sn sheet

100X 5D264

a. Specimen SS/Ti-3 in As-Welded Condition

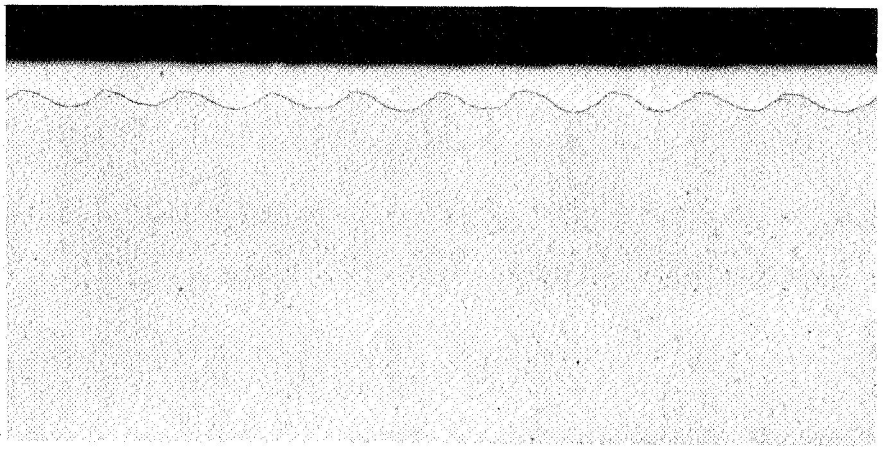

Cold-rolled 0.002-inch
Type 302 stainless steel

Annealed 0.050-inch
Ti-5Al-2.5Sn sheet

100X 5D394

b. Specimen SS/Ti-5 in As-Welded Condition

FIGURE 5. TYPICAL EXPLOSIVE WELDS OBTAINED IN THIN COMPOSITE SPECIMENS

Both welds illustrate the normal cyclical wave pattern expected in explosive welding. Pockets of solidified jet material may be seen distributed periodically along the interface.

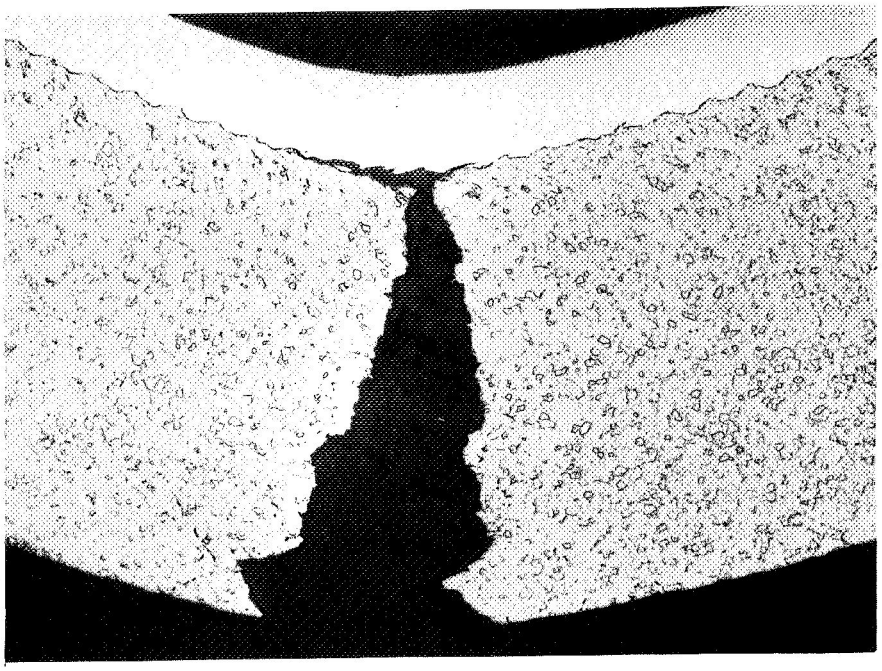

50X 5D173

a. Titanium Alloy Substrate in Tension; Minimum Bend Radius 3.24t

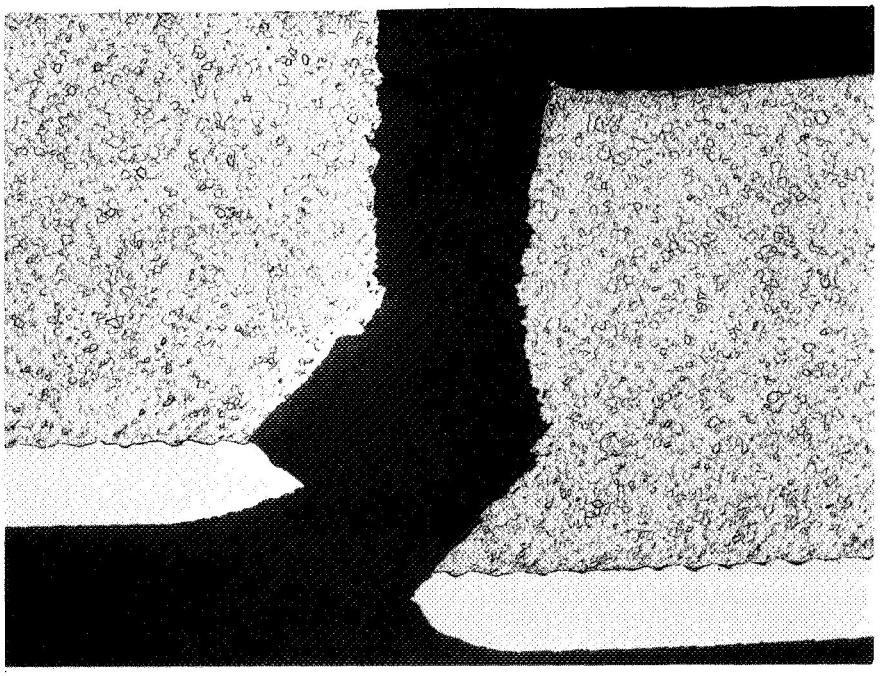

50X 5D171

b. Stainless Steel Cladding in Tension; Minimum Bend Radius 12.9t

FIGURE 6. EXPLOSIVELY WELDED THIN COMPOSITE SPECIMEN SS/Ti-1 AFTER BEND-TEST EVALUATION

Samples were tested in the as-welded condition.

Some improvement in composite ductility was realized by heat treatments at 1200 and 1400 F for 0.5 hour (Specimen SS/Ti-3 in Table 4). The benefit from heat treatment was much more pronounced for the samples bent with the stainless steel cladding stressed in tension. Figure 7 shows welded samples heat treated at 1200 F prior to bending to the R/t values shown. There was no visible damage in the sample bent with the titanium alloy stressed in tension (Figure 7a). The sample bent with the stainless steel member stressed in tension showed small cracks in the melt pockets at the weld interface (Figure 7b).

The 1400 F heat treatment resulted in a 0.5-mil diffusion zone at the weld interface. The ratios of minimum bend radius to sample thickness for these samples were deceptively low. Although these samples exhibited no external damage at the indicated bend-ratio values, subsequent metallographic examination revealed significant internal damage associated with the diffusion zone. The sample bent with the titanium alloy stressed in tension showed complete separation of the cladding from the substrate (Figure 8a). When another sample was bent with the cladding stressed in tension, numerous transverse cracks developed in the diffusion zone (Figure 8b). Both results are indicative of the presence of intermetallic compounds at the weld interface.

The following tabulation summarizes the hardness data obtained for two samples from thin composite specimens.

		Vickers Hardness, kg/mm^2					
		Stainless Steel Cladding[a]			Titanium-Alloy Base		
			0.006 Inch			0.040 Inch	
Specimen	Sample Condition	Near Weld	From Weld	Original	Near Weld	From Weld	Original
SS/Ti-1	As welded	403	398	395	348	322	265
SS/Ti-3	Welded, then heat treated at 1200 F for 0.5 hr	317	224	180	322	323	265

(a) A cold-rolled stainless steel foil was used in Specimen SS/Ti-1, while an annealed foil was used in Specimen SS/Ti-3.

The specimen in which annealed components were used exhibited a noticeable increase in bulk hardness, which can be attributed to the shock produced during welding. In the as-welded condition, the hardness interfacial zone was shown to be greater than the bulk hardness of the titanium member. The stainless steel member when used in the cold-rolled condition exhibited little bulk-hardness increase or gradient. Hardness in the titanium alloy was significantly reduced near the weld interface by heat treating at 1200 F for 0.5 hour. The heat treatment had little effect on the alloy hardness at more remote distances from the interface, nor did it affect the hardness of the stainless steel at any location.

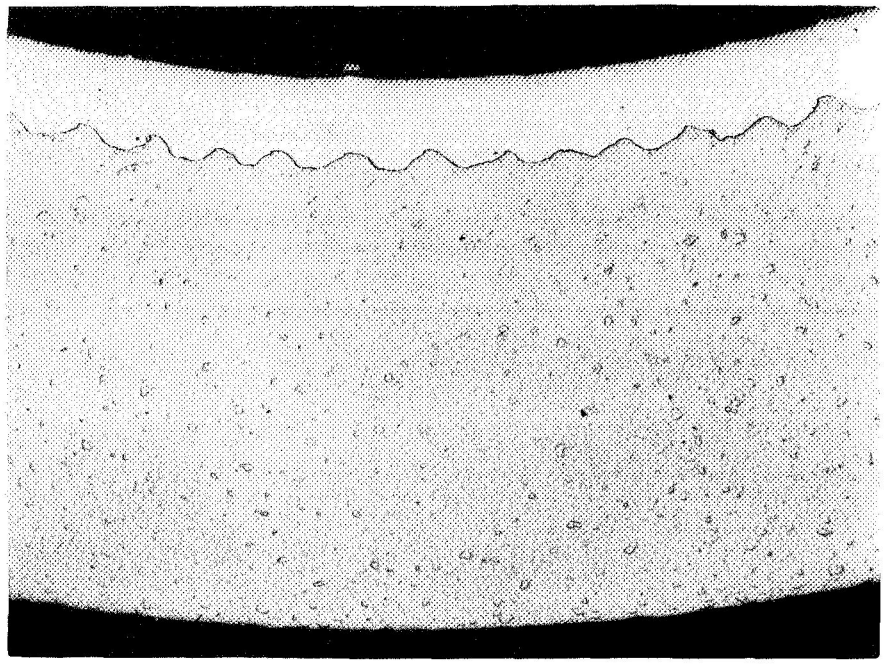

50X 5D534

a. Titanium Alloy Substrate in Tension; Minimum Bend Radius 2.69t

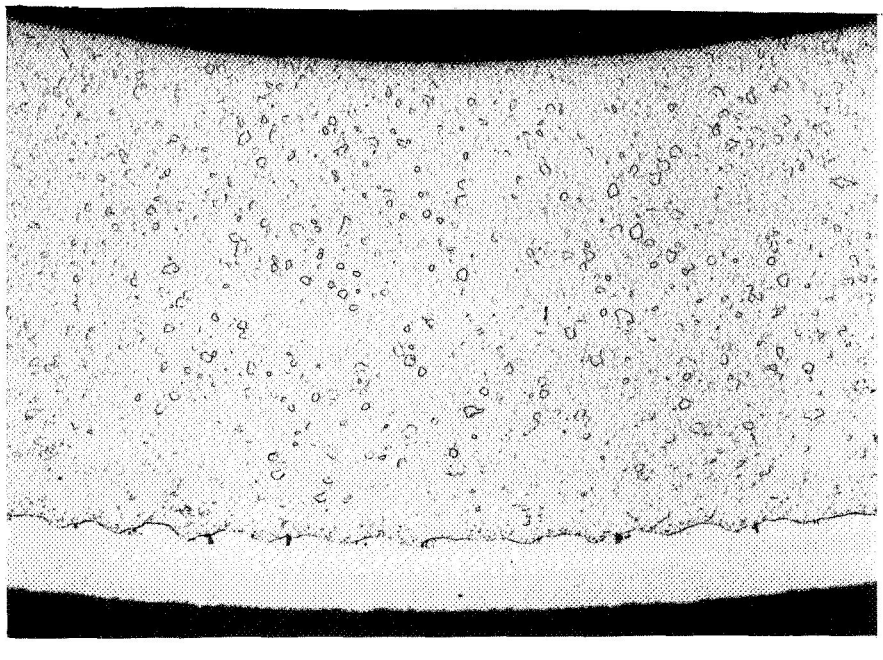

50X 5D738

b. Stainless Steel Cladding in Tension; Minimum Bend Radius 3.24t

FIGURE 7. EXPLOSIVELY WELDED THIN COMPOSITE SPECIMEN SS/Ti-3 AFTER BEND-TEST EVALUATION
Samples were heat treated in argon at 1200 F for 0.5 hour prior to testing.

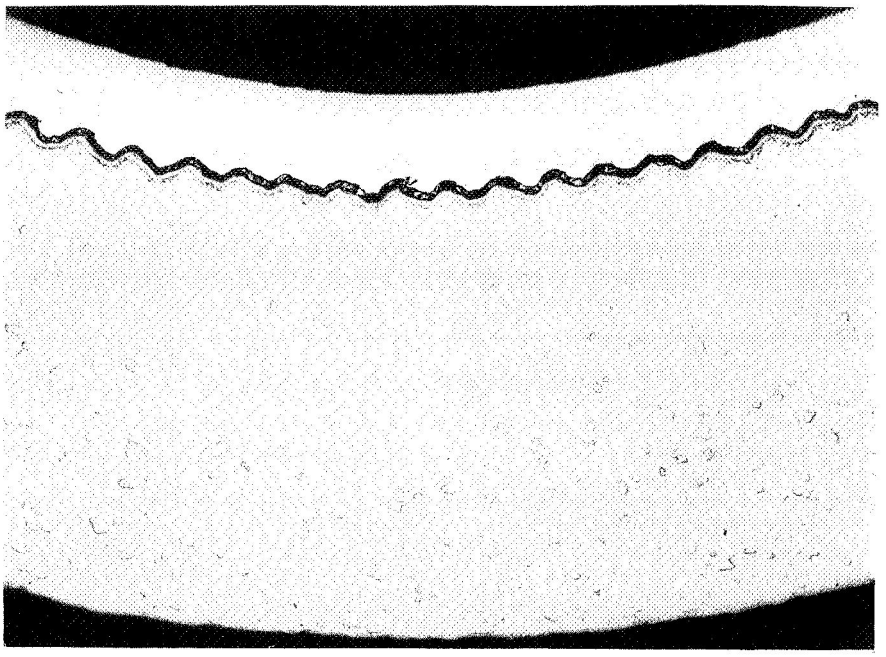

50X 5D397

a. Titanium Alloy Substrate in Tension; Minimum Bend Radius 1.62t

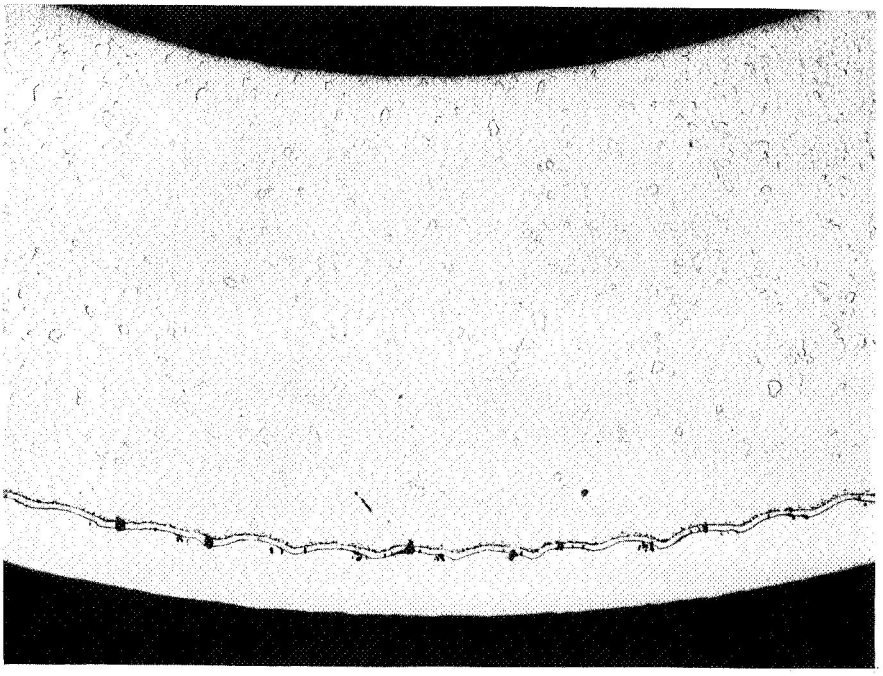

50X 5D396

b. Stainless Steel Cladding in Tension; Minimum Bend Radius 1.62t

FIGURE 8. EXPLOSIVELY WELDED THIN COMPOSITE SPECIMEN SS/Ti-3 AFTER BEND-TEST EVALUATION
Samples were heat treated in argon at 1400 F for 0.5 hour prior to testing.

Thick Composites. In contrast to the thin-composite results, it proved much more difficult to weld 0.020-inch-thick stainless steel to 0.5-inch-titanium-alloy plate and obtain a wavy or rippled interface. The parameters of mass ratio and standoff distance which were used to successfully weld the thin composites resulted in poor welds for the first two thick composites, Specimens SS/Ti-2 and -4 in Table 4. A typical weld exhibited an essentially straight interface with a thin and almost continuous layer of melt (Figure 9a). The stainless steel was easily peeled in specimens possessing this type of weld.

Additional experiments were conducted in an effort to produce better welds in the thick composites, Specimens SS/Ti-4 through -10. Welding parameters were increased, and annealed rather than cold-rolled stainless steel foils were employed. Some improvement in weld quality was achieved, as determined from metallography and peel tests. The weld obtained in Specimen SS/Ti-10, shown in Figure 9b, was the best obtained for the thick composite specimens. This weld showed the beginning of a wave pattern, with melt more periodically distributed along the interface. More effort was required to peel the stainless steel cladding from the titanium.

Bend tests were conducted only on samples taken from Specimen SS/Ti-10, as the welds in this specimen were considered to be the best that had been obtained with the thick composites. The bend-test data obtained from these samples are shown in Table 4 along with data from control samples taken from as-received 0.5-inch-titanium-alloy plate. Ductility of the welded composite in both the as-welded and welded-and-heat-treated conditions was significantly less than that of the control sample when the stainless steel cladding was stressed in tension. On the other hand, composite ductility was somewhat greater than that of the as-received plate material when the titanium was stressed in tension.

The 1200 F heat treatment clearly enhanced the ductility of the composite relative to the as-welded samples, when samples were tested with the titanium stressed in tension. A similar but smaller ductility increase was noted for samples bent with the stainless steel cladding stressed in tension. Although both the as-welded and welded-and-heat-treated samples failed while being bent with the largest available anvil (2.0-inch radius), the heat-treated sample bent to a greater angle (75 degrees versus 20 degrees) before failure occurred. Figure 10 shows the welded-and-heat-treated sample after bending with the cladding stressed in tension. This sample was similar in appearance to the somewhat less ductile as-welded sample. Failure in both samples was caused by the growth of cracks originating in melt pockets at the weld interface and propagating in the titanium alloy. These cracks in various stages of growth are clearly shown in Figure 10.

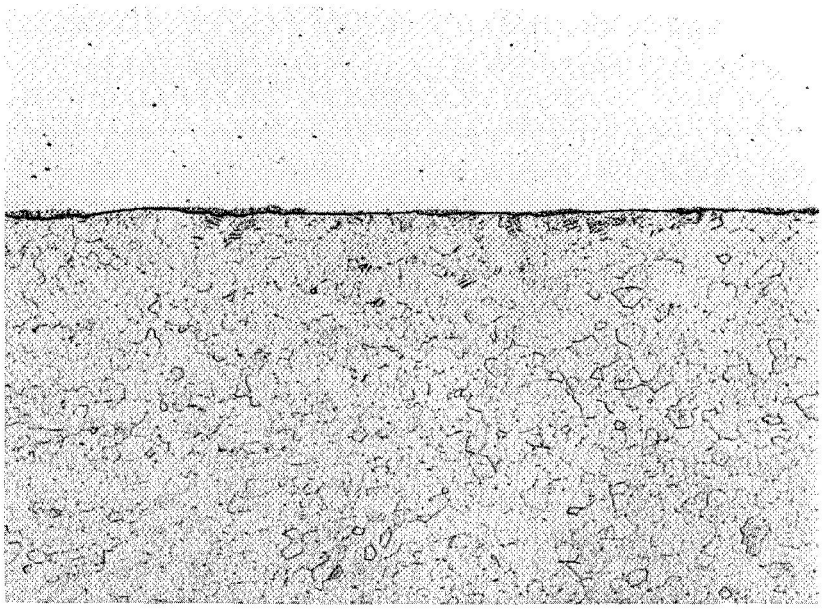

Cold-rolled 0.020-inch
Type 304L stainless steel

Annealed 0.5-inch
Ti-5Al-2.5Sn plate

100X 5D215

a. Specimen SS/Ti-2 in As-welded Condition

This specimen has essentially no wave pattern at the interface.

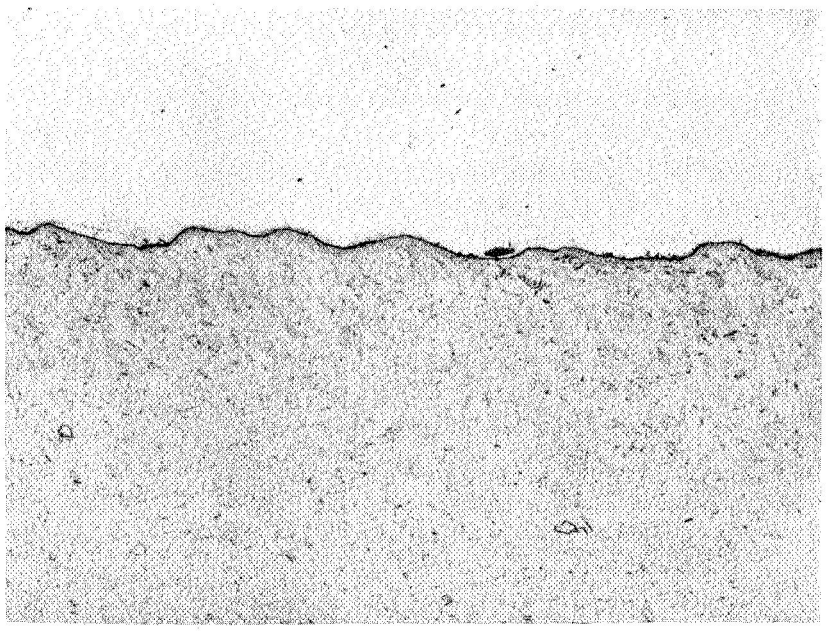

Annealed 0.020-inch
Type 304L stainless steel

Annealed 0.5-inch
Ti-5Al-2.5Sn plate

100X 5D795

b. Specimen SS/Ti-10 in As-Welded Condition

An improved wave pattern was obtained in this specimen.

FIGURE 9. TYPICAL EXPLOSIVE WELDS OBTAINED IN THICK COMPOSITE SPECIMENS

20X 8D381

FIGURE 10. EXPLOSIVELY WELDED THICK-COMPOSITE BEND-TEST SAMPLE

This portion of Specimen SS/Ti-10 was heat treated in argon for 0.5 hour after welding. Failure occurred after bending the sample ~75 degrees using a 2.0-inch radius anvil. The stainless steel cladding was placed in tension during the test.

A further attempt was made to improve weld quality of the thick composite by using anothe type of explosive, Pentolite. This effort was not successful and a microscopic examination of the separated component surfaces revealed no ripple pattern, although traces of the molten jet which forms during the welding process were found.

Average hardness data for two samples from thick composite specimens are shown in the following tabulation.

		Vickers Hardness, kg/mm^2					
		Stainless Steel Cladding(a)			Titanium-Alloy Base		
Specimen	Sample Condition	Near Weld	0.015 Inch From Weld	Original	Near Weld	0.031 Inch From Weld	Original
SS/Ti-2	As welded	385	370	360	385	345	294
SS/Ti-10	Welded, then heat treated at 1200 F for 1 hr	320	230	190	350	335	294

(a) A cold-rolled stainless steel foil was used in Specimen SS/Ti-2, while an annealed foil was used in Specimen SS/Ti-10.

As discussed previously in regard to the thin composite specimens, the annealed substrate and cladding members showed a significant overall hardness increase as a result of welding. A hardness increase was evident for both materials in the as-welded sample as the weld interface was approached. However, stainless steel used in the cold-rolled condition exhibited a smaller hardness increase and gradient as a result of welding. Heat treating at 1200 F for 1 hour decreased the hardness level in the titanium alloy near the weld interface, but had little effect at a distance of 0.031 inch from the interface.

Discussion of Results

The results of the welding-parameter study can best be analyzed and discussed in terms of the three basic parameters which are controlled in each welding experiment. These parameters are (1) explosive type, (2) explosive amount (explosive-cladding mass ratio), and (3) cladding-base standoff distance.

The sole purpose of the explosive in the welding process is to accelerate one component (cladding) so that it collides with a second, usually stationary component (base). To achieve welding in a metallurgical sense, a critical value of collision angle must be exceeded so that a shallow, molten jet forms. The jet is a mixture (or alloy) of the cladding and base materials

which cleans the mating surfaces as it sweeps along the collision interface. A second requirement for welding is that the collision pressure exceed the dynamic strength of both the cladding and base materials. The dynamic strength is usually taken to be the yield strength for the one-dimensional state of strain assumed to exist in these materials near the collision interface. A sufficiently high pressure insures that the clean, mating surfaces are plastically deformed (near the interface) and forced into intimate contact so that direct metal-to-metal bonding can take place on the atomic level. The most convenient way to satisfy both the collision angle and pressure requirements is to accelerate the cladding by a "running" or two-dimensional detonation front in a layer of explosive which is in contact with the cladding. In this arrangement, the cladding is bent through an angle as it is accelerated.

The most important property of the explosive for welding is its detonation velocity. This velocity influences the specific impulse (impulse per unit volume or impulse per unit area per unit thickness) delivered by a layer of explosive to the cladding. More importantly though, the explosive detonation velocity determines the rate at which welding proceeds along the collision interface when the cladding and base materials are initially arranged in the parallel configuration shown previously in Figure 4. It has been found that the rate of welding or detonation velocity determines how the molten jet is distributed once conditions for jet formation (collision angle) and dynamic yielding (collision pressure) have been satisfied. When an explosive is used whose detonation velocity is much greater than the hydrodynamic sound speeds of the materials being welded (supersonic case), the jet is deposited as a more or less continuous layer along a straight interface. Using an explosive having a detonation velocity equivalent to or subsonic with respect to the material sound speed leads to a rippling phenomenon and deposition of the jet in discrete pockets along a wavy interface. The latter type of weld is generally considered to be optimum for most material combinations. However, it is always desirable to minimize the volume of jet involved, particularly for materials which form hard, brittle compounds when alloyed.

The amount of explosive and the initial cladding-base standoff distance determine the velocity and angle at which the cladding strikes the base. The resulting collision velocity in itself determines the collision pressure, and in conjunction with the explosive detonation velocity, determines the collision angle. Explosive amount is usually expressed as loading density or as the mass of explosive per unit area of charge ($g/in.^2$). A more useful parameter as a welding variable is the explosive-cladding mass ratio, which is the ratio of explosive mass to that of the cladding for a unit area of each. Through the use of flash X-ray photography and detonation-velocity probes, it has been possible to "calibrate" the acceleration capability of a given explosive type and relate mass ratios to maximum cladding velocities and bend angles. The velocity and angle at which the cladding ultimately strikes the base may be less than maximum values which are based only on mass ratio. This occurs

if the cladding-base standoff distance is less than the "equilibrium" distance required for the cladding to be fully accelerated. Examination of many flash X-ray shadowgraphs has shown that an explosively accelerated cladding normally reaches maximum velocity for a distance of more than two cladding thicknesses. Through proper choice of standoff distance, this parameter can be eliminated as a critical welding variable in some situations.

On the basis of the preceding discussion, the stainless steel/titanium alloy welds achieved in the thin composite have the characteristics (rippled interface and isolated melt pockets) expected for the welding parameters used. The SWP-1 explosive has a detonation velocity (~9,500 ft/sec at ρ = 16 g/in.^{3}) which is subsonic with respect to the sound speeds of the stainless steel and titanium alloy. The combinations of mass ratio and standoff distance used did not result in much variation in collision velocity which averaged 1650 ft/sec based on flash X-ray data for the SWP-1 explosive. This velocity generates a collision angle of 10 degrees and a collision pressure of 75 kbar which are more than sufficient to form the jet and plastically deform the stainless steel and titanium-alloy components. Because the collision pressures for the thin composite specimens so greatly exceed the dynamic strength of the stainless steel cladding, cladding strength (annealed versus cold rolled) has little effect on the resulting weld characteristics.

Similar arguments concerning the effects of welding parameters on weld characteristics should also apply to the thick composites. Since the total mass being accelerated (cladding, shield, and buffer) for the thin and thick composites is about the same, their welding parameters would be expected to be similar for equivalent standoff distances. The fact that similar parameters (~1650-ft/sec collision velocity with SWP-1 explosive) produced much straighter weld interfaces and more continuous melt distribution in the thick composites indicates that other geometry differences may be important. One possible geometry factor is the much thicker titanium-alloy base in thick composite specimens, although the mechanism by which this could affect welding and weld characteristics is not clear.

Increasing the welding parameters (mass ratio mostly) up to a point produced somewhat stronger welds (on the basis of peel tests) which had better defined wave patterns and less continuous melt distributions. This trend, although based only on a few specimens, is difficult to explain since even the lowest collision pressures and angles used for the thin composites are much greater than those theoretically required for welding the stainless steel/titanium-alloy system. The greater strengths associated with more distinctly rippled interfaces is expected since this interface configuration permits more direct metal-metal bonding to take place.

Hardness measurements indicate that significant work hardening can occur in explosively welding stainless steel to Ti-5Al-2.5Sn. Most of the

hardness increase is confined to the regions in both materials near the weld interface and results from localized plastic flow and work hardening. The smaller hardness increases noted at more remote distances results from the rather high collision pressures (~75 kbar) produced during welding of these composite specimens. Heat treatment at 1200 F relieves much of the work hardening in the titanium alloy, but this temperature is too low to have much effect on the stainless steel member.

Both work hardening and the presence of melt pockets can have a detrimental effect on composite ductility, particularly when the weld and adjacent work-hardened regions are stressed in tension. Composites show greater ductility (lower minimum bend ratio) when the titanium alloy is stressed in tension. For this stress situation, the weld interface, regions adjacent, and the stainless steel cladding are in compression and composite ductility is determined only by the bend properties of the titanium-alloy component. In contrast, composite ductility is much lower (higher minimum bend ratios) when the weld interface and adjacent regions are stressed in tension. For this stress condition, composite ductility is determined not by the cladding which still shows considerable ductility (Figures 6b and 10), but rather is limited by the low tensile properties of the weld and adjacent regions of the titanium alloy. Cracks which originate in the brittle melt pockets propagate with relative ease into the work-hardened and notch-sensitive titanium alloy. Heat treatment at 1200 F removes much of the work hardening, but the inherent low resistance to crack propagation in the titanium alloy still limits the formability of the composite.

The rippled weld interface achieved for the Type 304 stainless steel/ Ti-5Al-2.5Sn alloy composite is considered to be the optimum type for this materials system. However, the jet produced during welding of this system contains hard and brittle particles, probably an iron-titanium compound. The presence of this melt, even as isolated pockets, and the notch-sensitive nature of the titanium alloy greatly weaken this weld when it is subjected to tensile stresses. The strength and ductility associated with the directly welded composite may be sufficient, considering the intended application. In the use of this material as flat stock to be formed into tankage structures, the stainless steel cladding will be on the inside. In that case, most of the bends would be made with the weld interface stressed in compression. The ductility under this stress situation may be such as to not require postwelding heat treatment. Possible weld degradation from heat treatment might therefore be avoided.

Welding of Composite Material for Testing

The purpose of this effort was to produce a quantity of composite material from Type 304L stainless steel and Ti-5Al-2.5Sn (ELI) components in the

two thickness combinations considered during the preliminary study. Two sizes of specimens were made in producing this composite material: 5 by 8 inches and 5 by 12 inches. The specimens were assembled using the parallel component arrangement shown previously in Figure 4. Welding parameters used for the two thickness combinations were:

(1) Thin composites

Explosive type - SWP-1

Mass ratio - 0.63 (7 g/in.^{2})

Standoff distance - 0.125 inch.

(2) Thick composites

Explosive type - SWP-1

Mass ratio - 0.67 (9 g/in.^{2})

Standoff distance - 0.125 inch.

The as-welded composites were given a heat treatment at 1200 F in an argon atmosphere to remove cold work and enhance their ductility. Because of the large mass of material involved, the composites were held at temperature for 2 hours. As a result of this heat-treatment cycle, the stainless steel cladding separated from the substrate in several of the thin and thick composite samples. In addition, the cladding of several other samples was easily peeled from the substrate. When peeling the stainless steel, a powdery material was noted at the weld interface.

The weld quality exhibited by these samples after heat treatment was definitely inferior to that evaluated during the preliminary studies. This weld degradation can be attributed to either the longer heat-treatment time used or to inadvertent overheating. Both of these might explain the material noted at the composite interface. This material is believed to be a diffusion product which formed during heat treatment. A check of the temperature record of the heat-treating cycle and the position of the composites relative to the temperature-controlling thermocouple in the furnace indicated the possibility that at least some of the composites could have been heated in excess of 1200 F.

A new set of composites was assembled and welded as described previously. The heat-treatment conditions and procedures were changed somewhat for this group to minimize the opportunity for excessive diffusion. The

samples were divided into several groups which were heated separately to 1200 F in vacuum, held for 1 hour, and then rapidly cooled by a flow of argon gas. Three of the thick composite samples showed indications of stainless steel separation. The remainder of the composites appeared suitable for machining into test specimens.

It is apparent from these and previous efforts that the explosive welds produced between Type 304L stainless steel and Ti-5Al-2.5Sn (ELI) were not of optimum quality and that further degradation could be caused by the 1200 F heat treatment. Although these welds exhibit the desired morphology (rippled interface and periodic distribution of melt in pockets), the brittle nature of the melt material and the notch sensitivity of the titanium alloy cause inherent weaknesses. Weld degradation during heat treatment is probably the result of shear stresses generated from the rather large differences in thermal-expansion coefficient between stainless steel and Ti-5Al-2.5Sn (approximately a factor of two over the temperature range 70 to 1200 F). As was observed, the thick composite welds are more subject to degradation since the thick substrate cannot bend and relieve an imposed shear stress. In contrast, the thin composites do bend, if they are free to do so, and relieve some of the shear stress. As a result, weld degradation would not be expected to be so pronounced.

Conclusions and Recommendations

The results of efforts to explosively weld composites of Type 304L stainless steel and Ti-5Al-2.5Sn (ELI) led to the following conclusions:

(1) Composites consisting of 0.002-, 0.004-, and 0.008-inch stainless steel on 0.05-inch titanium alloy sheet can be explosively welded. The resulting stainless steel/titanium alloy welds generally exhibit the rippled interface and periodic melt distribution patterns that are considered optimum for most material combinations.

(2) The welds possess an inherent weakness because of the brittle nature of the melt material formed during welding (intermetallic compounds) and the notch sensitivity of the titanium alloy adjacent to the weld interface.

(3) As-welded composite ductility is less than that of the titanium-alloy base metal. Heat treatment at 1200 F restores most of the composite ductility but causes degradation of the weld in some instances, particularly in the thick composites.

(4) Composites consisting of 0.02-inch stainless/0.5-inch titanium alloy can be welded but possess poor joint efficiency and do not exhibit a well-developed weld wave pattern.

There are two possible approaches which can be recommended to improve the properties of explosively welded stainless steel/titanium-alloy composites. The first of these is based on the assumption that weld strength and ductility of the as-welded composite are essentially adequate for the intended application and that a stress relief of the titanium-alloy component is desirable to decrease notch sensitivity. In this case, the stress-relief cycle employed would be modified to prevent degradation from atomic diffusion and thermally induced shear stress at the weld interface. The heating and cooling ramp of the cycle would have to be very carefully controlled to allow accommodation of the stresses produced. The slope of these ramps as well as the maximum permissible temperature and time would have to be determined through experiment.

Another approach would make use of an intermediate foil which is metallurgically compatible with both the stainless steel and the titanium alloy. Direct welding of the stainless steel to the titanium alloy produced a brittle melt material. Welds between a properly selected intermediate foil and the two end members would produce ductile melts. Weld strength and composite ductility should definitely be improved, as the source of cracks would be removed from the weld interface. Some of the candidate foils that might be considered for this indirect welding approach are tin, niobium, molybdenum, tantalum, vanadium, and aluminum. One such series of experiments using tantalum as the intermediate was performed as an adjunct to this program. The results of this effort are reported in Appendix A.

Physical Vapor Deposition

(C. T. Wan, D. L. Chambers, and D. C. Carmichael)

Physical Vapor-Deposition Techniques

Physical vapor deposition (PVD), or vacuum coating, is defined as a coating process in which a material in bulk form is transferred in atomic or molecular form through a vacuum to a collecting surface (the substrate), forming a deposit. The three basic processes of physical vapor deposition are (1) vacuum evaporation, (2) ion sputtering, and (3) ion plating. In vacuum evaporation, the source material is simply evaporated or sublimed and transferred to and condensed onto a collector surface. The evaporant can be an element or a compound, metallic or nonmetallic, organic or inorganic. At

low pressures of application, the atoms or molecules have a negligible collision rate with each other in the vapor, and radiate in straight lines from the source. In ion sputtering, lattice atoms are ejected from the target (source material) surface under the influence of incident ion bombardment, usually argon ions. The incident argon ions are generally created in the glow discharge of an inert-gas plasma and accelerated toward the target which is maintained at a high negative potential. The ejected atoms deposit on and coat the substrate by line-of-sight trajectories. In ion plating, the substrate is made the cathode in a spattering system. The source (coating) material is introduced independently as a vapor into the glow discharge where the atoms are ionized, and then are accelerated to the substrate to coat the substrate surface. This latter process has the capability to uniformly coat surfaces of complex geometry.

The physical vapor-deposition processes have the following advantages for the protective coating of materials:

(1) Complex alloy compositions can be deposited which cannot be applied by other coating methods.

(2) The part to be coated is maintained at a relatively low temperature during deposition.

(3) The part to be coated is exposed only to vacuum and the coating material, not to a reactive gas or a fluid as in chemical vapor deposition or electroplating.

(4) Coatings of high purity can be easily obtained without contamination by impurities from the process environment.

(5) Substrates with relatively complex geometry can be coated.

Recent developments in PVD processes have led to greatly increased deposition rates and to the present capability to apply coatings of virtually any material. These developments have led to important new uses of PVD processes in engineering applications, as well as in previous application areas of manufacture of thin-film optical and microelectronic devices. Diverse coating materials have been applied, including high-temperature alloys, refractory metals, light metals, precious metals and alloys, and dielectric materials (boron nitride, alumina, silica, glasses, and carbides). The vacuum atmosphere and the low substrate temperatures which can be used in PVD processes permit the deposition of these coatings onto parts of even a very reactive material or temperature-sensitive materials such as beryllium, titanium, hydrides, salts, and plastics.

All three of the basic PVD processes appear suited to the ultimate application of interest in this program. The immediate consideration, however, was to select the specific technique requiring the least development effort to fabricate coated specimens for evaluation of their characteristics. Sputtering has the attributes of ready retention of composition from the coating source material to the deposited material and excellent adherence and uniformity. The deposition time would have been too long within the scope of this program, however, for the very thick coatings (up to 15 mils) which it was originally considered might be necessary, even though deposition rates have recently been greatly increased (to 1 to 3 mils per hour). Ion plating is characterized by high deposition rates, excellent adherence, and excellent uniformity even on complex shapes. The technology for complex alloy deposition by this technique had not yet been sufficiently developed, however, for immediate use in this program. Therefore, the vacuum-evaporation technique, specifically using electron-beam heating of the coating source material, was selected for the fabrication of specimens in this program. The use of electron-beam heating with this technique, which has recently received considerable development effort for numerous applications, yields very high deposition rates, and minimizes fractionation of the elements in an alloy source material which occurs during the evaporation-condensation process owing to the differences in vapor pressure of the constitutents.

Using electron-beam vacuum evaporation, specific techniques and starting source-material compositions (to allow for the predictable and relatively small fractionation effect) have been developed at Battelle and elsewhere for the successful deposition of ductile, adherent, and protective high-temperature alloy coatings of specific composition. The techniques previously developed for stainless steel deposition onto substrate materials other than titanium could not be directly applied in this study because of the added constraint in this system to minimize the extent of diffusion between the coating and the titanium substrate. Previously employed process conditions were suitably adjusted to yield a reasonably close approximation to the Type 304L stainless steel composition desired. Within the scope of this program, effort was directed primarily to the development of the process for and the fabrication of coated specimens suitable to test the characteristics of stainless steel-coated titanium. Optimization of the process to produce a Type 304 stainless steel coating, or any other specific alloy, can be readily accomplished when deemed appropriate.

Description of Process Equipment

The deposition process was performed in a special vacuum coating chamber which is 30 inches in diameter and 42 inches long. The system has a 10-inch diffusion pump backed by a 15-cfm mechanical pump and has a

vacuum capability of 10^{-8} torr. A refrigerated baffle is placed between the chamber and the diffusion pump to stop the oil vapor from flowing into the chamber. All valves are pneumatically actuated. There is a water-cooled housing to dissipate the heat generated from the substrate heater and the electron beam.

The electron-beam guns employed in this study to melt the source material included a Pierce gun and two different open-hearth-type electron-beam guns. The Pierce gun was a Model 775 made by Brad Thompson Industries. It has a hot filament, bias cup, flat anode plate with large hole, and a focusing coil. The filament operates at -15 kv. This gun was used in the early part of the program but was not used later owing to the fact that the gun itself takes up too much substrate area, and its high operating voltage can cause splattering of the source material.

The first open-hearth-type electron-beam source employed was a Varian Vacuum Division Model No. 980-0103. It is a single-crucible electron-beam source. The electron beam is deflected more than 180 degrees by an integral permanent magnet and strikes the shielded and water-cooled crucible in a beam spot of about 3/16-inch diameter. The maximum power of the electron beam is 6 kw (6 kv at 1 ampere). This electron-beam source was used throughout the development of process parameters.

In the preparation of the test specimens, a single-crucible electron-beam source, Model No. 40-2023-203 made by Airco-Temescal, was used. The electron beam is deflected a full 270 degrees by an electromagnet to strike a shielded and water-cooled crucible. The maximum power of the electron beam is 10 kw (10 kv at 1 ampere).

A substrate holder which can hold an 8 by 8-inch substrate area was made of stainless steel plate. The substrates were placed 6 to 9 inches away from the evaporating source material. The substrates were heated by a pancake heater and also by a quartz-lamp radiation heater. The pancake heater was made by running heater wire coil in the troughs of an 8 by 8-inch ceramic plate. The heater was placed on the back side of the substrate holder. The substrates were heated through thermal conduction.

In radiation heating with the quartz lamps, four 1-kw quartz lamps are mounted such that the substrate, but not the source material, is in the line of sight of the quartz lamps. By this arrangement, the substrates are heated by the radiation of the quartz lamps and the quartz lamps are not coated by the evaporant.

A wire feeder was devised for replenishing the crucible with new source material. This technique is essential to the deposition of thick coatings, and also coatings with better controlled composition.

Study of Deposition Parameters

In the limited-scope development of the process for deposition of a stainless steel coating on a Ti-5Al-2.5Sn alloy by vacuum evaporation, six major parameters were investigated in order to obtain a good-quality coating:

(1) Degree of vacuum

(2) Distance between source and substrate

(3) Electron-beam power

(4) Substrate temperature

(5) Substrate surface cleanliness

(6) Postdeposition heat treatment.

Some experiments were also performed on methods for the maintenance of the source-material composition in the deposited coating.

In the development of the process parameters, the deposited coatings were evaluated for integrity, ductility, and adherence. The latter two properties were evaluated by a bend test involving the capability of a coated specimen to withstand bending through a radius of 2-1/2t (2-1/2 times the thickness of the substrate or 1/8 inch). The process parameters ultimately developed produced specimens which readily passed the bend test.

Degree of Vacuum. Because the substrate and source material may react with the residual gas in the vacuum chamber at the temperatures of the deposition process, it is essential that the process be carried out in a satisfactory degree of vacuum. Several coating runs were made at different pressures to establish the degree of vacuum necessary for a good deposit in this materials system. The results of these runs are presented in Table 5.

TABLE 5. THE EFFECT OF VACUUM ON THE COATING CHARACTERISTICS

Vacuum, torr	Coating Characteristics
1×10^{-4}	Dark gray and powdery
2×10^{-5}	Metallic and adherent
8×10^{-6}	Metallic and adherent

On the basis of these data, 2×10^{-5} torr was established as the maximum pressure allowed in the deposition process for fabricating coated specimens. Since this pressure was readily attainable, no further effort was made to determine the absolute maximum pressure at which the coating deposited will be metallic and adherent. The absolute maximum pressure could be significant in a production coating process, but it was not within the scope of this project to establish it.

Distances Between Source and Substrate. In evaporation deposition, the closer one can bring the source and the substrate, the higher will be the deposition rate. However, since the source can be visualized as a "point" for these considerations (although it is actually more complex) and the substrate is a relatively large planar area, too close a distance results in coatings with a variation in thickness, which is undesirable. Practically speaking, a compromise is made and the source-to-substrate distance is set to yield a reasonable deposition rate, with the required tolerance on the thickness of the coating.

Several experiments were conducted with source-to-substrate distance varying from 6 to 9 inches. Substrate configurations were varied for these tests to simulate the geometries used ultimately in fabricating the test specimens. Coating thickness was measured at the middle and near the ends of the test pieces at source-to-substrate distances of 6 to 9 inches. On the basis of the results, the actual tensile test specimens, which were 4 inches long and of dumbbell shape, were subsequently coated at a source-to-substrate distance of 7 inches. For the LOX-compatibility tests, 1-3/4 by 1-3/4-inch specimens were cut from coated substrates which were 1-3/4 by 7 inches. The thickness variation within each 1-3/4 by 1-3/4-inch area was less than 5 percent. On the basis of the data obtained, the specimens for fatigue testing should have a thickness distribution of about 15 percent or less in the actual test section. These variations in thickness, although far from the optimum which can be achieved, were considered to be satisfactory for this evaluation.

Electron-Beam Power. The electron-beam power directly controls the evaporation rate of the source and, thus, the deposition rate. In general, a lower deposition rate results in a denser coating. The density of the coating, however, is also a function of substrate temperature during deposition; higher substrate temperature will result in a denser coating for the same deposition rate. The deposition rates of stainless steel as a function of electron-beam power of the Varian electron-beam source are shown in Figure 11 for source-to-substrate distances of 4 inches and 5 inches. The deposition rate using the Temescal 2700 electron-beam source at 4 kw of beam power and at a source-to-substrate distance of 9 inches was measured to be 2 mils/hr. The maximum

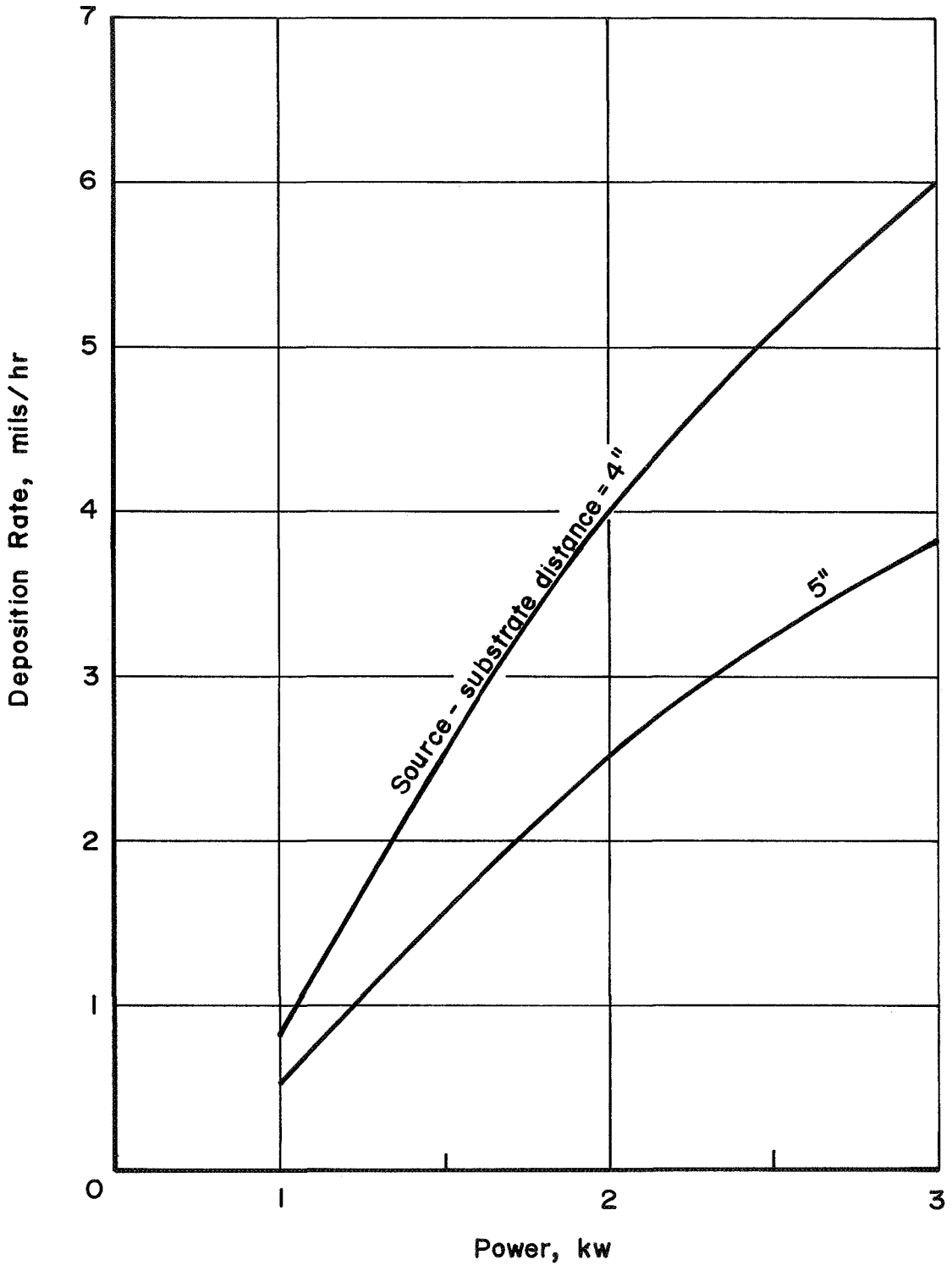

FIGURE 11. STAINLESS STEEL DEPOSITION RATE AS A FUNCTION OF ELECTRON-BEAM POWER

A Varian electron-beam source was employed.

beam power employed in the preparation of test specimens was 4 kw; most of the specimens were coated using a beam power of 3.5 kw.

Substrate Temperature. Substrate temperature plays a very important role in the adherence of the coating to the substrate as well as in the structure and mechanical properties of the coating. Higher substrate temperature usually improves the adherence of a metallic coating to a metallic substrate. It was, of course, important in the present process to heat the substrate to sufficiently high temperature for good adherence. The heating of the substrate was started only when the chamber pressure was lower than 3×10^{-6} torr, and the rate of increasing substrate temperature was adjusted such that the chamber pressure never exceeded 2×10^{-5} torr during heating. This procedure minimized oxidation of the substrate surface. During deposition, the substrate temperature must be maintained constant. The effect of substrate temperature on the adherence of the coating is shown in the following tabulation:

Substrate Temperature	Adherence of Coating
Room temperature	Poor
200 C	Poor
300 C	Good
Varied from 200 to 300 C during deposition	Poor

Accordingly, the substrate was maintained at 300 C during the fabrication of the test specimens.

Substrate-Surface Cleanliness. Several methods were investigated for cleaning the substrate surface: (1) vapor blast the surface, (2) abrade the substrate on a belt sanding machine, (3) abrade the substrate with fine steel wool, and (4) leach the substrate with a chemical reagent such as aqua regia. The effects of these treatments on the coating adherence were as follows:

Surface Preparation	Adherence of Coating
Vapor blast surface	Poor
Chemical leach with aqua regia	Poor
Abrade with fine steel wool	Good
Abrade with fine SiC paper	Good

Abrading with the fine steel wool was very time consuming. From other work, it is known that satisfactory (and convenient) vapor-blasting techniques could probably be determined with development. The cleaning method found most satisfactory for this program was abrasion of the substrate surface with a fine-grit SiC paper such as 400 grit; this method was used in the preparation of subsequent specimens.

Postdeposition Heat Treatment. The stainless steel coating as deposited using a substrate temperature of 300 C was brittle, and process development to determine the best substrate temperature to maximize adherence and ductility while minimizing diffusion was not within the scope of the program, as discussed subsequently. A stress-relieving heat treatment, however, was found to increase the ductility of the stainless steel coating. Vacuum heat treatment of the specimens at 1200 F for 1 hour not only increased ductility but also increased the adherence of the coating. Heating the specimen to 1300 F for 2 hours appeared to yield even better adherence. Most of the specimens prepared for test were vacuum heat treated at 1300 F for 2 hours; however, for evaluation, some specimens were heated to 1200 F for 1 hour, and some specimens were not heat treated at all.

Stainless Steel Composition. In the evaporation of an alloy, the component element which has a higher vapor pressure will evaporate faster than others which have lower vapor pressure. Therefore, the composition of the "bulk-evaporated" coating usually is not the same as that of the source material. The principal methods that are available to obtain the desired deposit composition are: (1) use codeposition methods with different sources for some elements or combination of elements; (2) feed an individual component metal which was found deficient in the coating to the evaporating source material in the crucible during the deposition process; (3) supply new alloy source material to the evaporating source material in the crucible during the deposition process. By these methods, exact composition control of alloys has been achieved for other applications. The third method was chosen for this deposition process. The new alloy source material, in the form of 30-mil-diameter wire, was fed to the crucible with a wire feeder. All the specimens prepared for the LOX-compatibility and mechanical-property tests were deposited with wire feeding of stainless steel to the source-material crucible.

The compositions of coatings deposited under ordinary bulk evaporation conditions and under the controlled wire-feeding conditions are shown in Table 6. Analyses were performed by the X-ray fluorescence method. Although no appreciable development work was performed within the scope of this program, it can be noted that quite good composition control was obtained by the wire-feeding method.

TABLE 6. COATING COMPOSITIONS ACHIEVED BY VACUUM DEPOSITION

Element	Compositions for Two Deposition Techniques, percent of element listed			Desired Type 304 Stainless Steel Composition, percent of element listed
	Bulk Evaporation	Wire-Fed Evaporation		
		Location A[a]	Location B[b]	
Cr	11.	18.7	19.2	18 to 20
Ni	9.2	11.4	8.5	8 to 12
Si	<0.5	<0.1	<0.1	1 max
Mn	<0.1	1.45	1.0	2 max
Fe	79.	69.	70.	65 to 71

(a) Analysis performed on the surface of coating as deposited.
(b) Coating detached from substrate and analysis performed on the substrate side of the deposit.

Fabrication of Test Specimens

Fabrication Procedure. To begin the fabrication process, the substrate surface was first cleaned by manually abrading the substrate with fine-grit paper until the surface appeared bright and metallic. The substrate was then degreased in trichloroethylene vapor for 4 minutes, rinsed in alcohol, and dried before being mounted to the substrate holder.

After the substrate holder was mounted inside the vacuum chamber, the chamber was pumped down to a vacuum of at least 2×10^{-6} torr. At this pressure, the substrate heater was turned on. With a pancake heater, the chamber pressure increased considerably as substrate temperature rose; with a quartz-lamp heater, the pressure increased only slightly. It usually took 1 hour for the pancake heater and 30 minutes for the quartz-lamp heater to raise the substrate temperature to 300 C while maintaining a good vacuum. When the substrate reached this temperature, the electron-beam evaporation was started by turning on the electron-beam power. The power was raised slowly so that the chamber pressure did not exceed 2×10^{-5} torr, and so that the source material in the crucible melted without splattering which results from uneven, spotty heating. After the beam power had reached the predetermined level, the deposition process was continued for the length of time required to obtain the thickness of the coating desired. The coated samples were cooled down under vacuum for 1 hour. Most coated samples were vacuum heat treated at 1200 F for 1 hour or 1300 F for 2 hours as follows:

Test Specimens	Heat Treatment	
	Temperature, F	Time, hr
All nondefected LOX-compatibility specimens	1300	2
All defected LOX-compatibility specimens	No heat treatment	
12 fatigue specimens	1300	2
12 fatigue specimens	No heat treatment	
4 tensile specimens	1300	2
5 tensile specimens	1200	1
All tensile-fracture-toughness specimens	1200	1

LOX-Compatibility Test Specimens. The specimens for the LOX-compatibility test program were 1.75-inch-square coupons. The substrate strips for fabrication of these specimens were 1.75 by 7 by 0.050 inch; from each of the substrate strips, four specimens were made. In each deposition run, four substrates, or a total of 16 specimens, were coated. The thicknesses of specimens from the LOX-compatibility test program were:

(1) 20 specimens having 0.1-mil-thick coating

(2) 20 specimens having 0.25-mil-thick coating

(3) 20 specimens having 0.5-mil-thick coating

(4) 20 specimens having 1.0-mil-thick coating

(5) 20 specimens having 0.2-, 0.3-, 6-, 1.5-, or 3-mil-thick coatings.

The coating procedures used in preparing these specimens were described above. The electron-beam power employed was 3 to 3.5 kw and the substrate temperature was maintained at 300 C throughout the deposition process. New source material in wire form was fed to the crucible of the electron-beam gun during deposition. The coated specimens were heat treated at 1300 F for 2 hours.

Specimens for Mechanical Testing. For the evaluation of mechanical properties of the coated specimens, 42 specimens were prepared. Thirty-three specimens 1 by 6 inches in area were for fatigue and tensile tests and

9 specimens of three specified shapes were for various notched tensile-fracture-toughness tests. The coating thicknesses of specimens for the fatigue and tensile tests ranged from 1 to 9 mils, and those of specimens for the fracture-toughness tests ranged from 4 to 6 mils.

The stainless steel-deposition procedures used in preparing these specimens are described above. The electron-beam power employed was 3.5 to 4 kw. Dense coatings were deposited at this electron-beam power. The substrate temperature was 300 C for the specimens for fatigue and tensile tests. A 400 C substrate temperature was used in the preparation of the fracture-toughness test specimens. The slightly higher temperature was employed to improve coating adherence. New source material in wire form was fed to the crucible of the electron-beam gun during deposition. Some specimens for fatigue and tensile tests were heat treated at 1300 F, some were heated at 1200 F, and some were not heat treated in an effort to minimize intermetallic-compound formation. The fracture-toughness test specimens were heat treated at 1200 F. Table 7 summarizes the characteristics of the test specimens.

TABLE 7. SUMMARY OF SPECIMENS SUBMITTED FOR EVALUATION

Type of Specimen	No. of Specimens	Area Dimensions, inches	Thickness of Coating, mils
LOX compatibility	20	1.75 x 1.75	0.1
Ditto	20	1.75 x 1.75	0.25
"	20	1.75 x 1.75	0.5
"	20	1.75 x 1.75	1.0
"	20	1.75 x 1.75	0.2, 0.3, 0.6, 1.5, or 3
Fatigue and tensile test	33	1 x 6	1 to 10
Fracture-toughness test	3	SF[a]	5 to 9
Ditto	3	SN[a]	5 to 9
"	3	SEN[a]	5 to 9

(a) As described elsewhere in the report.

Conclusions and Recommendations

In this investigation, satisfactory physical vapor-deposition techniques and conditions were determined for the preparation of the various stainless steel-clad titanium specimens which were required for the planned mechanical-property and LOX-compatibility tests. Coatings were achieved which were of suitable composition, ductility, adherence, and integrity to afford a high degree of protection to the substrate, even with remarkably thin coatings, as described elsewhere in this report. It is known from work on other applications that optimization of the coating composition and mechanical-property control can be achieved with appropriate development.

The process used for preparation of the vacuum-coated specimens in this program, involving relatively low-temperature deposition followed by a heat treatment, was found to result in an appreciable diffusion zone between coating and substrate. This interface layer evidently contained some of the brittle intermetallic compounds characteristic of this materials system. This effect can be minimized by decreasing the maximum temperature of the postcoating heat treatment, but such a process modification will also decrease the ductility and adherence of the coating. It may be possible to minimize sufficiently the extent of diffusion by raising the deposition (substrate) temperature slightly to achieve the desired coating ductility and adherence, and omitting the higher temperature heat treatment. This possibility should be investigated in any future, more comprehensive study. Another possible solution to this interface problem which appears attractive is to deposit a thin layer of a selected metal at the interface to serve as a compatibility aid. This thin intermediate layer would be deposited onto the titanium prior to deposition of the stainless steel. In the vacuum-coating process, such an initial step can be incorporated very conveniently into the same cycle used for deposition of the stainless steel coating.

The characteristics and development status of the stainless steel coating applied by the vacuum deposition process are recapitulated below:

Ductility. Ductile stainless steel coatings were achieved for the specimens in this program by postdeposition annealing of coatings applied at low substrate temperatures. Ductile coatings were also obtained by deposition at high temperature, which to the extent investigated appeared to result in a considerable diffusion layer. Study of intermediate deposition temperatures with deposition rate as an independent variable was not within the scope of this program, and these should be investigated in further work.

Adherence. Excellent adherence was obtained in specimens for evaluation in this program by postdeposition annealing of coatings applied at low

substrate temperatures. Considerations for intermediate-temperature deposition are the same as described above for ductility.

Composition. Good control of the composition of the stainless steel coatings was obtained by a wire-feeding technique. On the basis of results of other research programs, optimization of specific alloy compositions would be straightforward with development.

Integrity. Fabrication of specimens with no coating defects was entirely successful and would not require further development, as demonstrated in the LOX-compatibility tests. Even very thin coatings (less than 1 mil thick) afforded good protection of the titanium.

LIQUID OXYGEN COMPATIBILITY

(P. D. Miller and W. E. Berry)

Background

Previous studies have established that of the metals, titanium exhibits the greatest sensitivity to ignition by impact when immersed in liquid oxygen (LOX). Actually, titanium is about as sensitive to ignition as some organic materials. Zirconium is the only other metal that seems to behave similarly to titanium. Earlier research indicated that the ignition often experienced in LOX-titanium systems under impact required a combination of several factors, namely,

(1) Fresh surface

(2) Gaseous oxygen

(3) Pressure.

It is postulated that the impact force exposes a fresh surface of titanium at the same instant that gaseous oxygen is formed in the same area. Localized heating produced during the rupture or deformation is believed to cause the gaseous oxygen to form. In addition, it is believed that this gaseous oxygen is confined in a pit or crevice so that the impact can cause some compression to take place. Titanium is highly reactive with gaseous oxygen when a freshly formed surface is exposed at even moderate oxygen pressures. For example, under conditions of tensile rupture, an oxygen pressure of about 100 psi will initiate a violent burning reaction with titanium over the temperature range of -250 F to room temperature.

It is also significant that the oxides of titanium and zirconium are quite soluble in the molten metals, and thus fresh surfaces can be constantly maintained. It follows that in the presence of LOX, certain impact situations can satisfy the above conditions and a titanium-oxygen reaction can be initiated. The reaction will be self-sustaining if the heat balance is such that the heat furnished to the metal is greater than that lost to the surroundings. Under these circumstances, the oxide would be dissolved as rapidly as it is formed, thereby maintaining a fresh metal surface for continued reaction.

Surface conditions that can lead to greater incidence of reactivity are rough areas, the presence of chips or slivers of metals, and the presence of grit or other types of surface contamination. Of course, the impact force is

an important factor in bringing together the preferred conditions for initiation of reaction. The configuration of the impactor, along with its cleanliness and surface roughness, is also of importance.

The concern of the present study is with the significance of the above factors as they are related to the performance of Ti-5Al-2.5Sn (ELI) with Type 304L stainless steel. Obviously, no reactions are to be anticipated if the titanium is never in contact with the LOX. Accordingly, it is very important to consider conditions which could cause rupture of the stainless steel cladding. The ease with which the cladding can be ruptured will be a function of the cladding thickness and ductility. Hence, these factors need to be studied in some detail. It is visualized that original cladding defects could come from cracks in the cladding, poorly bonded areas, or the presence of foreign matter in the cladding or titanium. Then, during the operation of the component loaded with LOX, it would be necessary for an impact to occur at one of these damaged areas. This impact could come from two vibrating members, from a shock wave passing through the structure, or from a water-hammer-type pulse. The sheet could also be pierced from the outside by some foreign object or micrometeorite.

The program described in the following section of this report was designed to explore possible incoherences in the cladding system and to provide a good understanding of the performance of clad titanium sheets in LOX. Accordingly, titanium specimens clad with several candidate thicknesses of stainless steel were evaluated. The stainless steel cladding was applied by widely different procedures, i.e., explosive bonding and vapor deposition. Specimens from each coating system were impacted in a variety of ways while in contact with LOX. As-clad material, defected sheet, and material punctured during impact were evaluated for their reactivity.

Impact Apparatus and Testing Procedure

Impact Machine

The equipment and handling procedures for making the LOX-compatibility tests in general followed those outlined in MSFC-106 B and in ASTM-D2512-66T. An overall view of the impact machine is shown in Figure 12. The hold and release electromagnet and plummet can be seen at the top of the structure. The LOX filling crucible and line are shown to the right of the structure.

The plummet weight was 20 pounds and it was allowed to fall 43.3 inches, which supplied an impact energy of 75 ft-lb.

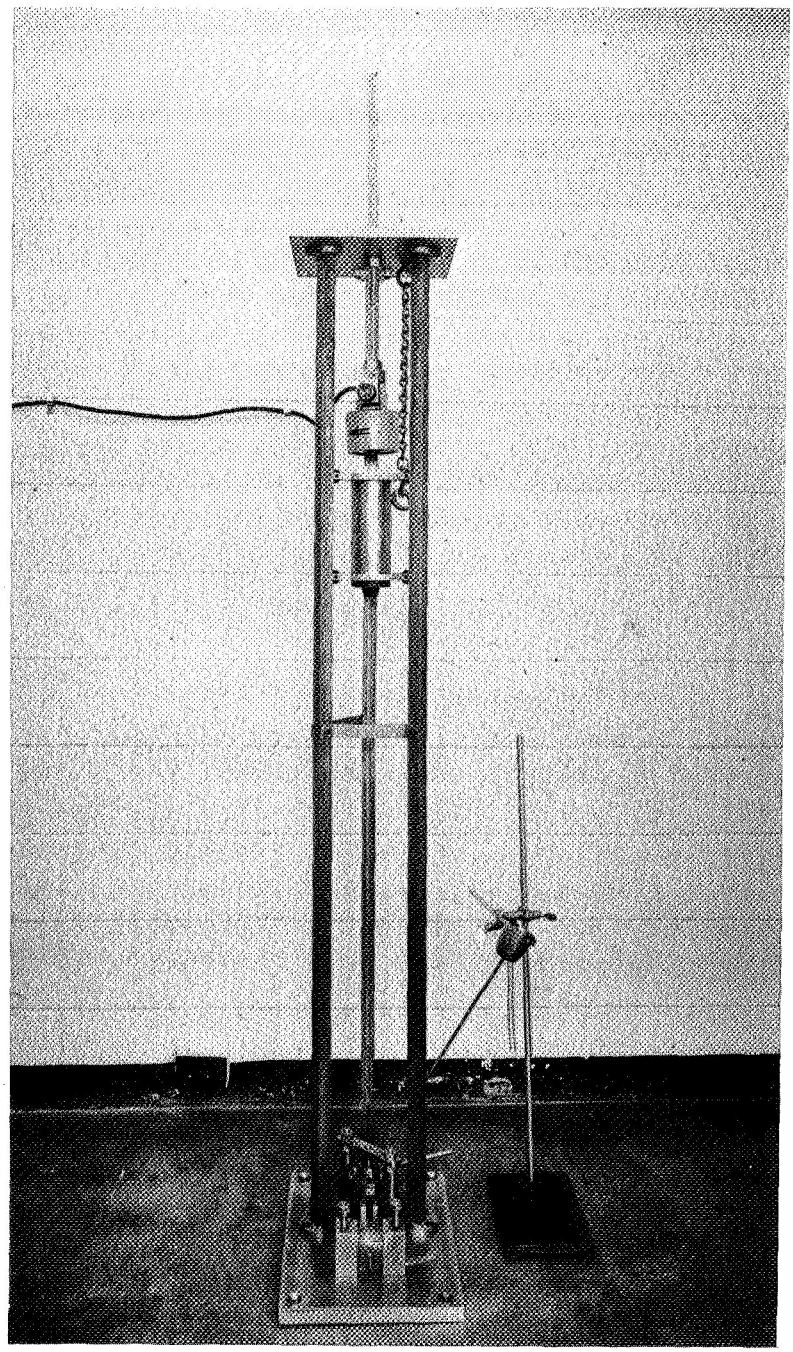

FIGURE 12. OVERALL VIEW OF IMPACT MACHINE

The nickel crucible with the tube welded in the bottom, located to the right of the structure, was used to fill the specimen holder with LOX.

The plummet was guided in channels milled in the upright members by means of ball-bearing races mounted at the tips of three pronged spiders fastened to each end of the plummet body.

Sample Holder and Striker

The specimens were titanium sheet with stainless steel claddings 8 mils thick and thinner. The 8-mil coating was applied by explosive welding, while the thinner coatings were applied by vapor deposition. The experimental specimens were in the form of disks 1.5 inches in diameter or squares 1 inch on a side, which were cut from the clad sheet. In order to insure that the LOX touched only the clad surface of the specimen, the pieces were mounted in a special holder shown in an exploded view in Figure 13. A disk was placed in a recess in the bottom holder plate at the center of the picture. A circular copper jacket was placed over the disk and the top holder plate was clamped to the bottom plate using six cap screws as illustrated in Figure 13.

An assembled holder mounted on the hardened anvil at the bottom of the impact assembly is shown in Figure 14. Also evident in the figure are the striker (mounted within the LOX cup), the striker retainer bar, and the end of the LOX filling tube. The two vertical members visible in the foreground of Figure 14 form the fulcrum of saddle for the lever bar used when the bottom piercing assembly was employed. Figure 15 illustrates the principle of the piercing assembly used for puncture experiments. The anvil was removed and the sample holder repositioned during external piercing experiments so that the plummet could strike the open end of the lever bar.

Two types of strikers were used and these are illustrated in Figure 13. The flat-faced striker was of hardened steel 1/2 inch in diameter conforming to the ABMA specifications. The striker with the rounded tip furnished a much more concentrated impact load to the specimen. It was made from hardened steel 1/2 inch in diameter and ground at one end to form a rounded tip with a 1/8-inch radius.

A hardened steel pointer ground to a narrow knife edge as shown in Figure 13 was used in the piercing studies.

Specimen Cleaning

Specimens, holders, strikers, jackets, and all pieces of equipment in contact with LOX during the experiments were cleaned and degreased prior to use. The cleaned pieces were then handled only by tweezers, metal tongs, or rubber gloves. The cleaning procedure was as follows:

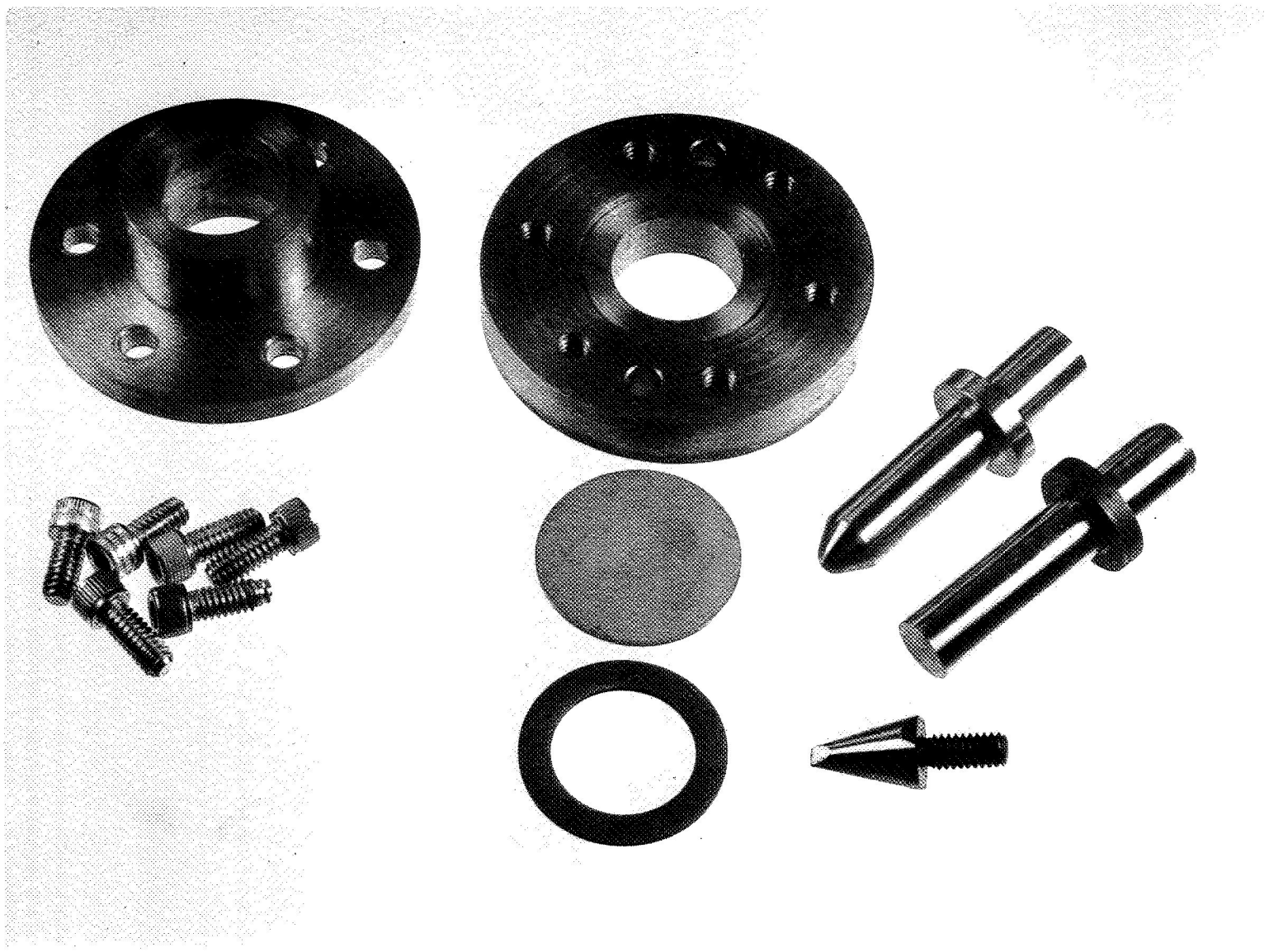

FIGURE 13. LOX-COMPATIBILITY SAMPLE-HOLDER ASSEMBLY AND STRIKER CONFIGURATIONS

A clad specimen and copper sealing gasket are shown in the center foreground.

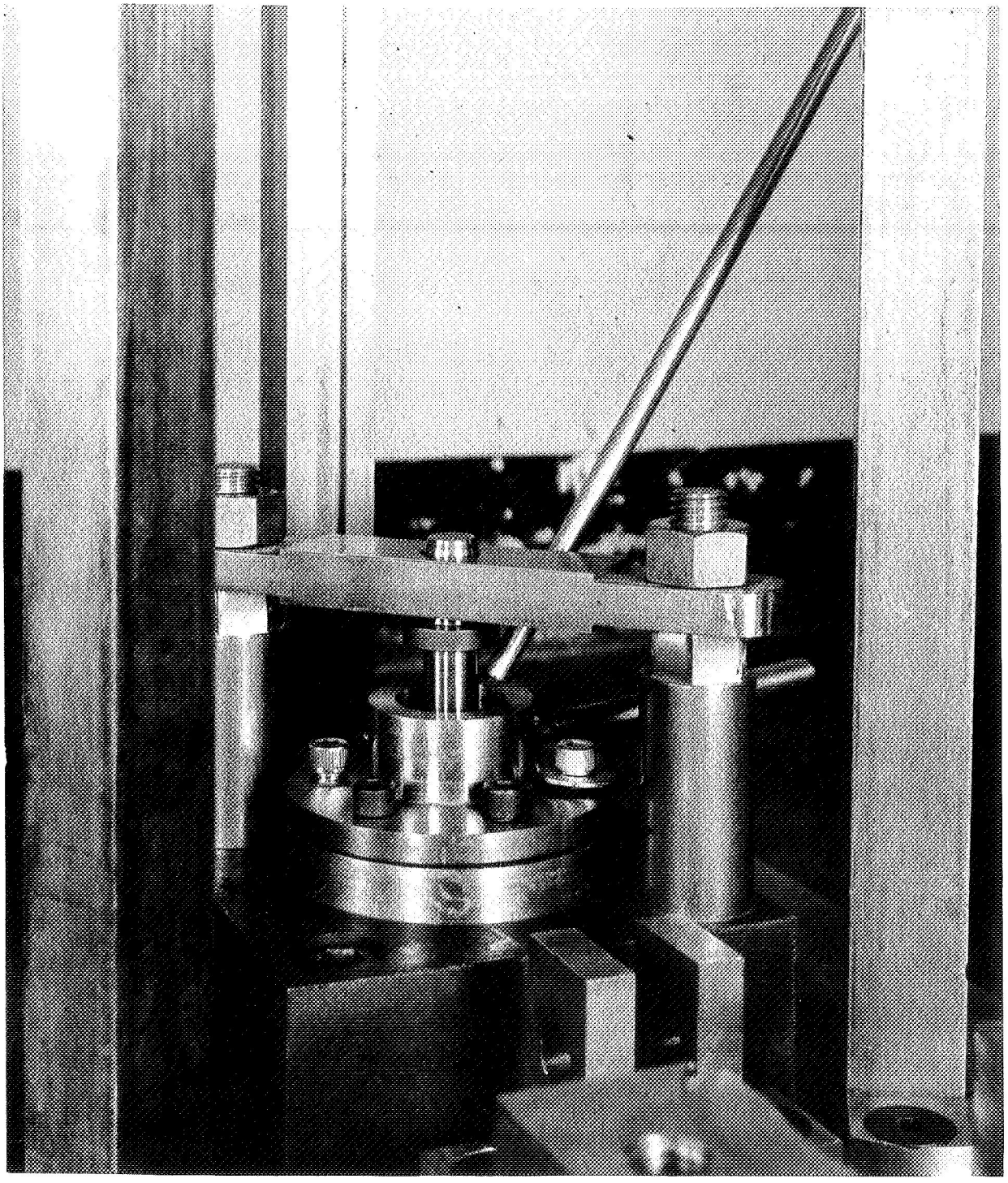

FIGURE 14. MOUNTED SAMPLE HOLDER RESTING ON ANVIL

The striker, retaining-bar, and LOX filling tube are also visible.

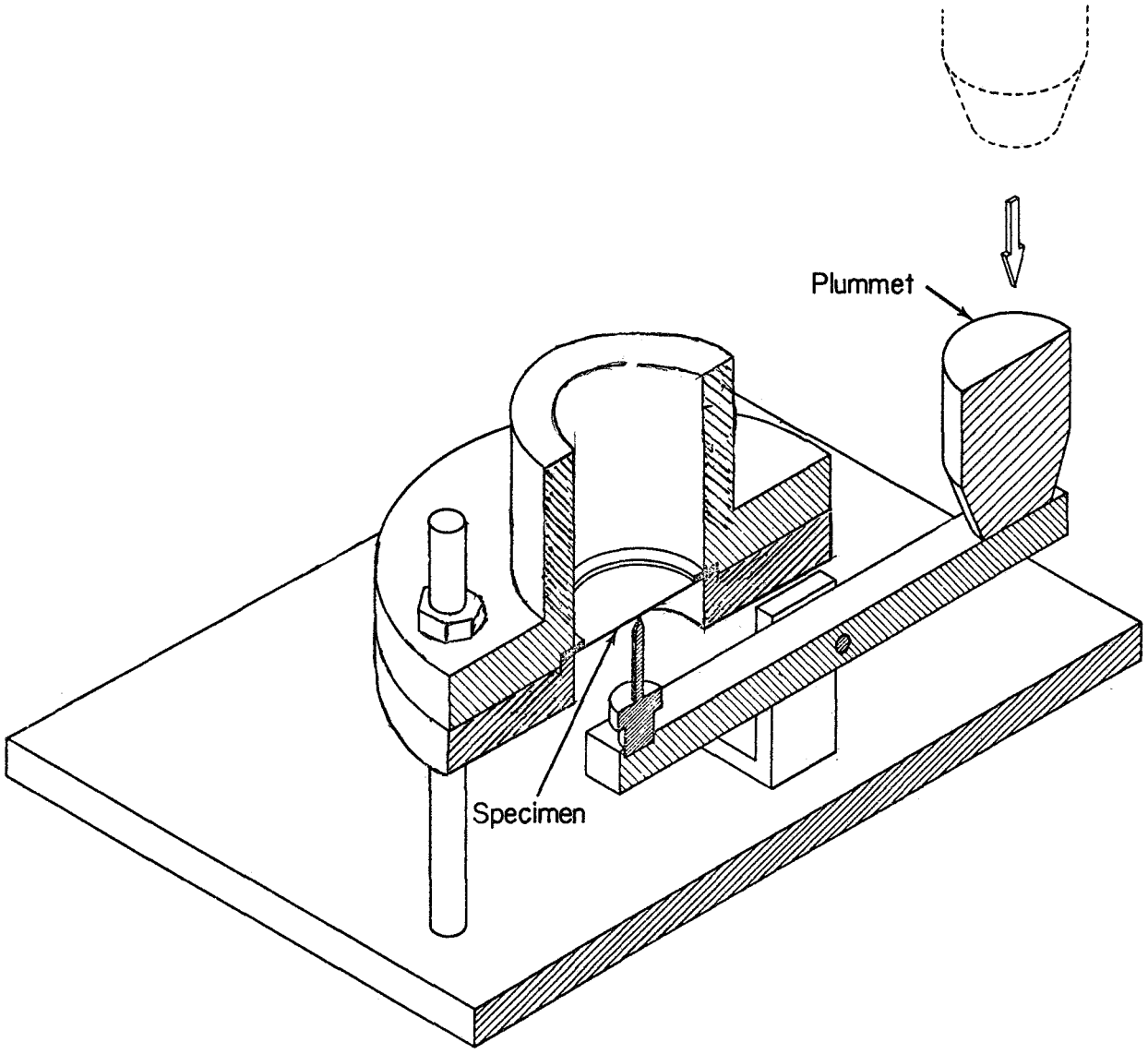

FIGURE 15. TEST FIXTURE FOR PUNCTURE EXPERIMENTS

Specimen was pierced from unclad surface; clad surface was in contact with LOX.

(1) Rinse in acetone and wipe with towel until all staining is absent.

(2) Soak in alkaline cleaner near boiling point for 15 to 30 minutes.

Cleaner composition:

15 g/l NaOH

15 g/l Na_3PO_4.

Since the above cleaner caused some discoloration of the titanium, the following cleaner was used in the preparation of intentionally defected specimens:

30 g/l sodium metasilicate

7.5 g/l sodium hydroxide

0.5 g/l Duponol.

(3) Water rinse in flowing tap water.

(4) Rinse in deionized water (boiling).

(5) Dry in oven at 212 F.

(6) Cool.

(7) Vapor degrease in trichloroethylene 15 minutes.

(8) Store in desiccator until used.

Specimen Evaluation

The assembled sample holder was immersed in LOX in a large stainless steel dewar until an equilibrium temperature was reached. The holder filled with LOX was placed on the anvil, the striker was inserted, the retainer bar was placed in position, and the LOX cup was refilled. It should be noted that even with a reaction some LOX always remained in the cup after a drop was conducted. The drop was conducted in a darkened room so that sparking or burning could be readily observed. The operator viewed the machine from an adjacent room through a Lucite window.

Two criteria were used to determine whether a reaction had occurred. First, a record was made of any visual flash of light at the instant of impact. Second, the impacted specimen was examined under a binocular microscope for evidence of a reaction. Evidence of a reaction may be manifested in several ways. In severe cases a burned or fused area is clearly visible, in other instances a burned area may be discolored by a thin film of oxide.

Compatibility Evaluation Data

Four types of evaluations were made:

(1) Ball impact of as-fabricated sheet

(2) Flat-faced impact of as-fabricated sheet

(3) Impact of defected sheet

(4) Sheet pierced from the titanium side.

Results are given in Table 8. A compilation of the individual test results is presented in Appendix B, Table B-1.

Impact of As-Fabricated Sheet

8-Mil-Thick Cladding. No reactivity was observed with 20 specimens with an 8-mil-thick stainless steel cladding when they were impacted with the ball-tipped striker. The force of the blow was sufficient to upset the sheet so that a dimple about 55 mils deep was formed. A smooth ductile flow of the stainless cladding was observed in all samples. The titanium on the back side of the samples was usually deformed enough to show lines of tensile rupture.

A fresh steel anvil was placed beneath the clad specimen for each drop.

1.0-Mil-Thick Cladding. No flash or other evidence of a reaction (burning) was observed on 19 specimens with a 1.0-mil-thick stainless steel cladding when impacted with the ball indenter. A slight amount of chipping of the stainless steel coating was noted near the crater on Specimen B-51 of this series. This is illustrated in Figure 16.

0.5-Mil-Thick Cladding. One of 20 specimens with a 0.5-mil-thick cladding exhibited a positive reaction when impacted in LOX (Figure 17). Two

TABLE 8. SUMMARY OF LOX-COMPATIBILITY RESULTS

Composite Thickness, mils				Number of	Results	
Titanium	Stainless steel	Defect	Type of Striker	Specimens	Flash	Reacted Area
50	8	No	Ball indenter	20	No	No
50	1	No	Ball indenter	19	No	No
50	0.5	No	Flat striker	5	No	No
50	0.5	No	Ball indenter	12	No	No
	0.5	No	Ball indenter	8	1	1
	0.5	No	Ball indenter (repeat)	1	1	1
50	0.4	No	Ball indenter	1	No	No
50	0.3	No	Ball indenter	4	No	No
50	0.2	No	Ball indenter	16	1	No
50	0.15	No	Ball indenter	2	No	No
50	0.1	No	Ball indenter	7	No	No
50	< 0.1	No	Ball indenter	2	No	No
50	8	35-mil hole	Ball indenter	20	2	4
50	1	16-mil hole	Flat striker	5	3	4
			Ball indenter	5	1	1
50	1	8-mil hole	Flat striker	5	No	No
			Ball indenter	5(a)	No	2
			Ball indenter	6	1	No
50	3	8-mil hole	Flat striker	2	No	No
			Flat striker	1(a)	No	1
			Ball indenter	1(a)	No	No
			Ball indenter	5	No	1
50	1	4-mil hole	Ball indenter	9	No	No
			Flat striker	1	No	No
50	8	No	Pierced from titanium side	20	3	11

(a) Second impact.

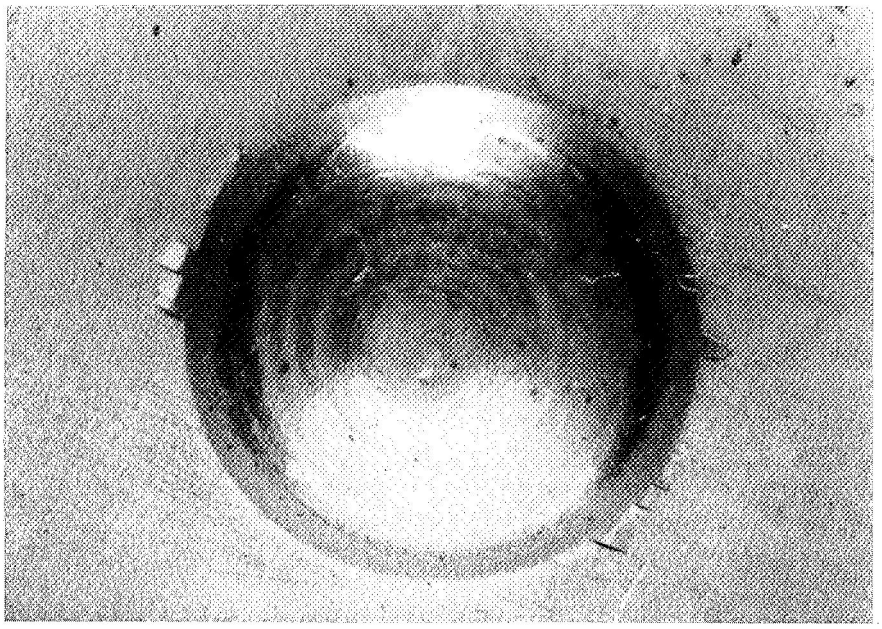

10X C-2962

FIGURE 16. CHIPPED COATING ON SPECIMEN B-51

Stainless steel cladding was 1 mil thick.

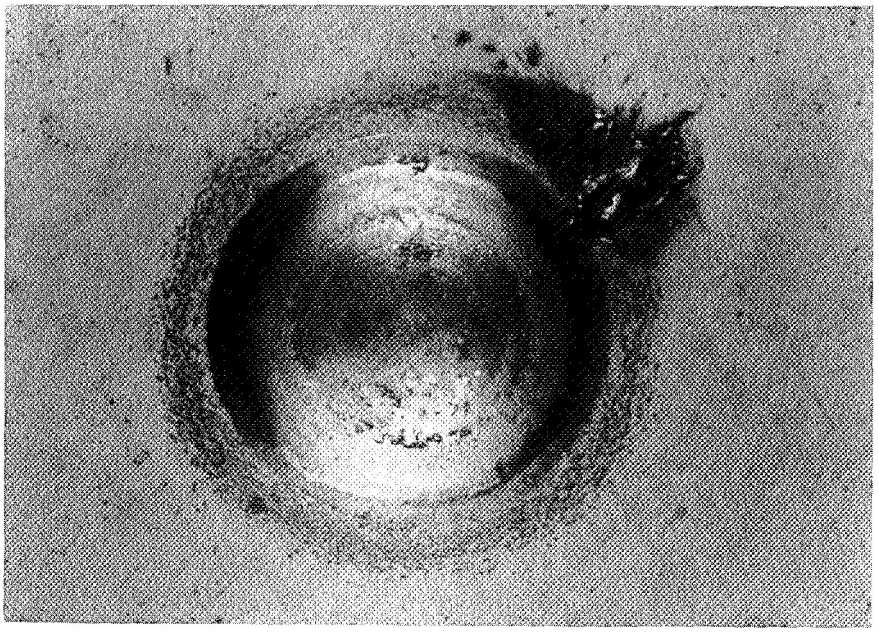

8X C-2963

FIGURE 17. BURNED AREA AT EDGE OF IMPACT CRATER OF SPECIMEN B-71

Stainless steel cladding was 0.5 mil thick.

groups of specimens were prepared on different dates. Some bond separation at the titanium-stainless steel interface, such as shown in Figure 18, was observed in specimens of the first (B57-B68) group. The second group of specimens, which include the specimen showing a reaction, exhibited a degree of coating fragmentation after impact, which indicates a brittle condition (Figure 19). A second impact test on one of these specimens (B73, Figure 20), which had passed the initial impact test, produced a reaction. Although further repeat tests were not performed, it was highly likely that many of the group of eight specimens that exhibited brittle behavior would have similarly reacted. It was concluded that an abnormal condition in the vacuum deposition process produced a poor coating. In light of subsequent results for yet thinner coatings, the reactions obtained with 0.5-mil-thick cladding are not believed to be indicative of the true performance of this cladding thickness.

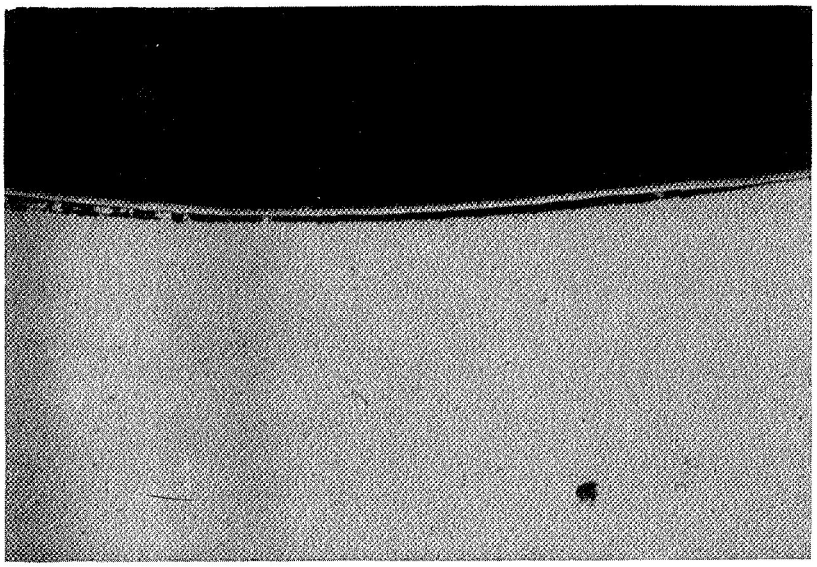

Type 304 stainless steel

0.050-inch Ti-5Al-2.5Sn sheet

100X B-39

FIGURE 18. COATING DELAMINATION AT BASE OF IMPACT CRATER

Metallographic section shown illustrates a 0.5-mil-thick vacuum deposited coating; no reaction occurred during the impact test.

Five specimens (F52 to F56) with a 0.5-mil coating were impacted using a standard ABMA flat striker. No visible indication of a reaction was noted in any case during the impact. In addition, microscopic examination of the important areas of each piece did not reveal any evidence of reaction.

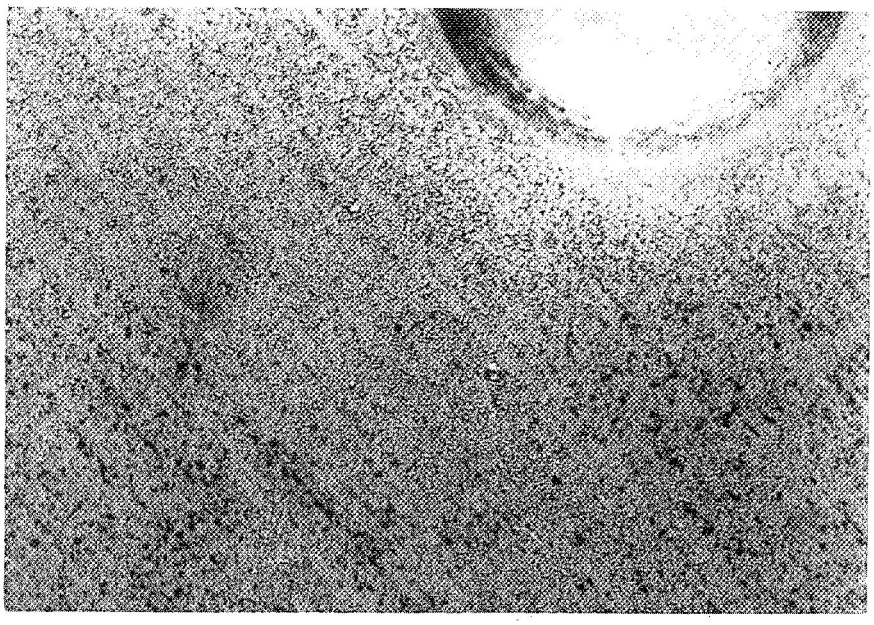

7X C-2964

FIGURE 19. SPECIMEN B-70 WITH 0.5-MIL STAINLESS STEEL CLADDING

Dark areas shown are portions of the cladding that have been shattered.

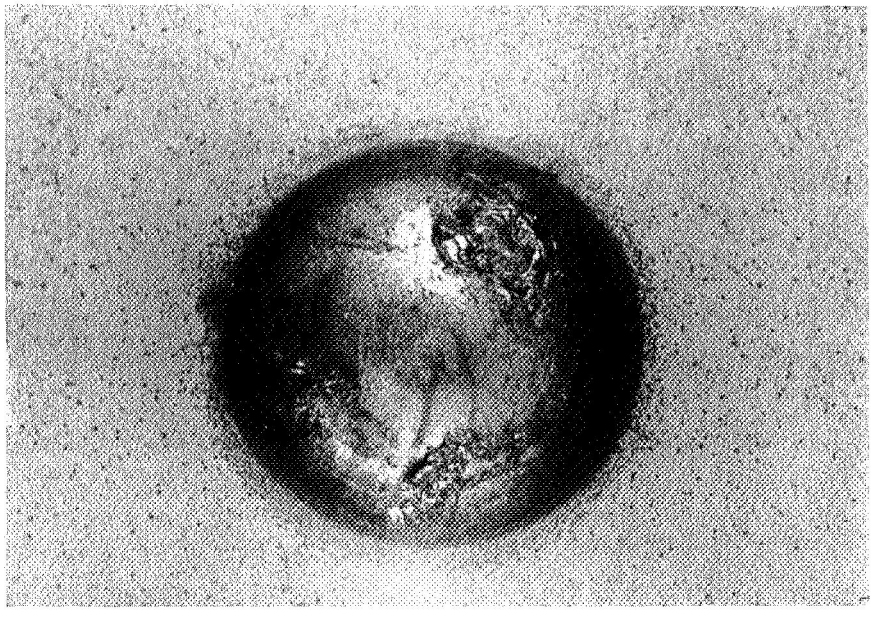

8X C-2965

FIGURE 20. BURNED AREAS RESULTING FROM SECOND IMPACT OF SPECIMEN B-73

Stainless steel cladding was 0.5 mil thick.

Thin Coatings. No reaction was observed upon ball impact of the following clad specimens.

1 - 0.4 mil thick

4 - 0.3 mil thick

2 - 0.15 mil thick

7 - 0.1 mil thick.

A flash was noted for 1 of 16 specimens with 0.2-mil-thick claddings when impacted with the ball striker. However, no reacted area could be found on either the specimen or the striker.

No reaction was observed on two specimens with a stainless steel coating less than 0.1 mil thick. The thickness of these coatings could not be determined by micrometer measurements, but some stainless steel was present as evidenced by the absence of staining in the cleaning solution. These results suggest that even very thin, ductile coatings of stainless steel afford protection against the reaction of titanium with LOX during impact.

Impact of Defected Sheet

It would be anticipated that reactivity would be experienced under conditions where defects in the stainless steel cladding allowed LOX to touch the titanium at the time of impact. In order to obtain a better understanding of the importance of such conditions, a study was made with clad sheet which had been defected in a known and controlled manner. This was done by drilling holes ranging from 4 to 35 mils in diameter through the cladding and several mils deep into the titanium base. Mechanical drilling was chosen over EDM or laser machining because drilling offered the least opportunity for substrate oxidation and/or contamination. Either of these could render the LOX test invalid. The effect of cladding thickness was explored as was the effect of striker configuration, i.e., ball versus flat.

Defect 35 Mils in Diameter. Twenty specimens clad with 8 mils of stainless steel were defected by drilling a hole 35 mils in diameter through the cladding to a total depth of about 12 mils. Thus titanium substrate was exposed to LOX during impact. The ball-tipped striker was placed over the hole before the sample cup was filled with LOX. Four specimens out of the series of 20 reacted with the LOX; two exhibited a flash. No sustained burning occurred in any instance. The reactivity was detected by examination of the specimen. A reacted piece always showed a blue discoloration in the

hole, as well as evidence of melting around the hole. A typical piece which reacted is shown in Figure 21. Note the area where molten metal had splattered around the hole. The severe deformation of the sheet that results from the ball-tipped striker is also illustrated in this photograph.

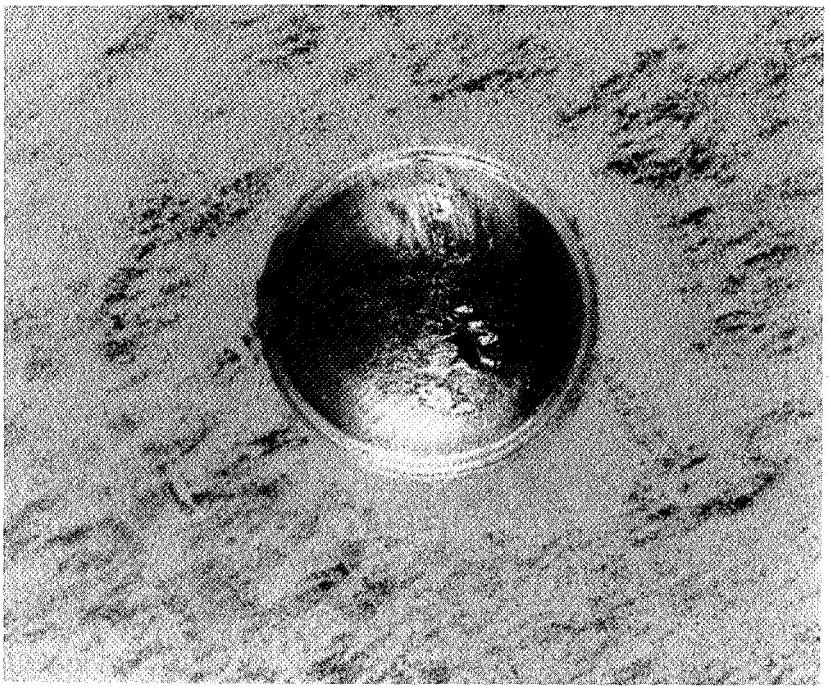

8X C2966

FIGURE 21. BURNED AREA IN IMPACT ZONE OF DEFECTED SPECIMEN BD-5

Specimen was defected by drilling a 35-mil hole through the 0.008-inch stainless cladding. A flash of light was observed during impact.

Defect 16 Mils in Diameter. Five specimens clad with 1 mil of stainless steel and defected with a 16-mil hole were impacted with a flat striker. Four of these showed reacted areas, and of these, three flashed during impact. The fifth specimen exhibited dark mottled areas around the impact crater. The cause may have been reactivity but it is possible that small flecks of the somewhat brittle coating were ejected from the surface.

Five additional similar specimens were impacted with the ball striker. One of these flashed upon impact and showed a reacted area when viewed under a microscope. The adhesion of the cladding of these specimens was poor.

Defect 8 Mils in Diameter. Five specimens clad with 1 mil of stainless steel and defected with an 8-mil hole showed no reaction when impacted with a flat striker. Two of these five specimens showed a reaction (no flash) around the defect when subjected to a second impact with the ball striker. Six additional specimens of this type were impacted with the ball striker. One of the six flashed during impact, but no fused or burned area was revealed by microscopic examination of the impacted area. Some mechanical chipping of the coating was seen around the crater on some of these pieces.

Two specimens clad with 3 mils of stainless steel and defected with an 8-mil hole showed no reaction when impacted with a flat striker. One of these showed no reaction when impacted further with a ball striker. The second piece was struck again with the flat striker and a reaction spot was observed at the hole area. Five additional specimens of this type were impacted with a ball striker. One contained an area where a reaction had occurred.

Defect 4 Mils in Diameter. Nine specimens clad with 1 mil of stainless steel and defected with a hole 4 mils in diameter and 4 mils deep showed no reaction when impacted with the ball impactor. Likewise, one additional specimen impacted with the flat impactor showed no reaction.

Pierced Sheet

It would be expected that reactivity could be experienced if a LOX vessel constructed from clad titanium were pierced from the outer surface. The performance of clad sheet under such conditions was studied in the present program.

A series of experiments was conducted in which the cup holding the LOX was pierced from the bottom side using the apparatus diagrammed previously in Figure 15. A flash of light was observed in 3 cases out of 20 when the specimen, which formed the bottom of the cup, was pierced from the titanium side (LOX touching the stainless steel). Eight of the 17 specimens which did not flash showed oxidized (discolored) areas in the vicinity of the titanium rupture when viewed under a microscope. In two instances areas which had become molten were observed. Hence, 11 out of the 20 specimens reacted in this type of evaluation. The appearance of a typical reacted specimen from the stainless steel side is illustrated in Figure 22. The ragged surface at the pierced hole is clearly evident.

8X C2967

FIGURE 22. APPEARANCE OF SPECIMEN P-6 AFTER PUNCTURE-IMPACT EXPERIMENT

The 0.008-inch stainless steel cladding surface is shown. Some discoloration and melting of thin section of titanium could be seen after impact. A flash was observed during rupture.

Discussion of Results and Conclusions

A summary of the LOX-compatibility results obtained from as-fabricated and intentionally defected sheet was presented in Table 8. It is apparent from these data that even very thin coatings of stainless steel provide effective protection again reaction, provided that the coating is ductile and well bonded to the titanium substrate. Under those circumstances, the titanium-alloy substrate is not exposed to LOX and no reaction is possible. In the as-fabricated condition, only two samples out of 96 showed any evidence of reaction after a single impact. The coating quality of those specimens which reacted was below normal and was indicative of the fact that chipping or fracture of the stainless steel coating could be expected to permit reaction. A third instance of reaction occurred in this test group; however, in this case a second impact was

required to cause reaction. The probability of reaction is greatly enhanced under such conditions if coating ductility is low and/or adherence less than perfect because small pieces of cladding metal can be loosened from the surface during the initial impact with an attendant loss of coating integrity. During a subsequent impact, the loosened particles aid in initiating the reaction.

The test series employing intentionally defected sheet specimens showed that a borderline condition between reaction and no reaction existed when a defect about 8 mils in diameter is present. No reactions were noted when a 4-mil-diameter defect is present. For the 8-mil-defect group of 25 specimens, a variety of results were obtained. For example, a flash of light was noted with Specimen 15-4-2 and a fused area was noted on Specimen 16-2-1 after the initial impact. Two specimens exhibited a fused area after the second impact. Poor adhesion was noted in many of the samples in this series. Hence, it would appear that adhesion, per se, was of less importance to reaction probability than a visible break in the coating. With the defect size increased to 16 mils, five out of the ten specimens exhibited fused areas after the first impact, four with the flat striker and one with the ball indenter. It should be noted that the cladding-to-substrate bond was broken on all specimens in this group when impacted with the ball-tipped striker. Four of the 20 specimens defected with a 35-mil hole showed a burned area after impact with the ball indenter. The cladding in this case was 8 mils thick, whereas those just discussed were coated with 1 mil of stainless steel. More extensive studies would be required to define completely the combined effects of hole size and thickness on reactivity.

The following conclusions may be drawn from the work performed in this segment of the program:

(1) The presence of a stainless steel coating of any finite thickness which is physically intact at the conclusion of impact would appear to preclude the possibility of LOX-titanium reaction.

(2) There is a high probability of reaction if an impact is sustained when LOX is in contact with the titanium substrate through a defect in the cladding, especially at defect sizes of 8 mils and greater.

(3) Reaction probability is extremely high when the composite is pierced. Over 50 percent of those samples evaluated revealed some evidence of reaction as a result of puncture.

(4) Striker shape, ball tipped or flat, did not appear to be a critical factor in the results of the evaluation of defected sheet. Both shapes were shown to be capable of producing reaction. The effect of striker geometry could not be adequately gaged in the case of as-fabricated sheet. Intuitively, the ball-tipped striker appeared the more potent threat through the action of secondary effects such as coating separation and chipping.

(5) There were no indications of a continuing or sustained burning with any specimen evaluated in this program. This, however, should not be interpreted to mean that sustained reactions could not be experienced in pressurized systems. In fact, previous experience with LOX-titanium phenomena indicates a high probability of sustained reaction in pressurized systems once the reaction has been initiated.

MECHANICAL PROPERTIES

Fatigue Properties

(D. E. Pettit and H. Mindlin)

Material

Five different stainless steel/0.050-inch Ti-5Al-2.5Sn (ELI) composite-material conditions were evaluated in this phase of the investigation. These conditions and the corresponding letter designation used to identify the specimens are presented below:

Letter Designation	Material Conditions
O	Bare 0.050-inch Ti-5Al-2.5Sn (ELI) alloy sheet
A, B	Explosively welded 0.008-inch Type 304 stainless steel/0.050-inch Ti-5Al-2.5Sn (ELI) alloy (Plates A and B from different runs)
C	Vacuum-deposited 0.001-inch stainless steel/0.050-inch Ti-5Al-2.5Sn (ELI) alloy, heat treated at 1300 F for 2 hr after deposition
D15, D17	Vacuum deposited 0.001-inch stainless steel/0.050-inch Ti-5Al-2.5Sn (ELI) alloy, not heat treated after deposition
D16	Vacuum deposited 0.003-inch stainless steel/0.050-inch Ti-5Al-2.5Sn (ELI) alloy, not heat treated after deposition.

Initially, an explosively welded 0.020-inch stainless steel/0.50-inch Ti-5Al-2.5Sn composite material was also to be evaluated. However, during the preliminary machining operations, it was observed that large sections of the stainless steel cladding peeled off, which indicated that a good bond had not been achieved. In view of the obvious bonding problem, these tests were discontinued by mutual agreement between Battelle Memorial Institute and NASA Lewis personnel.

Experimental Procedures

Specimen Preparation. All sheet-material specimens were machined from the as-received composite (or bare) sheet material to the fatigue-specimen configuration shown in Figure 23. The specimens were oriented parallel to the rolling direction of the 0.050-inch Ti-5Al-2.5Sn (ELI) alloy substrate. Prior to testing, the machined edges of the specimens were polished parallel to the longitudinal axis of the specimen with 600-grit SiC paper to remove any machining marks and assure a smooth unnotched surface. Surface-roughness measurements (rms values) were made on the as-received stainless-clad surface of each specimen prior to testing.

Test Procedures. All room-temperature tests were conducted in a standard 5-kip-capacity Krouse axial-load fatigue machine operating at a frequency of 1725 cycles per minute. Similarly, the cryogenic fatigue tests were conducted in a modified 5-kip-capacity Krouse axial-load fatigue machine shown in Figure 24 that was equipped with a cryogenic dewar and operated at a frequency of 1725 cycles per minute. The liquid-nitrogen level in the dewar was maintained constant by use of an automatic level probe that operated a solenoid valve on the liquid-nitrogen tank. Each specimen tested in liquid nitrogen was allowed to equilibrate under zero load for 1 hour in liquid nitrogen prior to testing. All specimens were cycled at a stress ratio R = 0.2 until failure (complete fracture) occurred or 10^7 cycles had been applied.

Fatigue Results

Bare 0.050-inch Ti-5Al-2.5Sn (ELI) Sheet Results. The initial fatigue tests were conducted at room temperature and in liquid-nitrogen (-320 F) for the bare 0.050-inch Ti-5Al-2.5Sn (ELI) substrate sheet material. These results, presented in Table 9, provided base-line data for comparison with the various composite conditions.

Explosively Bonded Stainless Steel/Ti-5Al-2.5Sn (ELI) Composite. The first series of composite material evaluated was the explosively welded 0.008-inch Type 304 stainless steel/0.050-inch Ti-5Al-2.5Sn (ELI) material. The fatigue results at room temperature and -320 F are presented in Table 10 for specimens from two separate bonding runs, Plates A and B. As shown in Table 10, the fatigue stress was computed on two bases. First, it was computed using the total cross-section area. Second, a stress

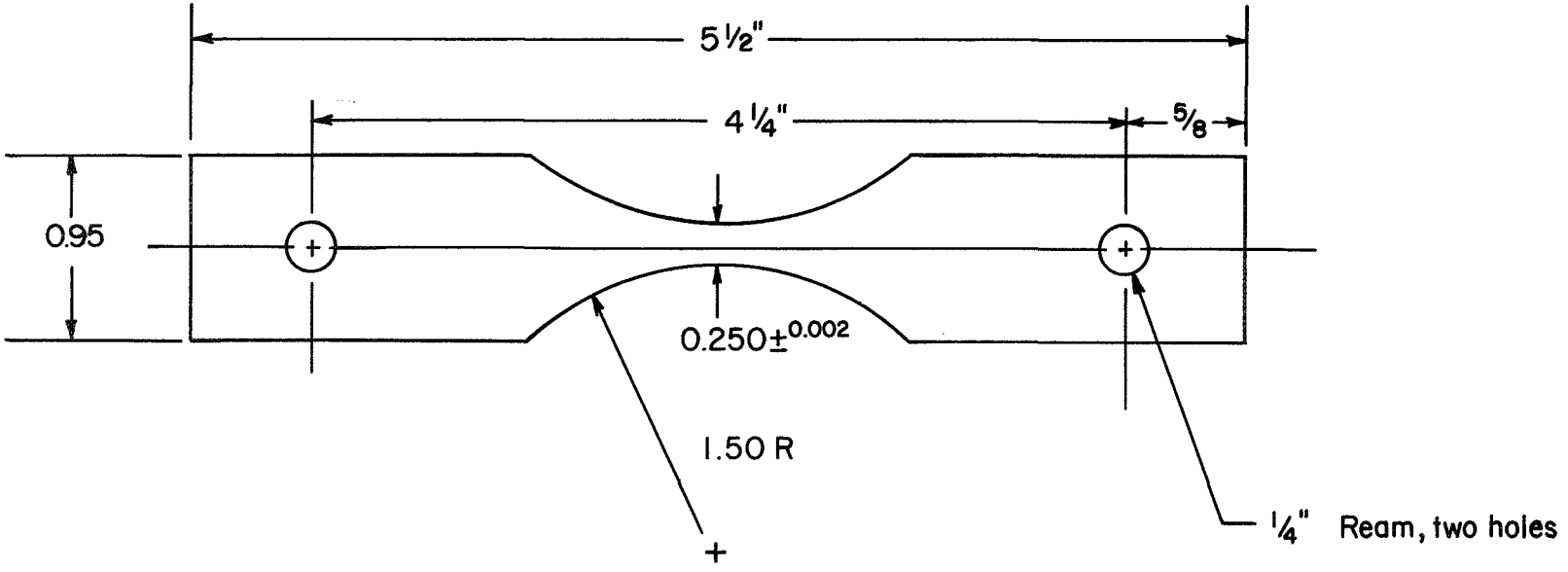

FIGURE 23. SHEET-MATERIAL FATIGUE-SPECIMEN CONFIGURATION

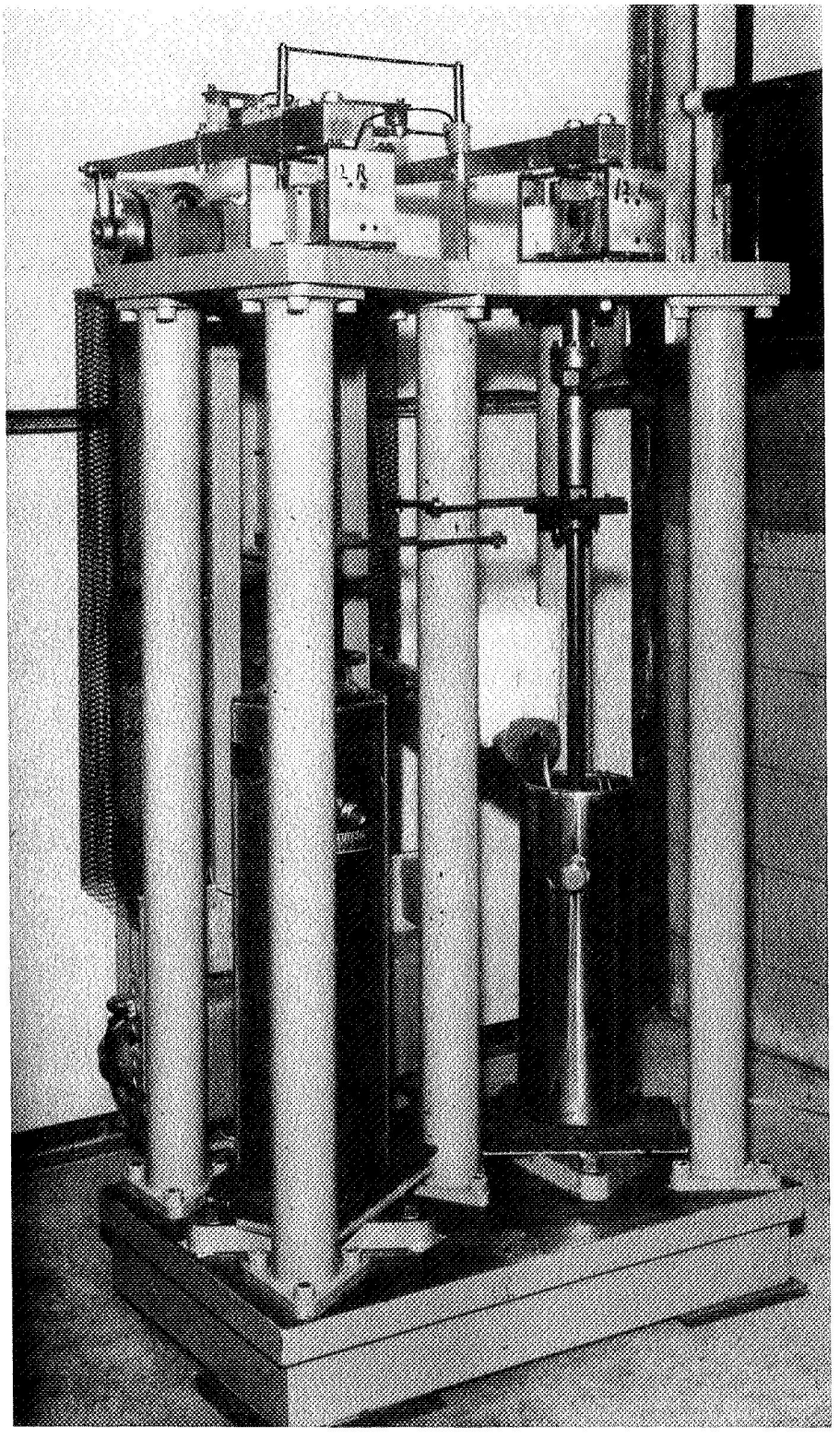

FIGURE 24. AXIAL-LOAD FATIGUE SETUP FOR TESTS AT LIQUID-NITROGEN TEMPERATURE

TABLE 9. FATIGUE RESULTS FOR BARE 0.050-INCH Ti-5Al-2.5Sn (ELI) SHEET MATERIAL AT ROOM AND CRYOGENIC TEMPERATURE, R = 0.2

Specimen	Surface Roughness, rms	Temperature, F	Maximum Stress (σ_{max}), ksi	Number of Cycles to Failure	Comments
0-1	30-32	75	85	9,551,600	--
0-2	30-32	75	100	133,000	--
0-3	30-32	75	95	1,237,000	--
0-4	30-32	75	90	977,700	--
0-5	30-32	75	105	87,600	--
0-6	30-32	-320	160	59,800	--
0-7	30-32	-320	140	371,400	--
0-8	30-32	-320	150	100,200	--
0-9	30-32	-320	130	1,594,000	Grip failure
0-10	30-32	-320	125	212,000	

TABLE 10. FATIGUE RESULTS FOR EXPLOSIVELY WELDED 0.008-INCH TYPE 304 STAINLESS STEEL/0.050-INCH Ti-5Al-2.5Sn (ELI) COMPOSITE MATERIAL AT ROOM AND CRYOGENIC TEMPERATURE, R = 0.2

Specimen	Surface Roughness, rms	Temperature, F	Maximum Stress, ksi (a)	Maximum Stress, ksi (b)	Number of Cycles to Failure	Comments
A-1	45-50	75	90	104	43,400	--
A-2	40-45	75	80	93	73,200	--
B-1	48-52	75	70	81	166,300	--
B-2	45-50	75	60	69.5	11,479,000	Did not fail
A-3	40-45	75	65	75.5	81,200	Very poor bond
B-3	45-50	-320	130	151	40,200	--
A-4	45-50	-320	110	128	41,000	--
B-4	45-48	-320	100	116	64,000	--
A-5	45-50	-320	80	93	130,000	--
B-5	45-50	-320	60	69.5	2,029,000	--

(a) Based on total specimen thickness.

(b) Based on nominal 0.050-inch titanium-substrate thickness only.

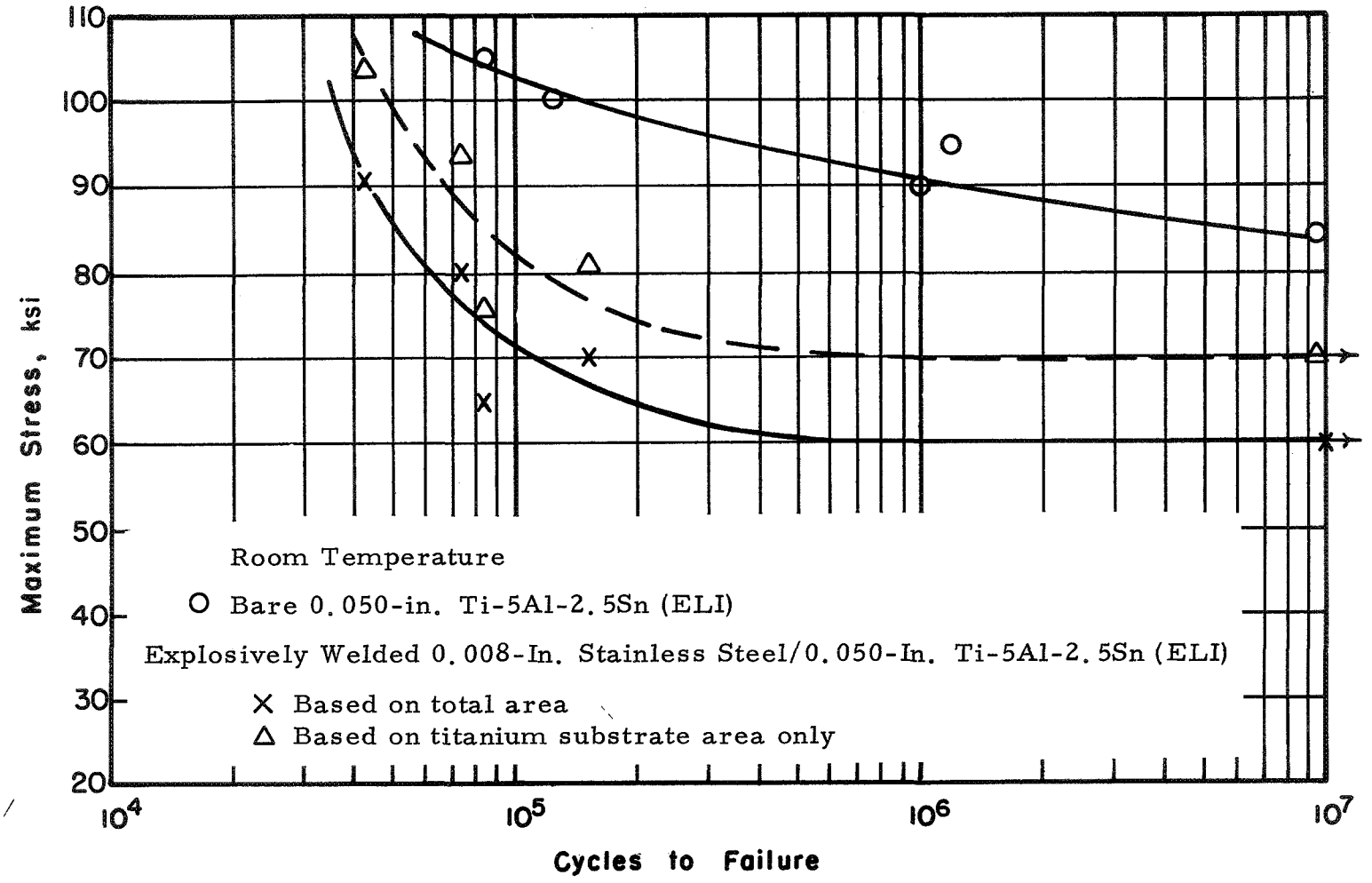

FIGURE 25. ROOM-TEMPERATURE AXIAL-LOAD FATIGUE RESULTS FOR BARE 0.050-INCH Ti-5Al-2.5Sn (ELI) AND EXPLOSIVELY WELDED 0.008-INCH STAINLESS STEEL/0.050-INCH Ti-5Al-2.5Sn (ELI), R = 0.2

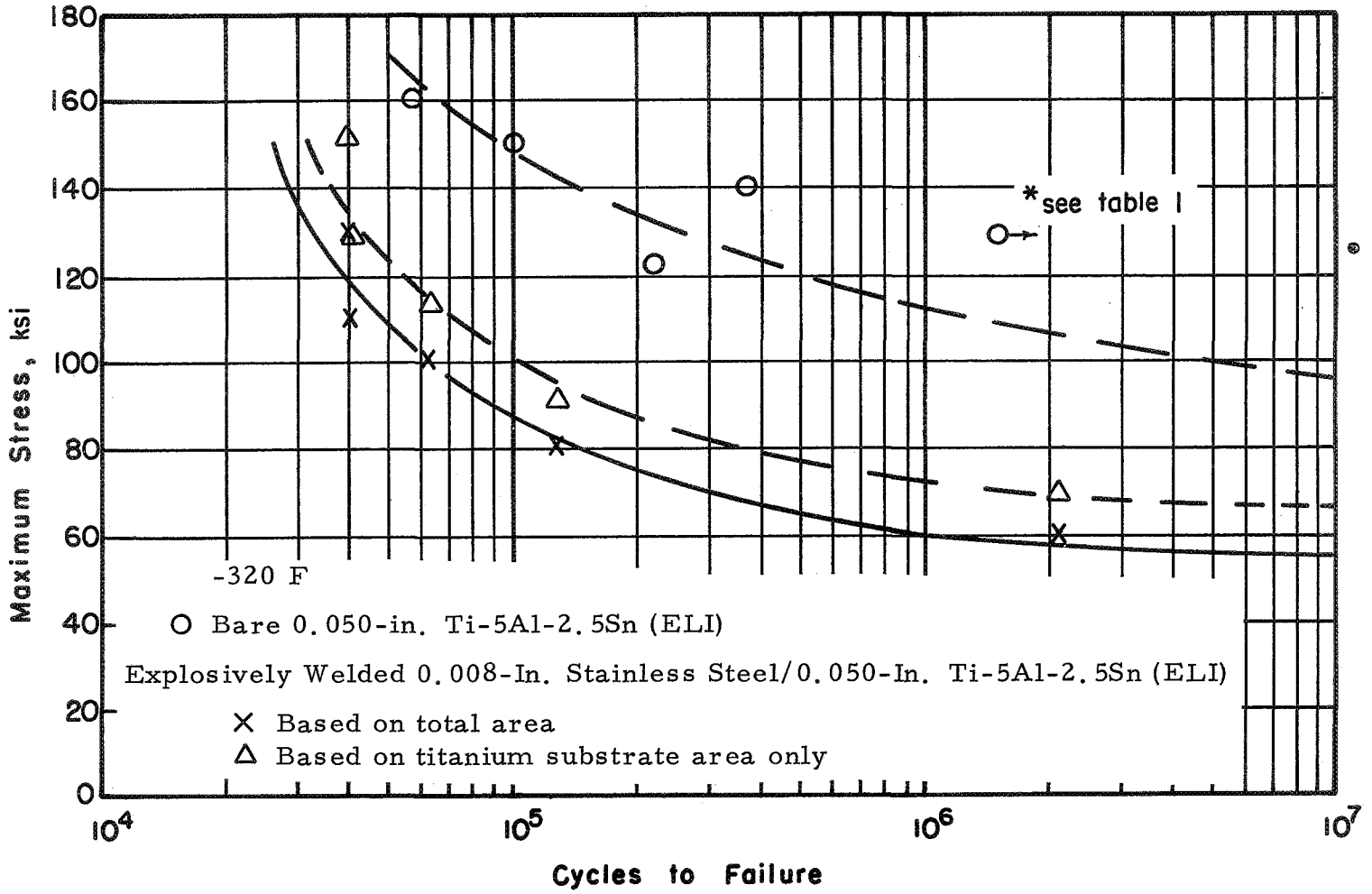

FIGURE 26. LIQUID-NITROGEN AXIAL-FATIGUE RESULTS FOR BARE 0.050-INCH Ti-5Al-2.5Sn (ELI) AND EXPLOSIVELY WELDED 0.008-INCH STAINLESS STEEL/0.050-INCH Ti-5Al-2.5Sn (ELI), R = 0.2

was computed on the basis of the nominal 0.050-inch titanium-substrate thickness, that is, it was computed on the assumption that the stainless steel would not carry a significant amount of the load. However, the room-temperature fatigue results (Figure 25) and the -320 F fatigue results (Figure 26) show that regardless of the basis of stress calculation, the explosively bonded material has a fatigue strength much lower than that of the bare titanium substrate at both room and cryogenic temperature.

In order to determine the factors that affected the fatigue properties of the titanium substrate after bonding, a posttest fractographic analysis of each of the failed specimens was conducted using a 7-30X stereomicroscope. During this analysis, it was observed that the failure initiated at the stainless steel/Ti-5Al-2.5Sn (ELI) interface for all of the explosively welded specimens. In Figure 27, typical initiation regions can be identified as the center of the "ridges" (at the bond interface) that characteristically are observed radiating away from the point of origin of a fatigue crack.

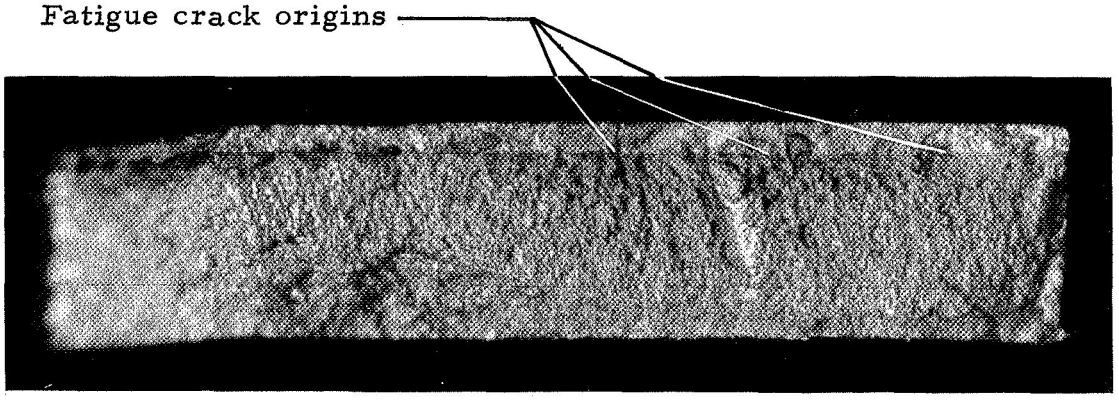

FIGURE 27. TYPICAL EXPLOSIVELY WELDED 0.008-INCH STAINLESS STEEL/0.050-INCH Ti-5Al-2.5Sn (ELI) SPECIMEN FAILED BY FATIGUE

During the fractographic examination, it was also noted that the bond quality of Specimen A-3, cut from the center portion of Sheet A, was very poor, as shown in Figure 28. This indicates that the bonding was not 100 percent effective across the sheet, and probably accounts for the very low fatigue strength observed for this specimen.

Subsequent to the fractographic analysis, a metallographic section was made of one-half of Specimen A-2 and the bond interface was then examined. The microstructure, shown in Figure 29, reveals a layer of extensively cracked intermetallic-compound material at the bond interface. The cracks

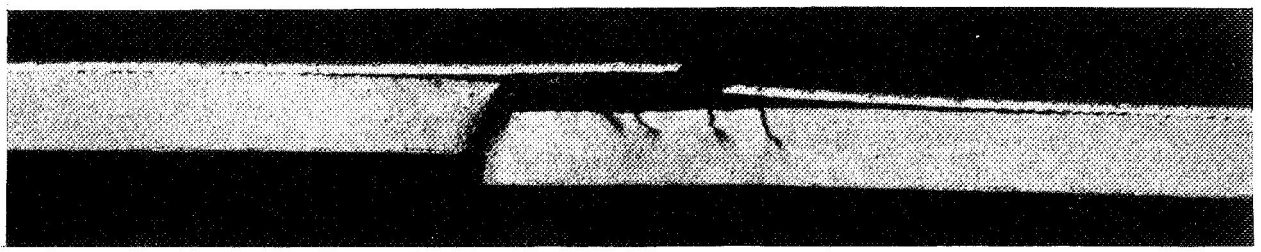

20X 7D728

FIGURE 28. EXPLOSIVELY WELDED SPECIMEN 1A-3 SHOWING EXTENSIVE SEPARATION OF BOND AND MULTIPLE CRACKING

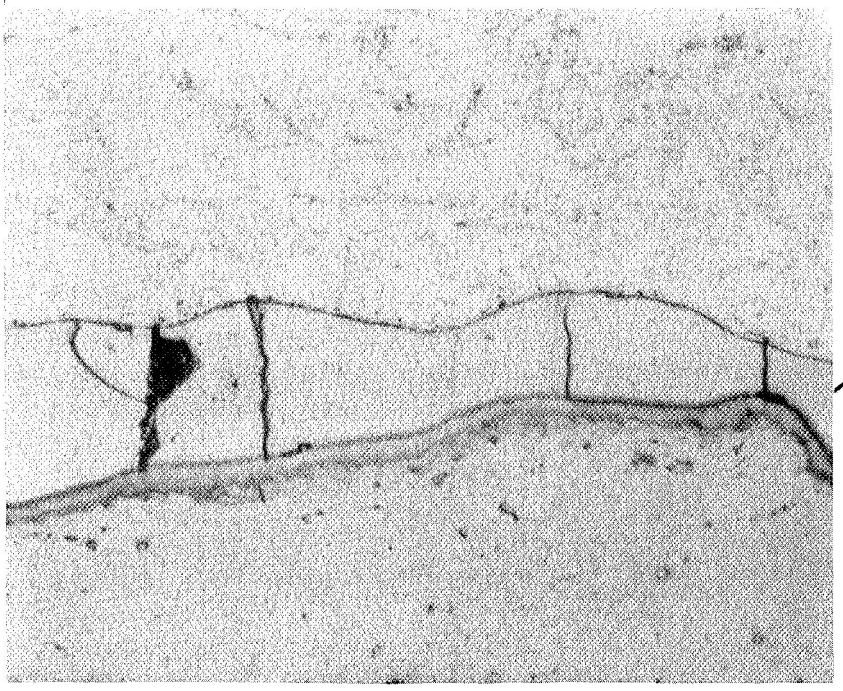

1000X 3E011

FIGURE 29. MICROSTRUCTURE OF EXPLOSIVELY WELDED STAINLESS STEEL/Ti-5Al-2.5Sn INTERFACE

formed in this apparently brittle layer probably provided the initiation sites for the fatigue failure. Thus, the poor fatigue strength of the explosively welded composite is believed to have resulted from the premature formation and subsequent fatigue propagation of cracks in a layer of intermetallic compound at the bond interface.

Vacuum-Deposited Stainless Steel/Titanium Composite. The third series of specimens was prepared from vacuum deposited 0.001-inch stainless steel/0.050-inch Ti-5Al-2.5Sn (ELI) sheet material that receive a postcladding heat treatment of 1300 F for 2 hr in vacuum. The fatigue results for this material at room temperature and at -320 F are presented in Table 11 and shown in Figures 30 and 31, respectively. In addition, the results of four tests at -320 F that were conducted at a stress ratio R = 0.1 are presented in Table 12 for reference only.

As shown in Figures 30 and 31, the fatigue properties of this composite were again much poorer than those of the unclad titanium substrate. If Figures 25 and 30 for the room temperature data and Figures 26 and 31 for the data at -320 F are compared, it is seen that the results of the 8-mil explosively welded and the 1-mil vacuum-deposited stainless steel composites are comparable when the stresses are based on the total specimen area. On the basis of substrate area only, the explosively welded material appears to have slightly better fatigue properties, the stresses for the 1-mil clad material being only about 2 percent higher than the stresses based on the total area. A determination of the typical scatter band for the two conditions, however, would be required before the apparent difference in fatigue behavior can be confirmed.

A fractographic examination of the failed specimens again showed fatigue-crack initiation to have occurred at the bond interface. No evidence of delamination was noted. A subsequent metallographic section of Specimen C-12 revealed the presence of intermetallic compounds at the bond interface, as shown in Figure 32. These brittle intermetallic compounds are believed to have served as the fatigue-crack initiation sites, resulting in the observed poor fatigue behavior of this composite.

Vacuum Deposited Stainless Steel/Titanium Alloy Composite With No Postcladding Heat Treatment. Since the intermetallic compounds observed at the bond interface in the previous group of vacuum-deposited stainless steel/titanium composite specimens were believed to have formed by interdiffusion during the postcladding heat treatment, three lots of vacuum-deposition composite samples that were not heat treated after cladding were evaluated at room temperature. The objective of this effort was to determine

TABLE 11. FATIGUE RESULTS AT ROOM TEMPERATURE AND AT -320 F FOR VACUUM-DEPOSITED 0.001-INCH STAINLESS STEEL/0.050-INCH Ti-5Al-2.5Sn COMPOSITE, R = 0.2

Specimen	Average Surface Roughness, rms	Cladding Thickness, mils	Maximum Stress, ksi (a)	Maximum Stress, ksi (b)	Number of Cycles to Failure	Comments
			Results at Room Temperature			
C-9	32	1	80	82	56,600	Failed
C-11	32	1.5	75	77	95,600	Failed
C-12	40	1.5	70	72	288,200	Failed
C-10	20	1	65	66	10,000,000	Did not fail
			Results at -320 F			
C-7	30	1	110	112	75,000	Failed
C-6	28	1	80	82	219,800	Failed
C-5	30	1.3	50	51	1,778,400	Failed outside minimum test section
C-8	32	1	45	46	11,000,000	Did not fail

(a) Based on total specimen thickness.
(b) Based on substrate thickness.

TABLE 12. FATIGUE RESULTS AT -320 F FOR VACUUM-DEPOSITED 0.001-INCH STAINLESS STEEL/0.050-INCH Ti-5Al-2.5Sn (ELI) COMPOSITE, R = 0.1

Specimen	Average Surface Roughness, rms	Cladding Thickness, mils	Maximum Stress, ksi (a)	Maximum Stress, ksi (b)	Number of Cycles to Failure	Comments
C-1	32	1	140	143	18,300	Failed
C-2	32	1	110	112	35,000	Failed
C-3	35	1	80	82	89,700	Failed
C-4	32	1	60	61	185,400	Failed

(a) Based on total specimen thickness.
(b) Based on substrate thickness.

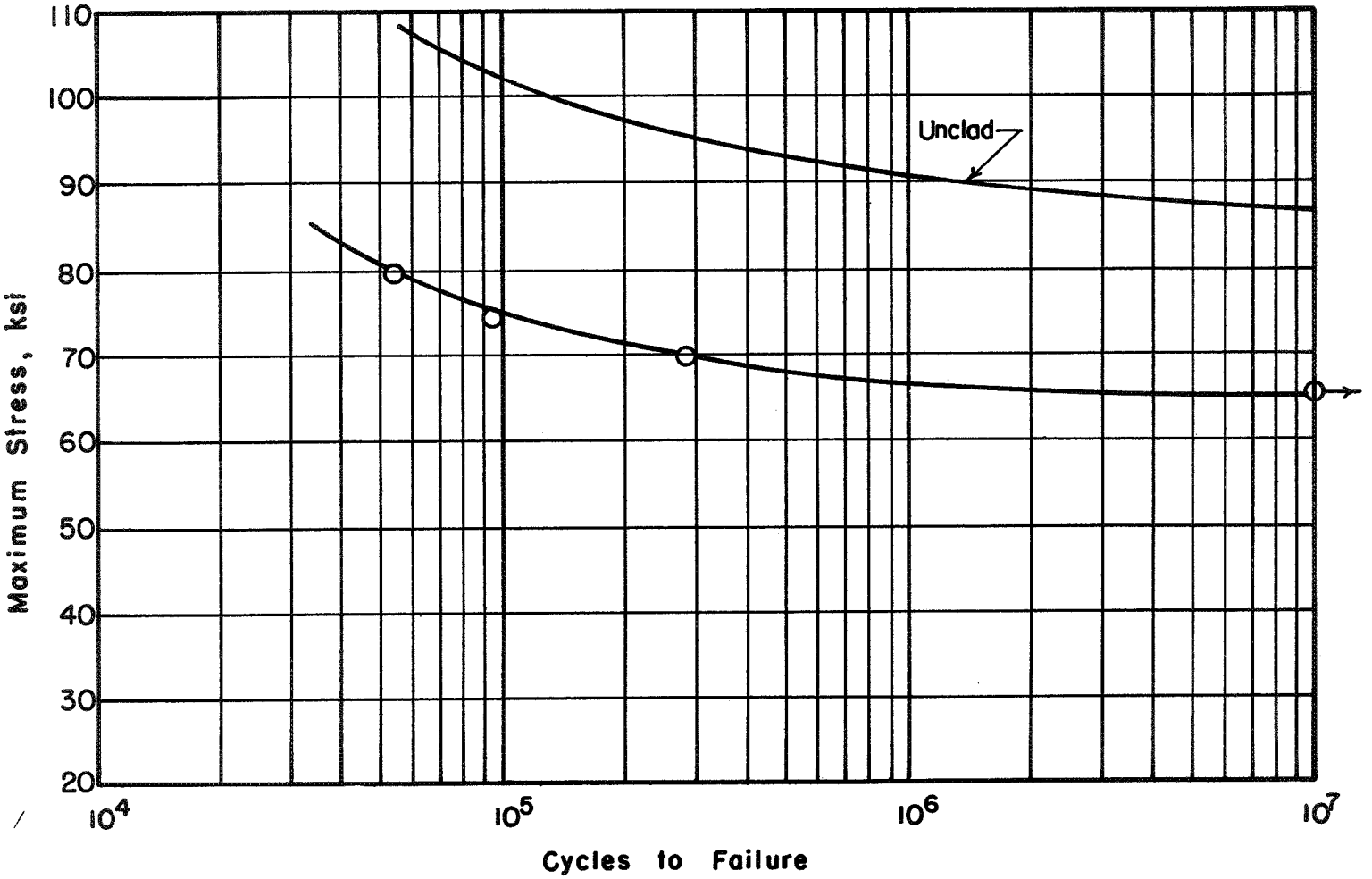

FIGURE 30. ROOM-TEMPERATURE AXIAL-LOAD FATIGUE RESULTS FOR VACUUM-DEPOSITED 0.001-INCH STAINLESS STEEL/ 0.050-INCH Ti-5Al-2.5Sn (ELI) ALLOY, R = 0.2

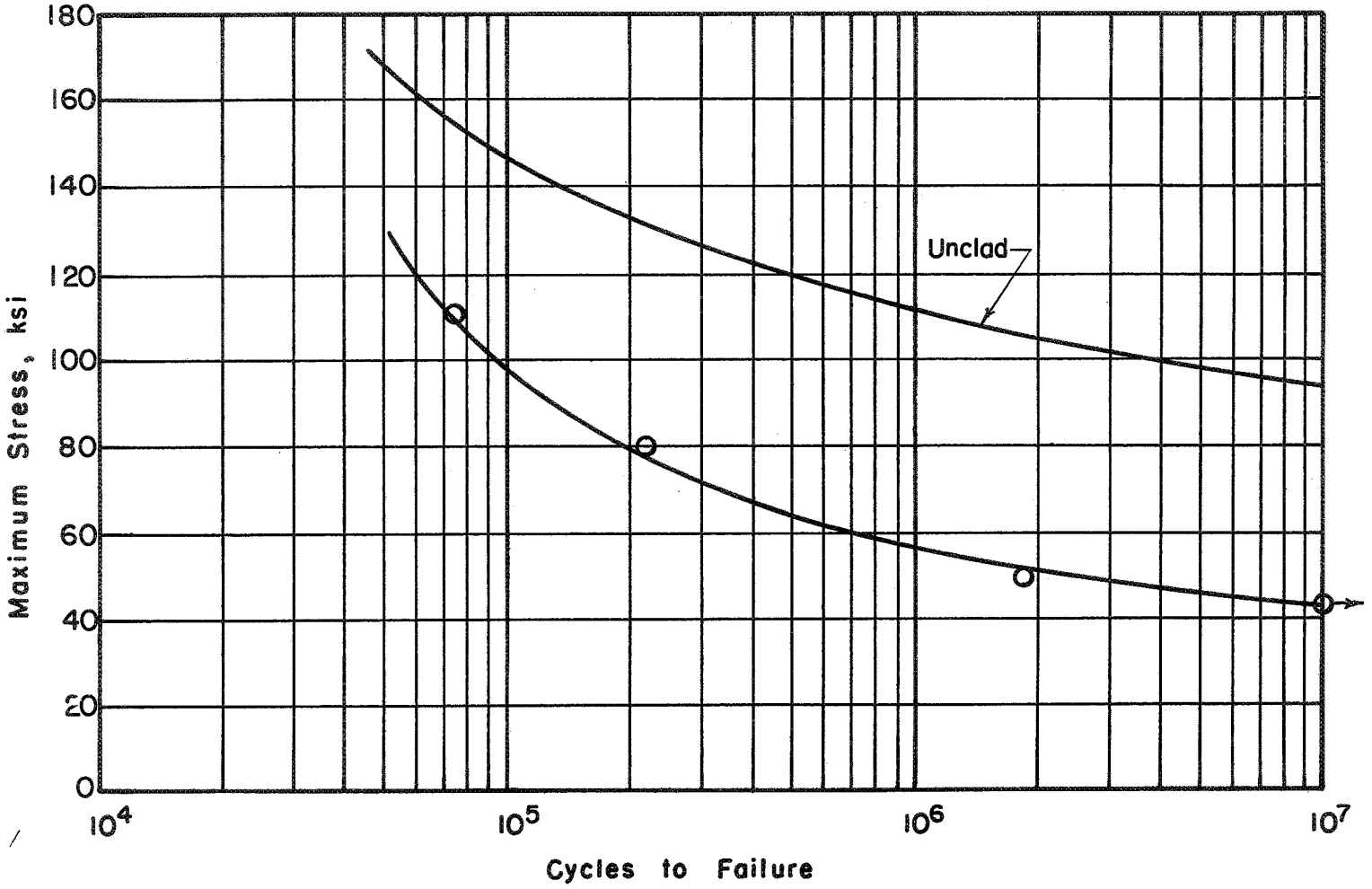

FIGURE 31. AXIAL-LOAD FATIGUE RESULTS FOR VACUUM DEPOSITED 0.001-INCH STAINLESS STEEL/0.050-INCH Ti-5Al-2.5Sn (ELI) ALLOY IN LIQUID NITROGEN, R = 0.2

whether the formation of these intermetallic compounds could be eliminated by omitting the postcladding heat treatment. Specimen Lot D16 had a 0.003-inch vacuum-deposited stainless cladding while Lots D15 and D17 represented two separate vacuum-deposition runs in which 0.001 inch of stainless was deposited on the titanium-alloy substrate. The results of the room-temperature fatigue tests for specimens from these three lots are presented in Table 13.

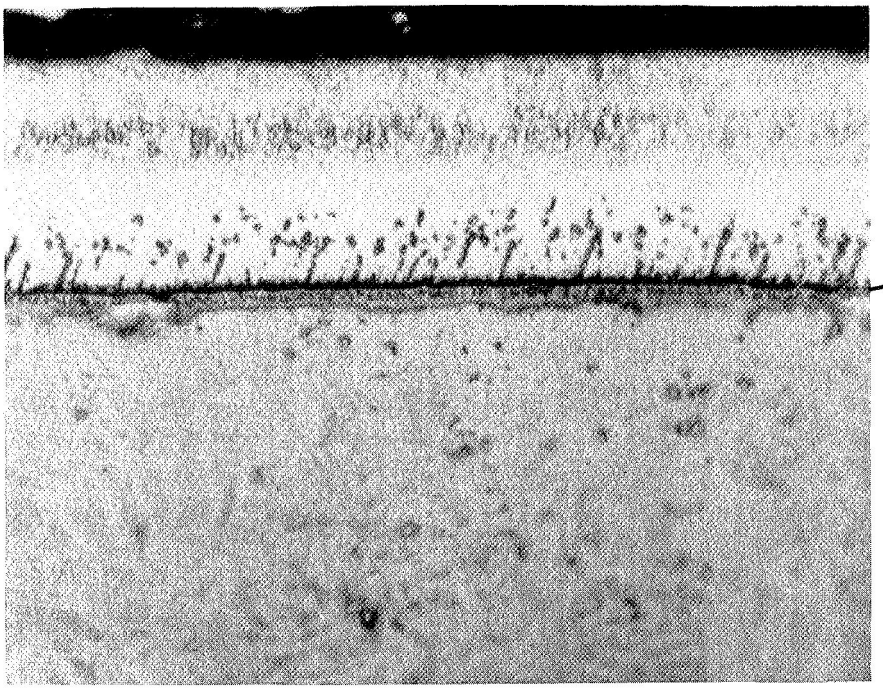

FIGURE 32. INTERFACE MICROSTRUCTURE OF VACUUM-DEPOSITED STAINLESS STEEL/Ti-5Al-2.5Sn ALLOY COMPOSITE

Specimen was heat treated in vacuum at 1300 F for 2 hours after deposition cycle.

A comparison of these results with the average curves for the unclad titanium-alloy substrate and the vacuum deposited, 0.001-inch stainless steel-clad specimens with a postcladding heat treatment is shown in Figure 33. As shown in Figure 33, elimination of the postcladding heat treatment unexpectedly resulted in a further degradation of fatigue properties, probably because of residual stresses left unrelieved by the lack of a postcladding heat treatment.

TABLE 13. ROOM-TEMPERATURE FATIGUE RESULTS FOR VACUUM-DEPOSITED STAINLESS STEEL/0.050-INCH Ti-5Al-2.5Sn (ELI) ALLOY WITH NO POSTCLADDING HEAT TREATMENT, R = 0.2

Specimen	Average Surface Roughness, rms	Cladding Thickness, inch	Maximum Stress, ksi (a)	Maximum Stress, ksi (b)	Number of Cycles to Failure	Comments
			Lot D16			
D16-3	6	0.003	70	74	36,300	Failed
D16-5	10	0.003	60	64	53,700	Failed
D16-6	8	0.003	50	53	117,800	Failed
D16-7	7	0.003	40	42	245,000	Failed
			Lot D17			
D17-4	8	0.001	80	82	30,600	Failed
D17-5	7	0.001	70	72	54,700	Failed
D17-6	9	0.001	60	61	105,200	Failed
D17-7	7	0.001	50	51	222,000	Failed
			Lot D15			
D15-5	11	0.001	60	61	<200,000	Machine did not shut off; had not failed at 150,000 cycles
D15-6	11	0.001	50	51	227,300	Failed
D15-7	--	0.001	--	--	--	Not tested - coating peeled off during machining
D15-8	12	0.001	40	41	463,800	Failed

(a) Based on total specimen thickness.
(b) Based on substrate thickness.

Figure 33 also tends to indicate a further decrease in fatigue behavior with increasing cladding thickness, at least in the as-coated condition. However, if the stresses are based on the titanium substrate only, the 3-mil-clad material stress levels would be raised 4 percent relative to the stresses of the 1-mil-clad material, thus reducing the apparent difference in fatigue behavior with cladding thickness. In addition, insufficient data are available to determine the normal scatter bands for the two thicknesses, so no conclusion regarding the effect of cladding thickness appears warranted.

Fractographic examinations of the specimens from Lots D15, D16, and D17 indicate that failure initiated at the bond interface as was previously observed. Only Specimen D15-7 showed any evidence of delamination of the cladding. Metallographic examination of Specimen D16-5 revealed that even

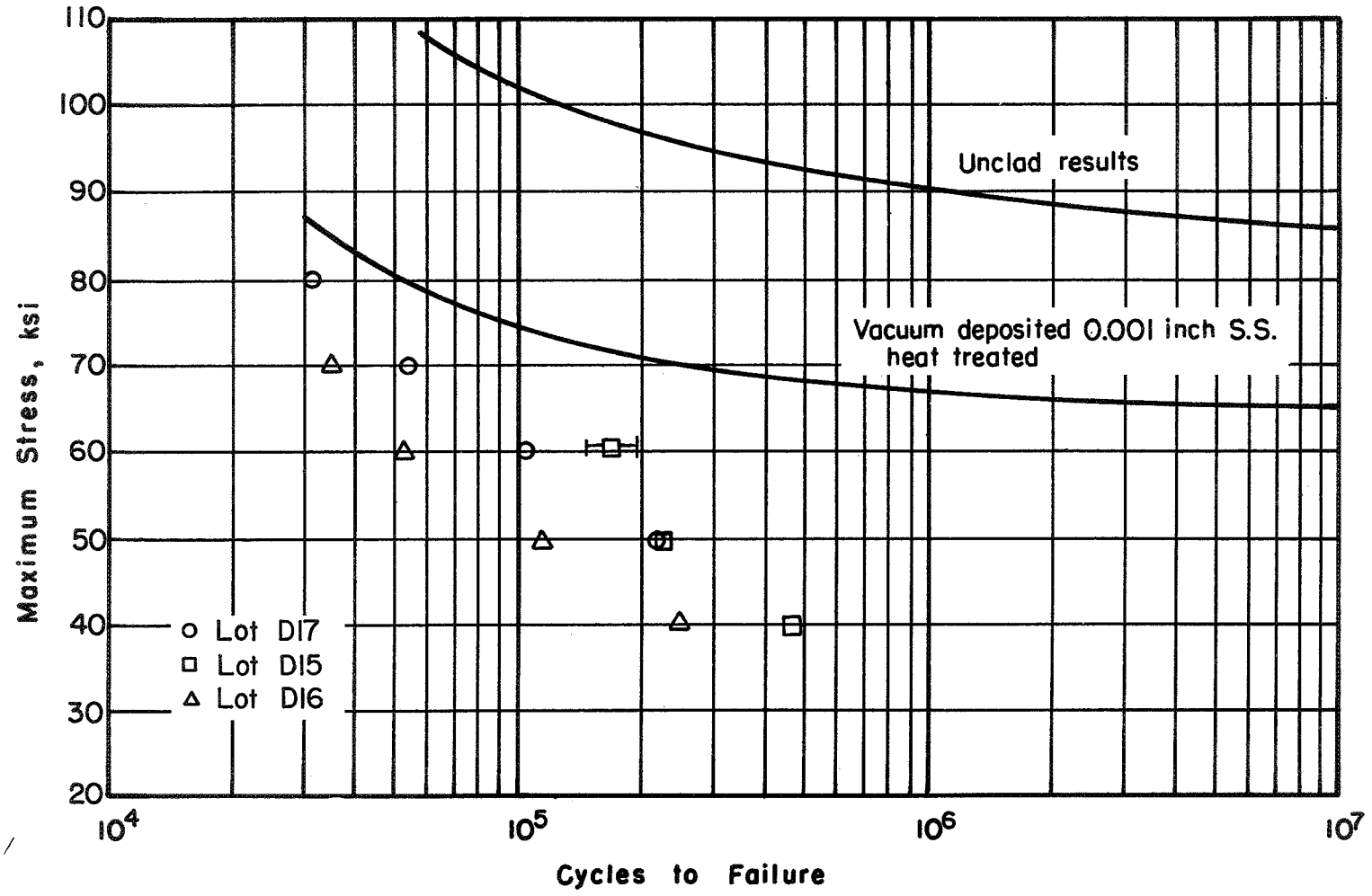

FIGURE 33. ROOM-TEMPERATURE FATIGUE BEHAVIOR OF VACUUM-DEPOSITED STAINLESS STEEL/0.050-INCH Ti-5Al-2.5Sn (ELI) ALLOY WITH NO POSTCLADDING HEAT TREATMENT, R = 0.2

though no postcladding heat treatment had been used, some intermetallic compounds had still formed. This is shown in Figure 34. Note also in Figure 34 the layers caused in the stainless cladding by interruptions of the coating cycle.

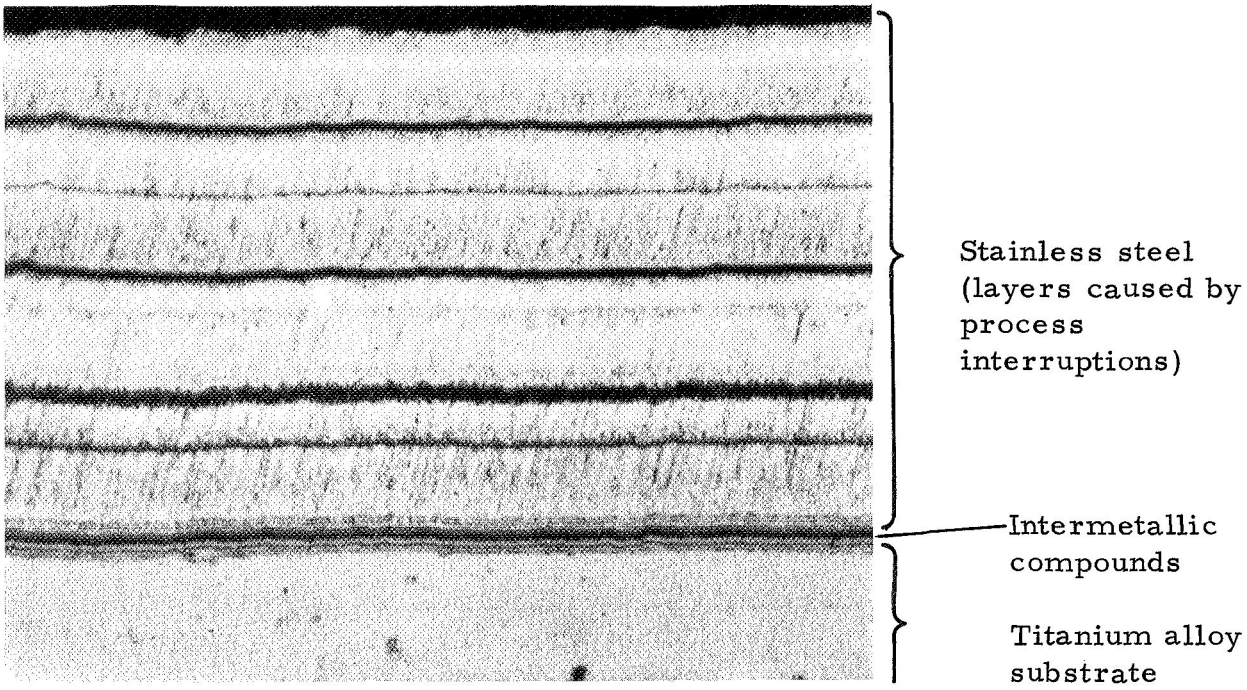

FIGURE 34. INTERFACE MICROSTRUCTURE OF VACUUM-DEPOSITED STAINLESS STEEL/Ti-5Al-2.5Sn ALLOY COMPOSITE WITH NO POSTCLADDING HEAT TREATMENT

Conclusions

On the basis of the results of this phase of the investigation, the following conclusions were drawn:

(1) The explosively welded stainless/titanium composite and the vacuum-deposited stainless/titanium composites with and without a postcladding heat treatment, exhibit a fatigue strength much lower than that of the unclad titanium substrate.

(2) The lower fatigue properties of the three composites studied are believed to have resulted from the premature formation of fatigue cracks in areas of brittle intermetallic compounds found at the bond interface.

(3) The elimination of the postcladding heat treatment of the vacuum-deposited stainless/titanium composite was not sufficient to eliminate the formation of intermetallic compounds at the bond interface.

Tensile and Fracture Toughness Properties

(J. S. Perrin and D. R. Ireland)

Experimental Procedures

Tensile Test Procedure. Conventional unaxial tensile tests were run on clad and unclad sheet specimens at ambient temperatures and -320 F. The geometry and size of the specimen are shown in Figure 35. The tests were performed in a 20,000-pound Instron tensile testing machine at a crosshead speed of 0.02 ipm. The cryogenic temperature was obtained by total immersion of the specimen in liquid nitrogen. Temperature was monitored by a thermocouple embedded in the upper grip fixture. Loading of the specimen was not started until the temperature had been maintained at -320 F for at least 20 minutes. Load and deflection were continuously recorded during testing. A standard Instron extensiometer was used for the deflections up to and slightly past yield, and during the remainder of the test, deflection was estimated from crosshead motion. Elongation values were based on a 1-inch gage length and determined by measuring the specimens before and after testing. The ultimate tensile strength was determined from the maximum load recorded during the test and the cross-sectional area of the specimen before testing. The load at 0.2 percent offset strain was determined from the load-deflection records; initial cross-sectional area of the specimen was used to calculate yield strength. For the clad specimen, the cross-sectional area employed in the strength calculations was that of the substrate and not the combined area of cladding and substrate.

Fracture-Toughness-Test Procedure. The compact-tension (CT) specimen shown in Figure 36 was used to evaluate the plane-strain fracture toughness (K_{Ic}) of clad and unclad plate. These specimens were fatigue precracked to a depth of approximately 0.06 inch below the initial slot with

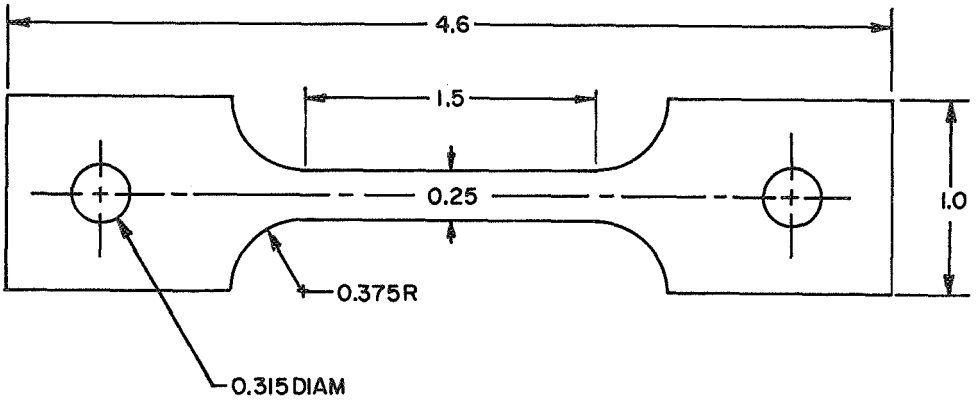

FIGURE 35. TENSILE-SPECIMEN CONFIGURATION

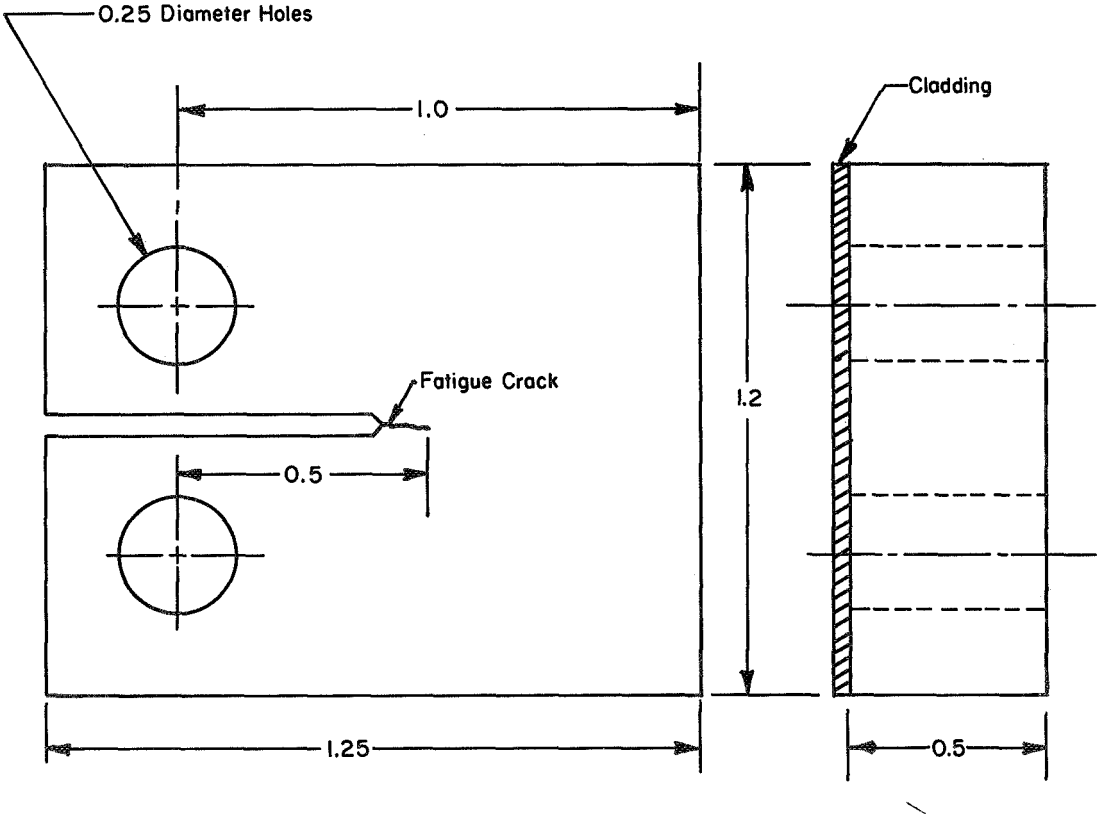

FIGURE 36. COMPACT-TENSION-SPECIMEN CONFIGURATION

a crack growth rate of approximately 0.001 inch per 1000 cycles. Load and displacement were recorded during the test. Displacement was measured by a double-cantilever-beam gage patterned after that recommended by ASTM Commiteee E-24 and described in STP410. This gage provided a satisfactory linear record of load-displacement up to fracture in the -320 F tests conducted. The cryogenic temperature was obtained and monitored by the same procedures as used in sheet tensile testing. The fracture load (P) was clearly evident by a sharp deviation from linearity. The K_{Ic} value was calculated from the following relationship

$$K_{Ic} = \frac{R\sqrt{a}}{Bw} 23.12 - 67.67 \left(\frac{a}{w}\right) + 97.31 \left(\frac{a}{w}\right)^2 ,$$

where a is crack length, w is specimen width, and B is specimen thickness. For the clad samples, B was assumed to be the Ti-SA1-2.5Sn substrate thickness.

The clad sheet material was evaluated by testing defected tensile specimens of the three designs shown in Figure 37. The SN (side notched) and SF (surface flawed) specimens are of the same general geometry and size as those used in uniaxial tensile testing. However, the SN specimen has a 0.008-inch-deep flaw across the cladding side, and the SF specimen has a semielliptical flaw, 0.008 inch deep and 0.006 inch long in the titanium substrate beneath the stainless steel cladding. The SEN (single edge notched) specimen has a through-thickness (i.e., cladding and substrate) slot, with the ligament cross section below the slot being the same as that of the uniaxial tensile specimen. In all three specimen types, the flaws were produced by electrical-discharge machining (EDM) with root radii of approximately 0.002 inch and a slot width less than 0.006 inch. The previously described procedures (temperature environment and crosshead speed) employed for uniaxial tensile tests were repeated for flawed tensile specimen tests. All SF and SN specimens behaved like a standard uniaxial tensile specimen but with reduced elongation. Therefore, the test records were evaluated by the procedures used for unflawed tensile tests. That is, a 0.2 percent offset yield strength and a ultimate fracture strength were determined for each test. However, the SEN specimen load-deflection records closely resembled that expected of a conventional fracture-mechanics test. That is, there was only a slight deviation from linearity prior to fracture. From these tests, a fracture strength was computed from the net section area and fracture load. In addition, an estimate of plane-stress fracture toughness (K_c) was obtained from the following relationship:

$$K_c = \frac{R\sqrt{a}}{Bw} 1.99 - 0.41\,(a/w) + 18.7\,(a/w)^2 - 38.48\,(a/w)^3 + 53.85\,(a/w)^4 ,$$

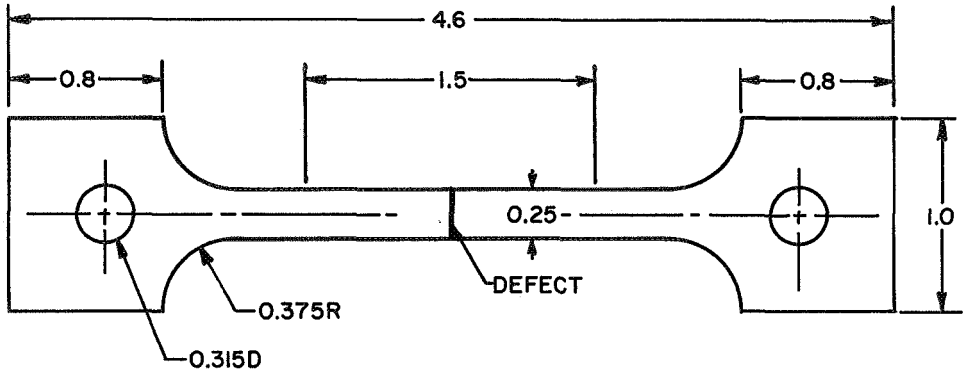

(a) Side-Notch Defect, Uniform Depth Equal to Cladding Thickness

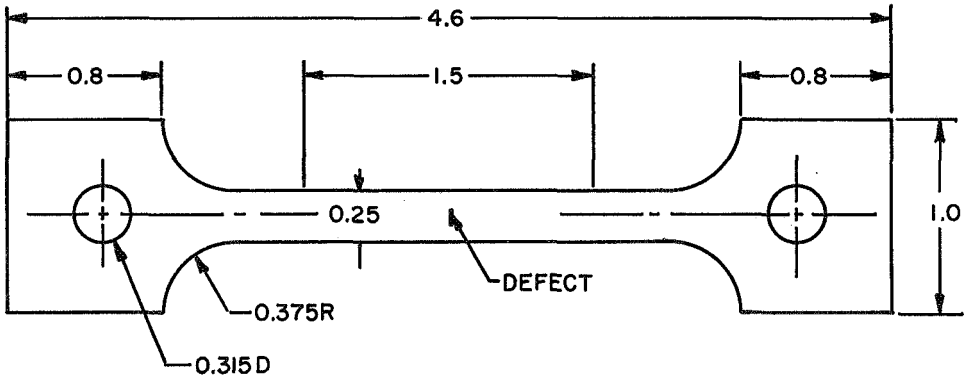

(b) Surface-Flaw Defect, Semielliptical Surface Flaw In Substrate Beneath Cladding

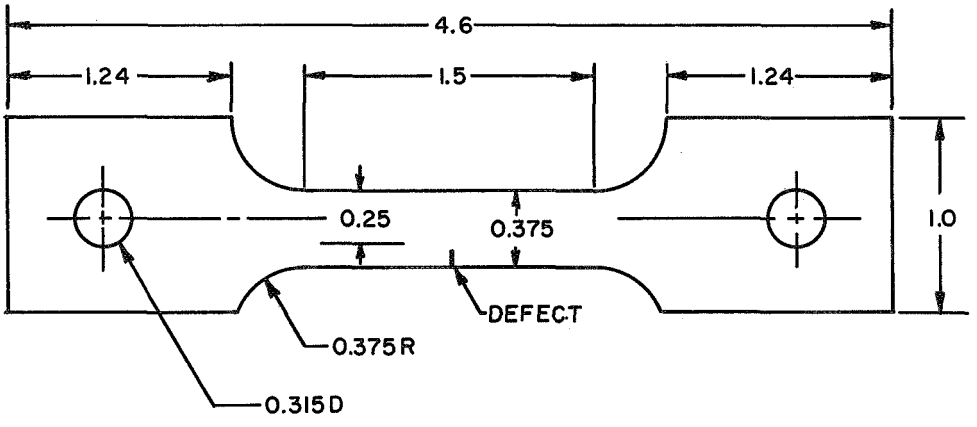

(c) Single-Edge-Notch Defect, Through-Thickness Slot

FIGURE 37. DEFECTED-CLADDING TENSILE SPECIMENS

where a is the slot depth, w is the cross-section width, and B is the thickness of the specimen. For all flawed tensile specimens (SN, SF, and SEN), the various strength values were calculated with the specimen thickness being that of the Ti-5Al-2.5Sn substrate only.

Tensile-Test Results and Discussion

The tensile properties of unclad sheet at room temperature and at -320 F were determined. Six tensile specimens of the 0.050-inch-thick substrate [Ti-5Al-2.5Sn (ELI)] material were prepared. The results of these tests are as follows:

Temperature, F	0.2% Yield Strength, ksi	Ultimate Strength, ksi	Elongation, percent
70	105.6	117.0	22
70	99.0	109.8	22
70	104.0	115.9	22
-320	188.5	190.8	20
-320	180.5	190.0	22
-320	179.5	187.0	22

The tensile strength of a stainless steel/titanium-alloy-sheet composite – 0.008-inch Type 304L stainless steel explosively welded to 0.050-inch Ti-5Al-2.5Sn (ELI) – was determined. The results of those tests which were computed on the basis of substrate thickness only are as follows:

Temperature, F	0.2% Yield Strength, ksi	Ultimate Strength, ksi	Elongation, percent
70	125.5	137.5	21
70	(a)	143.0	20
70	128.4	138.6	23
-320	194.0	211.0	39
-320	189.0	208.0	25
-320	188.9	212.8	37

(a) Extensometer error obviated yield-strength evaluation.

The tensile strength of a stainless steel/titanium-alloy-sheet composite – 0.002-inch Type 304 stainless steel vacuum-deposited on 0.050-inch Ti-5Al-2.5Sn (ELI) – was determined. The composite was heat treated in vacuum at 1300 F for 2 hours after deposition. The results of these tests using a substrate-thickness base are tabulated below:

Temperature, F	0.2% Yield Strength, ksi	Ultimate Strength, ksi	Elongation, percent
70	101.5	112.3	23.5
-320	176.4	188.3	23.7
-320	172.7	187.7	23.8
-320	174.5	185.8	26.1

The tensile strength of a stainless steel/titanium-alloy-sheet composite – 0.005-inch Type 304 stainless steel vacuum-deposited on 0.050-inch Ti-5Al-2.5Sn (ELI) – was determined. The composite was heat treated in vacuum at 1200 F for 1 hour after deposition. The results of these tests again using a substrate-thickness base were as follows:

Temperature, F	0.2% Yield Strength, ksi	Ultimate Strength, ksi	Elongation, percent
70	108.0	123.7	15
-320	174.3	186.4	15
-320	169.9	179.8	13
-320	180.9	194.7	10

The average values of the various tensile test series are summarized in Table 14. The tensile properties of the unclad sheet were found to compare favorably with published results for similar material. Presence of the vacuum-deposited stainless steel coating did not seem to affect these tensile properties. The explosively clad composite exhibited an increase in yield strength and ultimate strength. This may be due to the effects of the shock pulse inherent in the cladding process rather than to the mere presence of the cladding. There was also an apparent improvement in cryogenic ductility which may also be linked with shock-pulse effects on the substrate material. There were a few instances in which the cladding separated from the substrate in a zone adjacent to the fracture. Both explosively welded and vacuum-deposited claddings exhibit this behavior. In general, the tensile-test results revealed no deleterious effect on the tensile behavior of Ti-5Al-2.5Sn (ELI) substrate as a result of either cladding process evaluated.

Fracture-Toughness-Test Results and Discussion

Compact tension tests were performed to evaluate the fracture toughness at -320 F of bare 0.5-inch Ti-5Al-2.5Sn (ELI) plate and that of plate clad with 0.020-inch-thick Type 304L stainless steel. Two types of bonding were employed: (1) direct bonding of cladding on substrate and (2) indirect

TABLE 14. AVERAGE TENSILE PROPERTIES OF UNCLAD AND STAINLESS STEEL-CLAD Ti-5Al-2.5Sn

Specimen Type	Test Temperature, F	0.2% Yield Strength, ksi	Ultimate Strength, ksi	Elongation, percent
0.050-in. Ti alloy	70	103	114	22
0.050-in. Ti alloy/ 0.008-in. SS explosively bonded	70	132.3	139.3	21
0.050-in. Ti alloy/ 0.002-in. SS vacuum deposited	70	101.5	112.3	23.5
0.050-in. Ti alloy/ 0.005-in. SS vacuum deposited	70	108.0	123.7	15
0.050-in. Ti alloy	-320	183	189	21
0.050-in. Ti alloy/ 0.008-in. SS explosively bonded	-320	190.4	211	34
0.050-in. Ti alloy/ 0.002-in. SS vacuum deposited	-320	174.5	187.2	24.5
0.050-in. Ti alloy/ 0.005-in. SS vacuum deposited	-320	175.1	187.0	13

bonding with a thin tantalum layer between the cladding and the substrate. Both were accomplished by the explosive welding process. Two specimens of each material were prepared and tested. The specimens were fatigue precracked and tested according to the recommended procedures of ASTM Committee E-24. The results, which are presented in Table 15, indicated that the cladding process had little, if any, effect on the fracture-toughness properties of the substrate plate.

TABLE 15. COMPACT-TENSION FRACTURE-TOUGHNESS TEST RESULTS

Specimen Type	Crack Size, in.	Fracture Load(a), lb	K_{Ic}, ksi $\sqrt{in.}$
Bare plate	0.46	3025	49.0
	0.46	2860	46.4
Clad plate, Process 1	0.46	2660	45.7
	0.45	2875	48.0
Clad plate, Process 2	0.52	2245	44.8
	0.51	2250	44.3

(a) Based on substrate thickness only.

The fracture resistance of clad and unclad sheet [0.050-in.-thick Ti-5Al-2.5Sn (ELI)] material was evaluated by -320 F tests of defected tensile specimens. The specimens employed are identified as SF, SN, and SEN which were described previously. In general, the SEN-specimen test results resembled those obtained in conventional fracture mechanics and the SN and SF specimen test results were similar to those obtained from a conventional uniaxial tensile test. Typical load-deflection records for SF, SN, SEN, and unflawed-tensile-specimen tests are shown in Figure 38. The results of the flawed-tensile-specimen tests are listed in Table 16.

It is apparent from the data in Table 16 that the explosively clad sheet material has decreased fracture toughness and increased tensile strength properties. This behavior suggests that the explosive shock pulse has altered the properties of the titanium substrate, rather than the change being due to the simple presence of the stainless steel cladding. The increase in fracture and/or ultimate strength is approximately 10 percent and the attendant decrease in toughness is approximately 30 percent. The results from the vacuum-deposited composite material may not be conclusive. The

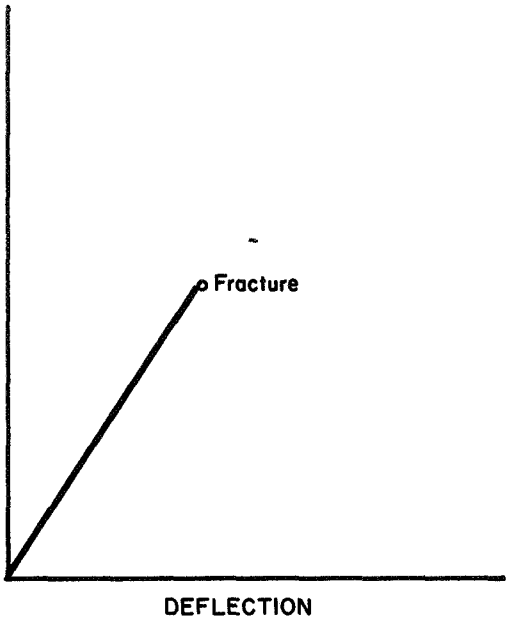

(a). SEN Specimen

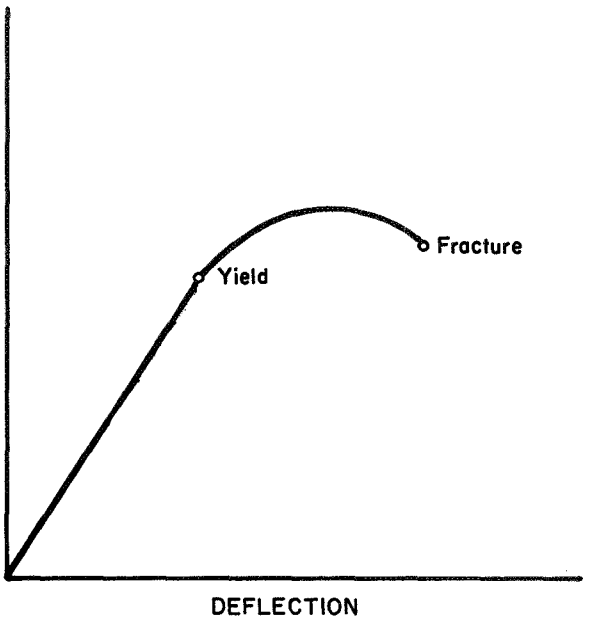

(b). SN Specimen

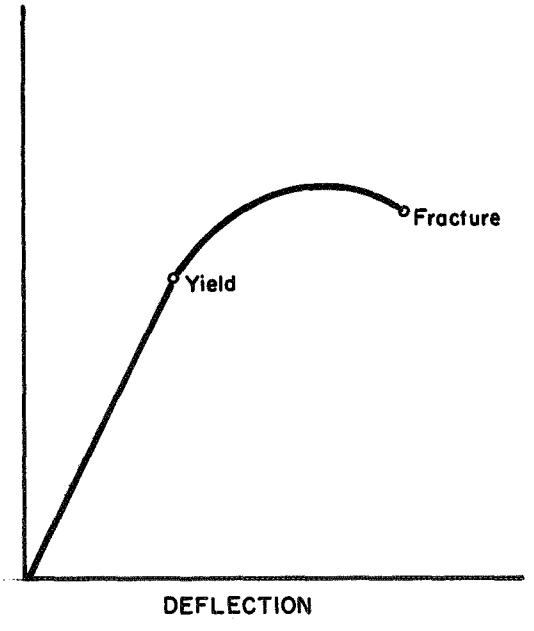

(c). SF Specimen

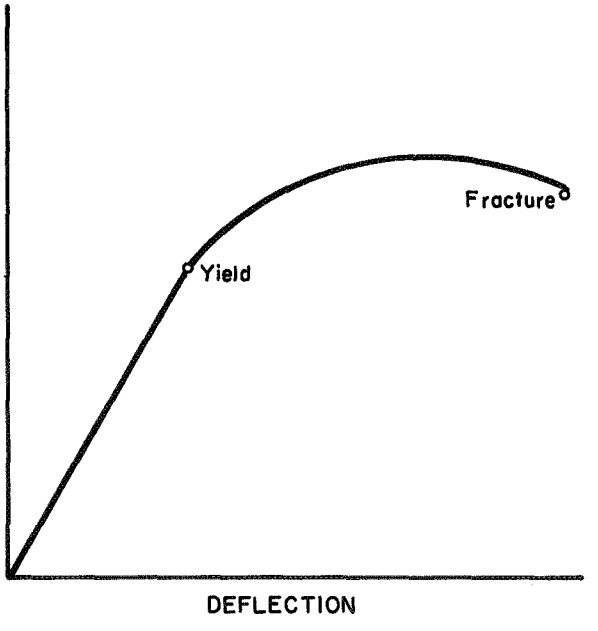

(d). Tensile Specimen

FIGURE 38. TYPICAL LOAD-DEFLECTION RECORDS

cladding separated from the substrate early in the test cycle. Hence, the stainless steel had no influence on the test per se. However, the tests did evaluate the effect of the coating process on substrate properties, and the results of these tests are in good agreement with those for bare titanium sheet.

The above fracture-toughness tests of plate and sheet material has shown that the cladding does not have an appreciable effect on the mechanical response of the composite. However, the explosive cladding process may have an adverse effect on the fracture resistance of the sheet material. This latter effect is probably the result of the substrate being slightly shock hardened by the explosive-welding shock pulse.

TABLE 16. FLAWED-TENSILE-SPECIMEN FRACTURE-TOUGHNESS RESULTS

Material	Specimen Type	0.2% Yield Strength, ksi	Fracture Strength(a), ksi	K_c Fracture Toughness, ksi $\sqrt{in.}$
Bare sheet	SEN		144.5	115
	SN	177.4	183.5	
0.050-in. Ti alloy/	SEN		204	77.2
0.008-in. SS ex-	SEN		225	80
plosively bonded	SEN		228	81.2
	SEN		220	78.3
	SN(b)	188.4	200.8	
	SN(b)	200.8	218	
	SN(c)	199.4	207.5	
	SN(c)	199.4	216.2	
0.050-in. Ti alloy/	SEN		149.3	108.4
0.005-in. SS	SEN		142.7	110
vacuum deposited	SEN		140.3	110
	SN(b)	155.1	163.9	
	SN(b)	162.3	170.5	
	SN(b)	151.8	158.9	
	SF	191.9	202.9	
	SF	187	200.7	
	SF	190.3	201.8	

(a) Based on substrate thickness only.
(b) Flawed on cladding side of composite.
(c) Flawed on substrate side of composite.

CONCLUSIONS

In each of the previous sections of this report, conclusions of a somewhat more detailed nature were drawn pertinent to the technical area under discussion. In summary, the following general conclusions may be drawn on the basis of the overall experimental effort:

(1) A capability for producing stainless steel-clad Ti-5Al-2.5Sn sheet and plate with a wide variety of cladding thickness by explosive welding and physical vapor deposition has been demonstrated. However, the joint efficiency of explosively welded composites consisting of 0.02-inch stainless/0.5-inch Ti-5Al-2.5Sn plate was found to be low.

(2) Formation of brittle intermetallics between the constituents of the cladding and substrate alloys prevent the attainment of optimum properties of the stainless steel/Ti-5Al-2.5Sn composite. The physics of compound formation is believed to be quite different in the two cladding processes evaluated, but further study in that area was beyond the scope of this program.

(3) Further development emphasizing the use of candidate barrier materials to prevent interdiffusion of the intermetallic-forming species of the system should be pursued.

(4) A 0.0005-inch-thick stainless steel cladding over Ti-5Al-2.5Sn appears to preclude the possibility of LOX-titanium reaction with a high degree of reliability. The coating must remain physically intact to insure reliability.

(5) There is a substantial probability of reaction with LOX if an impact is sustained by the composite at a point at which a defect greater than 0.004 inch in effective diameter exists. Reaction during an impact event that pierces the composite is extremely probable.

(6) Stainless steel-clad Ti-5Al-2.5Sn prepared in this program exhibited a fatigue strength much lower than that of the unclad titanium-alloy substrate. It is almost certain that intermetallic-compound formation was responsible for the decrease observed. This was also responsible for cladding delamination noted in LOX and tensile tests.

(7) Neither of the cladding techniques evaluated appeared to have a deleterious effect on tensile-strength properties.

(8) The presence of a stainless steel cladding per se was found to have an insignificant effect on the fracture-toughness behavior of the Ti-5Al-2.5Sn substrate. Similarly, the physical vapor deposition process did not appear to affect fracture behavior.

(9) It is believed that the value of a bilaminate composite for space-booster-hardware fabrication has been demonstrated. The two shortcomings pointed up in the study, shortened fatigue life and possible fracture-toughness degradation in one case, can be eliminated by the exclusion of brittle phases at the composite interface and by the capability to stress relieve at the higher temperatures that a mutually compatible barrier material would provide.

APPENDIX A

EXPLOSIVE-WELDING EXPERIMENTS UTILIZING A TANTALUM INTERLAYER

APPENDIX A

EXPLOSIVE-WELDING EXPERIMENTS UTILIZING A TANTALUM INTERLAYER

After the explosive-welding segment of the program had been completed and while the final report was being prepared, a few experiments were conducted in which one of the recommended approaches for improving welds between 0.020-inch Type 304L stainless steel and 0.5-inch Ti-5Al-2.5Sn (ELI) was considered. This approach involved the use of an intermediate layer of tantalum which is metallurgically compatible with both the stainless steel and the titanium-alloy components. These experiments produced a significant improvement in the quality of welds between the stainless steel and titanium alloy.

The first step of the interlayer approach involved explosively welding 0.003-inch tantalum foil to 0.020-inch Type 304L stainless steel sheet. A vacuum hold-down technique was used to insure that the foil was put down in a smooth layer. This welded composite was next flat-annealed between platens by heating for 0.5 hour at 1800 F in vacuum. The stainless steel/tantalum composite was then explosively welded to 0.5-inch Ti-5Al-2.5Sn plate. The stainless steel-tantalum/titanium alloy composite was subsequently heat treated for 1 hour at 1200 F in vacuum and flattened in a roller-leveler.

Evaluation of specimens processed in this manner revealed that welds with good strength and ductility were produced using either SWP-1- or SWP-6-type explosives. Figure A-1 illustrates a typical interface. The stainless steel-tantalum welds tend toward a somewhat overdeveloped wave pattern, although this does not affect the weld properties. The tantalum-titanium alloy welds were almost straight, with a periodic distribution of alloy pockets along the interface. Peel tests always resulted in failure at the tantalum-titanium alloy weld, but the effort required to peel the specimens indicated that the welds had significant strength and were evidently not degraded by the presence of alloy pockets. The ductility of the welded composite was further evidenced by its low minimum bend radius. Bend radii of 2.5t were obtained. This value compares very favorably with the 2t value for the bare titanium alloy.

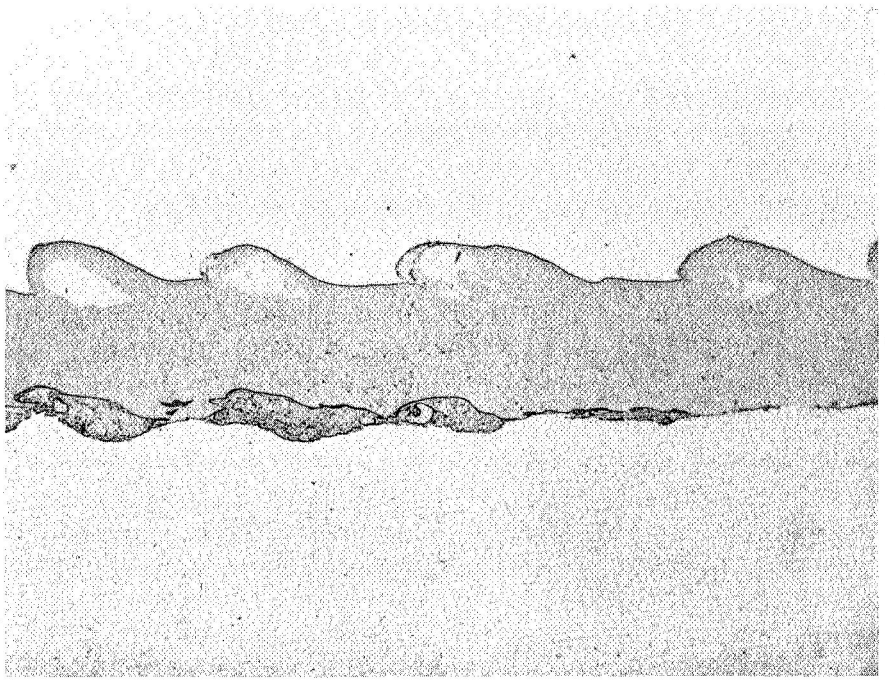

250X 3E831

FIGURE A-1. EXPLOSIVELY WELDED COMPOSITE INTERFACE

The tantalum interlayer was first welded to the stainless steel cladding. This composite was then welded to the titanium-alloy plate.

APPENDIX B

INDIVIDUAL TEST RESULTS FROM LOX-COMPATIBILITY STUDY

TABLE B-1. RESULTS OF LOX-COMPATIBILITY STUDIES

Specimen	Cladding Thickness, mils	Defect Diameter, mils	Striker	Results	
				Flash	Fused Area
B-1	8	None	Ball	No	No
B-2	8	None	Ball	No	No
B-3	8	None	Ball	No	No
B-4	8	None	Ball	No	No
B-5	8	None	Ball	No	No
B-6	8	None	Ball	No	No
B-7	8	None	Ball	No	No
B-8	8	None	Ball	No	No
B-9	8	None	Ball	No	No
B-10	8	None	Ball	No	No
B-11	8	None	Ball	No	No
B-12	8	None	Ball	No	No
B-13	8	None	Ball	No	No
B-14	8	None	Ball	No	No
B-15	8	None	Ball	No	No
B-16	8	None	Ball	No	No
B-17	8	None	Ball	No	No
B-18	8	None	Ball	No	No
B-19	8	None	Ball	No	No
B-20	8	None	Ball	No	No
B-33	1	None	Ball	No	No
B-34	1	None	Ball	No	No
B-35	1	None	Ball	No	No
B-36	1	None	Ball	No	No
B-37	1	None	Ball	No	No
B-38	1	None	Ball	No	No
B-39	1	None	Ball	No	No
B-40	1	None	Ball	No	No
B-41	1	None	Ball	No	No
B-42	1	None	Ball	No	No
B-43	1	None	Ball	No	No
B-44	1	None	Ball	No	No
B-45	1	None	Ball	No	No
B-46	1	None	Ball	No	No
B-47	1	None	Ball	No	No
B-48	1	None	Ball	No	No
B-49	1	None	Ball	No	No
B-50	1	None	Ball	No	No
B-51	1	None	Ball	No	No

TABLE B-1. (Continued)

Specimen	Cladding Thickness, mils	Defect Diameter, mils	Striker	Results	
				Flash	Fused Area
F-52	0.5	None	Flat	No	No
F-53	0.5	None	Flat	No	No
F-54	0.5	None	Flat	No	No
F-55	0.5	None	Flat	No	No
F-56	0.5	None	Flat	No	No
B-57	0.5	None	Ball	No	No
B-58	0.5	None	Ball	No	No
B-59	0.5	None	Ball	No	No
B-60	0.5	None	Ball	No	No
B-61	0.5	None	Ball	No	No
B-62	0.5	None	Ball	No	No
B-63	0.5	None	Ball	No	No
B-64	0.5	None	Ball	No	No
B-65	0.5	None	Ball	No	No
B-66	0.5	None	Ball	No	No
B-67	0.5	None	Ball	No	No
B-68	0.5	None	Ball	No	No
B-69	0.5	None	Ball	No	No
B-70	0.5	None	Ball	No	No
B-71	0.5	None	Ball	Yes	Yes
B-72	0.5	None	Ball	No	No
B-73	0.5	None	Ball	No	No
B-73[a]	0.5	None	Ball	Yes	Yes
B-74	0.5	None	Ball	No	No
B-75	0.5	None	Ball	No	No
B-76	0.5	None	Ball	No	No
B-77	0.4	None	Ball	No	No
B-78	0.3	None	Ball	No	No
B-79	0.3	None	Ball	No	No
B-80	0.3	None	Ball	No	No
B-81	0.3	None	Ball	No	No
B-82	0.2	None	Ball	No	No
B-83	0.2	None	Ball	No	No
B-84	0.2	None	Ball	No	No
B-85	0.2	None	Ball	No	No
B-86	0.2	None	Ball	No	No
B-87	0.2	None	Ball	No	No
B-88	0.2	None	Ball	No	No

TABLE B-1. (Continued)

Specimen	Cladding Thickness, mils	Defect Diameter, mils	Striker	Results	
				Flash	Fused Area
B-89	0.2	None	Ball	No	No
B-90	0.2	None	Ball	No	No
B-91	0.2	None	Ball	No	No
B-92	0.2	None	Ball	No	No
B-93	0.2	None	Ball	No	No
B-94	0.2	None	Ball	No	No
B-95	0.2	None	Ball	No	No
B-96	0.2	None	Ball	No	No
B-106	0.2	None	Ball	Yes	No
B-97	0.15	None	Ball	No	No
B-98	0.15	None	Ball	No	No
B-99	0.1	None	Ball	No	No
B-100	0.1	None	Ball	No	No
B-101	0.1	None	Ball	No	No
B-102	0.1	None	Ball	No	No
B-103	0.1	None	Ball	No	No
B-104	0.1	None	Ball	No	No
B-105	0.1	None	Ball	No	No
B-107	< 0.1	None	Ball	No	No
B-108	< 0.1	None	Ball	No	No
BD-1	8	35	Ball	No	No
BD-2	8	35	Ball	No	No
BD-3	8	35	Ball	No	No
BD-4	8	35	Ball	No	No
BD-5	8	35	Ball	Yes	Yes
BD-6	8	35	Ball	No	No
BD-7	8	35	Ball	Yes	Yes
BD-8	8	35	Ball	No	Yes
BD-9	8	35	Ball	No	No
BD-10	8	35	Ball	No	No
BD-11	8	35	Ball	No	No
BD-12	8	35	Ball	No	No
BD-13	8	35	Ball	No	No
BD-14	8	35	Ball	No	No
BD-15	8	35	Ball	No	No
BD-16	8	35	Ball	No	No
BD-17	8	35	Ball	No	No
BD-18	8	35	Ball	No	No

TABLE B-1. (Continued)

Specimen	Cladding Thickness, mils	Defect Diameter, mils	Striker	Results	
				Flash	Fused Area
BD-19	8	35	Ball	No	Yes
BD-20	8	35	Ball	No	No
17-A-1	1	16	Flat	No	No
17-A-2	1	16	Flat	Yes	Yes
17-B-1	1	16	Flat	Yes	Yes
17-B-2	1	16	Flat	No	Yes
15-4-1	1	16	Flat	Yes	Yes
15-4-2	1	16	Ball	No	No
15-4-3	1	16	Ball	Yes	Yes
15-7-1	1	16	Ball	No	No
15-7-2	1	16	Ball	No	No
15-7-3	1	16	Ball	No	No
15-2-1	1	8	Flat	No	No
15-2-2	1	8	Flat	No	No
15-2-3	1	8	Flat	No	No
15-2-4	1	8	Flat	No	No
15-2-5	1	8	Flat	No	No
15-2-1A[a]	1	8	Ball	No	No
15-2-2A[a]	1	8	Ball	No	No
15-2-3A[a]	1	8	Ball	No	Yes
15-2-4A[a]	1	8	Ball	No	No
15-2-5A[a]	1	8	Ball	No	No
15-4-1	1	8	Ball	No	No
15-4-2	1	8	Ball	Yes	No
17-C-1	1	8	Ball	No	No
17-C-2	1	8	Ball	No	No
17-D-1	1	8	Ball	No	No
17-D-2	1	8	Ball	No	No
16-1-1	3	8	Flat	No	No
16-1-2	3	8	Flat	No	No
16-1-1A[a]	3	8	Ball	No	No
16-1-2A[a]	3	8	Flat	No	Yes
16-2-1	3	8	Ball	No	Yes
16-4-1	3	8	Ball	No	No
16-8-1	3	8	Ball	No	No
16-8-2	3	8	Ball	No	No
17-A-1	1	4	Flat	No	No
17-A-2	1	4	Ball	No	No

TABLE B-1. (Continued)

Specimen	Cladding Thickness, mils	Defect Diameter, mils	Striker	Results	
				Flash	Fused Area
17-A-3	1	4	Ball	No	No
17-B-1	1	4	Ball	No	No
17-B-2	1	4	Ball	No	No
17-B-3	1	4	Ball	No	No
17-C-1	1	4	Ball	No	No
17-C-2	1	4	Ball	No	No
17-C-3	1	4	Ball	No	No
17-D-1	1	4	Ball	No	No
P-1	8	None	Pierce	No	No[(b)]
P-2	8	None	Pierce	No	Yes
P-3	8	None	Pierce	No	Yes
P-4	8	None	Pierce	Yes	Yes
P-5	8	None	Pierce	Yes	Yes
P-6	8	None	Pierce	Yes	Yes
P-7	8	None	Pierce	No	No
P-8	8	None	Pierce	No	No
P-9	8	None	Pierce	No	Yes
P-10	8	None	Pierce	No	No
P-11	8	None	Pierce	No	No
P-12	8	None	Pierce	No	No
P-13	8	None	Pierce	No	Yes
P-14	8	None	Pierce	No	Yes
P-15	8	None	Pierce	No	Yes
P-16	8	None	Pierce	No	No
P-17	8	None	Pierce	No	No
P-18	8	None	Pierce	No	No
P-19	8	None	Pierce	No	Yes
P-20	8	None	Pierce	No	Yes

(a) Second impact.

(b) This and the following results indicate the existence or nonexistence of either a fused or colored area.

DISTRIBUTION LIST

	Copies
National Aeronautics and Space Administration	
Lewis Research Center	
21000 Brookpark Road	
Cleveland, Ohio 44135	
Attention: Contracting Officer, MS 500-313	1
Chemical Rockets Division, MS 500-205	10
Technical Report Control Office, MS 5-5	1
Technology Utilization Office, MS 3-19	1
AFSC Liaison Office, MS 501-3	2
Library, MS 60-3	2
T. W. Godwin, MS 500-203	28
National Aeronautics and Space Administration	
Washington, D. C. 20546	
Attention: Code RPX	2
RPL	2
Scientific and Technical Information Facility	
P.O. Box 33	
College Park, Maryland 20740	
Attention: NASA Representative	6
Code CRT	
National Aeronautics and Space Administration	
Ames Research Center	
Moffett Field, California 94035	
Attention: Library	1
C. A. Syvertson	1
National Aeronautics and Space Administration	
Flight Research Center	
P.O. Box 273	
Edwards, California 93523	
Attention: Library	1
National Aeronautics and Space Administration	
Goddard Space Flight Center	
Greenbelt, Maryland 20771	
Attention: Library	1

DISTRIBUTION LIST
(Continued)

	Copies
National Aeronautics and Space Administration John F. Kennedy Space Center Kennedy Space Center, Florida 32931 Attention: Library	1
National Aeronautics and Space Administration Langley Research Center Langley Station Hampton, Virginia 23365 Attention: Library	1
National Aeronautics and Space Administration Manned Spacecraft Center Houston, Texas 77001 Attention: Library	1
National Aeronautics and Space Administration George C. Marshall Space Flight Center Huntsville, Alabama 35812 Attention: Library Keith Chandler, R-P&VE-PA	1 1
Jet Propulsion Laboratory 4800 Oak Grove Drive Pasadena, California 91103 Attention: Library C. D. Coulbert, MS 67-201	1 1
Defense Documentation Center Cameron Station Alexandria, Virginia 22314	1
Air Force Rocket Propulsion Laboratory (RPR) Edwards, California 93523	1
Director (Code 6180) U. S. Naval Research Laboratory Washington, D. C. 20390 Attention: H. W. Carhart	1

DISTRIBUTION LIST
(Continued)

	Copies
Air Force Aero Propulsion Laboratory Research & Technology Division Air Force Systems Command United States Air Force Wright-Patterson AFB, Ohio 45433 Attention: APRP (C. M. Donaldson)	1
Aerojet General Corporation P.O. Box 1947 Sacramento, California 95809 Attention: Library	1
Chrysler Corporation Space Division New Orleans, Louisiana 70150 Attention: Librarian	1
General Electric Company Flight Propulsion Lab Department Cincinnati, Ohio 45215 Attention: Library	1
Rocketdyne, A Division of North American Rockwell Corporation 6633 Canoga Avenue Canoga Park, California 91304 Attention: Library, Department 596-306	1
TRW, Incorporated TAPCO Division 23555 Euclid Avenue Cleveland, Ohio 44117 Attention: Library	1
United Aircraft Corporation Pratt and Whitney Division Florida Research and Development Center P.O. Box 2691 West Palm Beach, Florida 33402 Attention: Library	1

DISTRIBUTION LIST
(Continued)

	Copies
Mr. Eugene W. Broache Defense Division Westinghouse Electric Corporation Baltimore, Maryland	1
General Dynamics Convair Division P.O. Box 1128 San Diego, California 92112 Attention: A. Hurlich, Mail Zone 572-00	1
The Boeing Company Aerospace Group Seattle, Washington Attention: R. E. Regan	1
Gould, Incorporated Technical Center 540 E. 105th Street Cleveland, Ohio 44108 Attention: C. F. Davies, Composite Development Section	1